SELFISH MISBEHAVIOR IN 802.11 WIRELESS NETWORKS

Antoniy Ganchev

A thesis
in
The Department
of
Computer Science and Software Engineering

Presented in Partial Fulfillment of the Requirements
For the Degree of Doctor of Philosophy (Computer Science)
Concordia University
Montréal, Québec, Canada

September 2011

Concordia University
School of Graduate Studies

This is to certify that the thesis prepared

By: **Antoniy Ganchev**

Entitled: **Selfish Misbehavior in 802.11 Wireless Networks**

and submitted in partial fulfillment of the requirements for the degree of

Doctor of Philosophy (Computer Science)

complies with the regulations of this University and meets the accepted standards with respect to originality and quality.

Signed by the final examining commitee:

Dr. Ahmed A. Kishk ______________________ Chair
Dr. Michel Barbeau ______________________ External Examiner
Dr. Mourad Debbabi ______________________ Examiner
Dr. Jaroslav Opatrny ______________________ Examiner
Dr. Horhannes Harutyunyan ______________________ Examiner
Dr. Lata Narayanan ______________________ Supervisor

Approved ______________________
Chair of Department or Graduate Program Director

September 12, 2011 ______________________
Dr. Robin A. L. Drew, Dean
Faculty of Engineering and Computer Science

Abstract

Selfish Misbehavior in 802.11 Wireless Networks

Antoniy Ganchev, Ph.D.
Concordia University, 2011

Media access protocols in wireless networks require each contending node to wait for a backoff time chosen randomly from a given range, before attempting to transmit on a shared channel. However, selfish stations might try to acquire an unfair portion of the channel resources, at the expense of the cooperating nodes, by not following the protocol specifications. For example, they might choose smaller backoff values more often than would be dictated by pure chance. In this thesis, we study how to detect such misbehavior as well as how nodes might be induced to adhere to the protocol.

We first introduce a game-theoretic framework that models an abstracted version of the medium access protocol as a strategic static game. We are interested in designing a game which exhibits a unique Nash equilibrium corresponding to a pre-specified full-support distribution profile. In the cooperation inducement context, the Nash equilibrium for the game would correspond to protocol compliance on behalf of the participating nodes. We identify an exact condition on the number of players and the number of their strategies that must be met to guarantee the existence of such a game.

Further, we propose a new protocol called XVBEB in order to determine based on the stations' backoff values choices whether they are behaving accordingly or selfishly. We describe how to deduce the backoff values in XVBEB based on observations of transmissions by nodes in the network and the collision timeline, which is rarely feasible with the IEEE 802.11 backoff procedure. Given a set of backoff values used by a XVBEB node, we describe how to conclude with a specified level of certainty whether the node is indeed adhering to the protocol.

Finally, we evaluate the performance of a network of XVBEB nodes and compare it against a standard IEEE 802.11 network. Simulation results show that the throughput of XVBEB is better than that of 802.11 for saturated CBR traffic. Furthermore, XVBEB also exhibits lower packet loss, delay and delay variation than 802.11 for both VBR and VoIP traffic for a variety of load conditions.

Acknowledgments

In 2004, I have enrolled in a computer science doctorate program at Concordia University. It has been a bumpy ride as I had to overcome many obstacles along the way. During the past five or six years I have been working full time, so I had to dedicate countless sleepless nights and weekends to achieve my goal - the writing of this thesis. I often ask myself the question whether I would do it again if I had the chance to go back in time. Today, I am certain I had made the right choice as I am confident that the results in this thesis were well worth the efforts.

Dr. Lata Narayanan, my thesis supervisor, deserves special thanks. Aside from being the only person with whom I could discuss my work, a discussion (or sometimes a heated debate) with her has never failed to provide me with a new direction to overcome the numerous challenges I had to face. Nonetheless, her broad experience helped me a lot to develop academic writing and presentation skills. If it was not for her feedback, the presentation and the writeup of my thesis would not be up to the quality of the actual achievements.

I would also like to thank Prof. Sunil Shende for his assistance for the results presented in Chapters 3 and 4, as well as Prof. Chadi Assi for his valuable input for the work in Chapter 6.

Finally, I would like to dedicate this thesis to my father. Without his continuous support over the years, I would not be nowhere near the person that I am now.

Contents

List of Figures

List of Tables

Chapter 1

Introduction

The number of wireless network deployments has been significantly increasing over the last decades as many businesses and home users have started to appreciate the benefits of wireless communications. Ease of setup and mobility are a few of the benefits that made such networks widely used. Therefore, many research groups focused their attention on enhancing the existing standards and creating new standards for mobile communications. Wireless Local Area Networks (WLANs) can be classified in two major categories: Mobile Ad Hoc Networks (MANETs) and Infrastructure-Based Wireless Networks. MANETs consist of a set of mobile devices communicating with each other via wireless links in the absence of any fixed infrastructure. The second type is observed when mobile nodes communicate with peers with the help of base stations, which are networked to each other through wired links. Typical MANET instances are military and disaster recovery operations; library and airport networks are examples of infrastructure-based wireless networks.

Most traditional physical, data link and network layer protocols were developed for use in wired networks and are not suitable for use in wireless environments. Therefore, new standards had to be developed to address many important concerns such as node mobility, insecure and unreliable wireless links, and power constraints. Some physical and data link layer protocols for mobile communications are suitable for use in both MANETs and infrastructure-based networks, whereas ad-hoc networks require particular routing protocols. Because of the lack of designated routing devices, all nodes must act as routers forwarding packets on behalf of the others.

1.1 Data link layer protocols for wireless communications

Our work focuses exclusively on studying the behavior of data link layer protocols. The first such protocol was ALOHA [Abr70], developed for packet radio networks, the precursor of today's ad hoc networks. In ALOHA, a wireless node or terminal that has data simply transmits, and if it finds out later that there was a collision, it re-transmits. By dividing time into fixed length slots, and allowing packet transmission only at time slot boundaries, Slotted ALOHA reduces the time spent in collisions thereby doubling the throughput [Rob75].

In most modern protocols, a mechanism is implemented on the data link layer aiming to avoid simultaneous transmissions on the same channel. Such mechanisms are often called Carrier Sense Multiple Access (CSMA) schemes. A station that has a message to transmit must verify whether there the channel is free; if so, it attempts to send the message. If, however, there is another transmission in progress, it wait until the channel becomes free and then wait again for some random interval before attempting a transmission. Additional improvements to this access scheme are achieved by implementing a second wait period in an effort to avoid the possibility that two or more waiting nodes try to send their packets at the same time, which would result in a collision. This procedure is also called a Carrier Sense Multiple Access with Collision Avoidance (CSMA/CA) scheme. The p-persistent [KT75] protocol was one of the earliest CSMA/CA schemes. A node wishing to transmit first senses the channel. If the channel is idle, it transmits with probability p, and defers the decision to transmit by one slot with probability $1 - p$.

Most of the analysis in this thesis concentrates on the most widely used wireless medium access protocol IEEE 802.11 [IEE07], so we present its detailed mode of operation. The IEEE 802.11 standard specifies participants' behavior at both physical and data link layers. On the physical layer, the transmission frequencies are split into channels to avoid interference between different networks within the same transmission range. On the data link layer, it is a slotted CSMA/CA scheme designed to resolve simultaneous channel access attempts from multiple hosts.

The protocol provides two mechanisms to solve the contention problem: PCF (point coordination function) and DCF (distributed coordination function). PCF is based on a polling scheme where the point coordinator (access point) polls each station in its polling list. In IEEE 802.11 DCF, which is a fully distributed mechanism, the responsibility for resolving media access conflicts is distributed between all participating nodes. Each node maintains a special value CW (contention window). Before transmitting, a node senses if the channel is free for a DIFS (DCF inter frame spacing) period of time. If no other transmission is detected, the station makes a transmission attempt. If the channel is sensed busy, the participant initiates a *backoff procedure* (Figure 1).

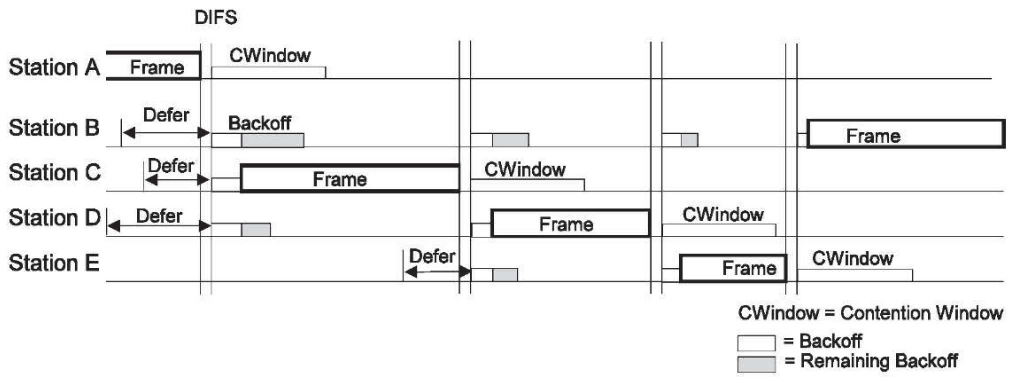

Figure 1: IEEE 802.11 Contention

When entering in backoff state, a station selects a *random* backoff value from the $[0, CW]$ interval and sets its backoff counter to the selected value. When the channel becomes idle again, the station waits for a DIFS period and decreases its backoff counter by one after each time slot the channel is sensed idle. If at some point the medium becomes busy again, the backoff procedure is put on hold until the channel becomes available. When the channel becomes available again, the node waits for another DIFS interval and continues the countdown from the value of the backoff counter when the backoff procedure was suspended. Once the backoff counter reaches 0, the node makes another transmission attempt (Figure 2).

In contrast to wired networks, transmitting wireless station do not get feedback from the medium when collisions occur. Therefore, to determine whether the transmission of a data packet has been successfully received or if the packet has been lost (e.g. due to a collision), the recipient should send a confirmation packet back

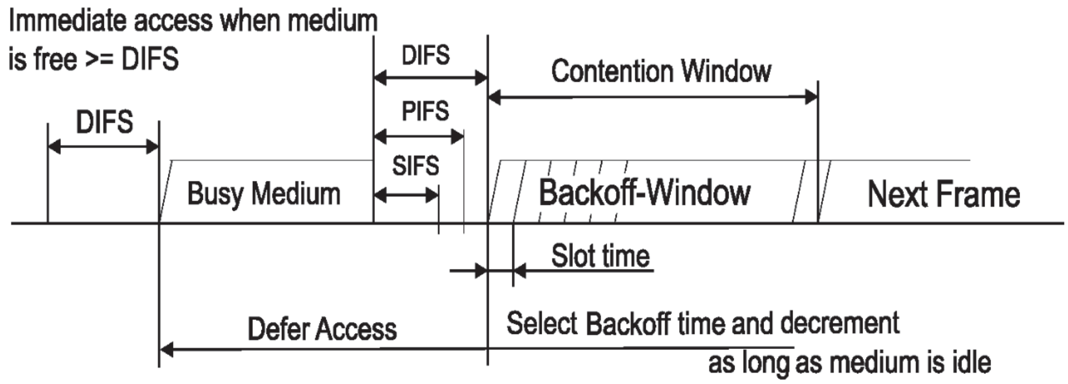

Figure 2: IEEE 802.11 Transmission

to the sender. A transmission is deemed to be successful if the sender receives an ACK (acknowledgment) packet back from the receiver. This mechanism is called *basic access*. The basic access handshake is shown in Figure 3.

In efforts to reduce collision times and to solve the hidden node problem, an optional *RTS/CTS* (Request to Send/Clear to Send) mechanism has been specified. Instead of sending a full data packet, a transmitting station sends a short RTS control packet to the destination. If the receiver replies with a CTS control packet, the sending node starts transmitting the data. Figure 4 illustrated the RTS/CTS handshake.

The benefit of the RTS/CTS mechanism is that if two or more nodes transmit at the same time, the collision time would normally be much shorter than if lengthy data packets collided thus reducing the dirty utilization of the channel. In the basic access mechanism (no RTS/CTS being used), however, there is no wasted time in RTS/CTS frames exchange, and, therefore, a bigger portion of the channel clean utilization is used for data traffic and less bandwidth is wasted for control frames.

If, at some point the sender fails to receive a CTS or ACK packet (depending

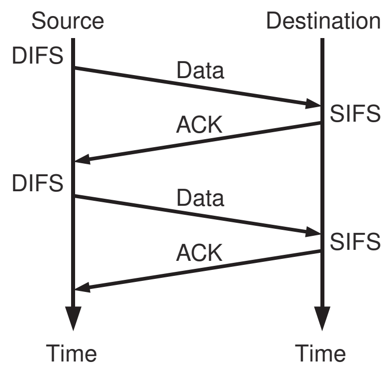

Figure 3: IEEE 802.11 Basic Access Handshake

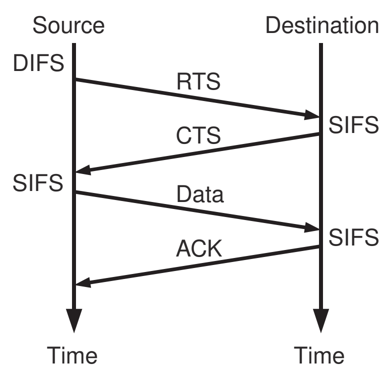

Figure 4: IEEE 802.11 RTS/CTS Handshake

on the access mechanism in use), it evokes a collision recovery procedure. The transmitting station should double its CW value (subject to some CW_{max}) and follow the backoff algorithm again. Once the transmission succeeds, it should reset its CW to a CW_{min} value.

In IEEE 802.11, carrier sensing is achieved in two ways: physical and virtual sensing. Virtual sensing is implemented to help nodes conserve their power resources. When a node is sending a packet, it calculates the expected communication duration. This interval is then indicated in the NAV (network allocation value) value contained within the MAC header. All listening nodes should refrain from transmission for the duration of this interval. When RTS/CTS is used, the NAV is also included in the CTS packet because there might be nodes in the destination's transmission range that cannot overhear the RTS packet sent by the source (Figure 5).

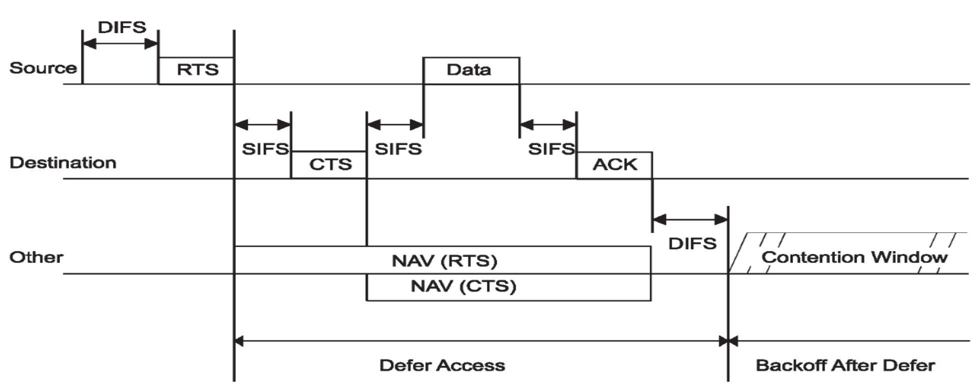

Figure 5: IEEE 802.11 RTS/CTS

Because of the nature of the wireless links, a node cannot transmit big chunks of data simultaneously. IEEE 802.11 DCF uses fragmenting to solve this problem. It has a MTU (maximum transmission unit) of 2304 bytes; however, when fragmentation is used, the MTU is reduced to 1500 bytes. Each DATA-ACK fragment serves as virtual RTS-CTS sequence thus reserving the channel for the next fragment.

1.2 Cooperation issues in mobile networks

Lack of central authority to provide control and management over the network operation can be observed in both types of wireless networks. This makes the wireless environments more vulnerable and imposes additional constraints on the design of communication protocols. Aside from the obvious security concerns, some participants could try to exploit the autonomous nature in order to achieve gain in different aspects such as achieving higher bandwidth or saving battery life. This gain is almost always achieved at the expense of the participants that adhere to the communication rules. Such behavior is often referred to as *selfish* or *greedy misbehavior*.

Note that such misbehavior could occur in the traditional wired networks; however, it is unlikely to happen because nodes are physically attached to the same backbone and usually belong to same organization.

It is important to distinguish selfish from malicious agents. Selfish nodes' goal is to maximize their own benefit which may impact the network operations in a negative way. Malicious nodes' purpose, on the other hand, is to obscure the network operations; saving energy, for example, is not a priority.

By design, all network and media access protocols work under the assumption that the participants strictly follow the protocol specifications, which makes them susceptible to selfish misbehavior. Greediness may occur in all layers of the protocol stack [CGM04].

We briefly the describe the non-cooperation problem at the network layer. Two general approaches for ad-hoc routing protocols have been developed [RT99]: reactive and proactive protocols. Proactive protocols are similar to the conventional routing protocols, i.e. all nodes maintain routing tables and routing decisions are taken by the intermediate nodes. Frequent topology changes are typical for ad-hoc environments resulting in high traffic overhead for routing table updates. As an alternative, reactive routing protocols do not require routing table maintenance. The routes are established only as needed, and the path that the packet should take is piggybacked by the sender into the packet header. A connection between two nodes is established in two phases: route discovery and packet forwarding. Reactive routing protocols are considered more suitable for ad-hoc environments.

A node may act selfishly trying to maximize or conserve its power resources in several ways:

1. Forwarding phase: each data packet having source/destination different from the current node is discarded.

2. Routing phase for reactive protocols (AODV [PBRD03], DSR [JMH]): not replying to route request, route reply, and route error messages.

3. Routing phase for proactive protocols (FSR [GPHC], OLSR [CJ03]): not cooperating in the propagation of routing information throughout the network.

This thesis focuses on selfish misbehavior at the data link layer. All CSMA/CA schemes assume that all participants strictly follow the protocol specifications in order to achieve an operational point of the network on the data link layer. However, this assumption may not be always valid, especially in the presence of autonomous nodes. For example, a node may have an incentive to increase its own throughput. This could be easily achieved by transmitting right after the channel is sensed idle instead of invoking the backoff procedure.

Unfortunately, there are numerous ways in which a station can gain advantage by not adhering to the protocol guidelines:

- Choosing small backoff values: Instead of choosing randomly, a selfish node could choose a smaller value. For example, if a cheater intentionally selects a backoff value of 0 each time it needs to access the communication medium, it will have the highest chance to access the media as soon as it becomes free.

- Not doubling CW after collision: after a collision, a node may not invoke the collision recovery procedure. Thus, the node would be always choosing its backoff values from $[0, CW_{\min}]$, thereby utilizing values for backoff

- Manipulating the NAV value: if a node increases this value, it can assure that all other agents will remain idle even after the end of the current transmission.

- Not conforming to the DIFS and SIFS intervals: such behavior will increase the chances of getting access to the medium.

- Scrambling others' data and control frames: such behavior would push other stations to invoke the collision recovery procedure, thus forcing them to double their CW values.

Note that not obeying the inter-frame spacing intervals or manipulating the

NAV values could be easily detected from the other participants. Scrambling others frames require the node to use energy resources for transmissions. Thus, the easiest ways for a participant to behave selfishly without being noticed is to choose lower backoff or not to double its contention window values. This two possibilities are special subcases of a generalized misbehavior: the station is choosing its backoff values according to a distribution different than the specified uniform distribution.

In the presence of two or more cheaters, a disastrous situation could occur. For instance, if two participants always choose 0 as their backoff value, only collisions will occur on the channel, and the network will collapse.

Finally, note that a participant might be misbehaving without even being aware of it. This could happen if manufacturer of wireless equipment aims to increase its popularity by incorporating lower backoff values in its products, which would lead to better performance compared to the products of its competitors. In recent work, Tinnirello et al. [TGN09] tested a number of Wi-Fi cards and discovered that some products were not conforming to the IEEE 802.11 specifications and the size of the contention window was smaller than the value given in the protocol specifications.

1.3 Thesis statement

The main goal of this thesis is to model and analyze data link layer protocols in order to detect and prevent selfish misbehavior on the part of wireless nodes. More specifically, we focus our attention on greedy nodes that manipulate the backoff procedure by choosing their backoff values based on other than the uniform distribution in $[1, CW]$. The objective is to provide an incentive to the participants to strictly follow the backoff algorithm and to detect stations that do not obey the protocol specifications.

Using the *rationality* assumption of game theory (i.e. that all participants seek to maximize their utility), we aim to create a game theoretic framework for the CSMA/CA backoff procedure and to answer the question whether it is possible to design an incentive scheme within that model that would allow for enforcement of protocol compliance. In other words, is it possible to design a game that has a unique Nash equilibrium such that it is in the nodes' best interest to strictly follow the specified procedure? If so, the player utilities in the game could be used as incentives to the wireless stations to enforce cooperation.

As previously noted, the participants in IEEE 802.11 backoff procedure are required to choose their backoff values uniformly at random over the entire backoff range. However, we also investigate protocols based on distributions differing from the uniform. Is it always possible to design games with a unique outcome regardless of the desired distribution? Are there any restrictions imposed by the number of participants or their strategies? What would be the effect on the network performance when alternative backoff schemes are used to detect and prevent selfishness? Would there be any negative impact on throughput, packet loss and packet delay?

Finally, we attempt to address scenarios when the rationality assumption is not satisfied. In practice it might not be feasible to implement an incentive scheme (as calculating equilibria might be a time and resource consuming process), or some nodes simply decide to behave selfishly regardless of the incentives they would be awarded. Therefore, we seek to create a selfishness detection scheme to identify greedy but not necessary rational nodes based on the choices of their backoff values. Are there some backoff protocols that are more amenable to detect such misbehavior?

1.4 Thesis contributions

In this thesis, we solve the problems discussed in Section 1.3. We first design a game-theory framework to be used as an incentive to protocol compliance. We also take a more practical approach to detect selfish misbehavior. In particular, we make the following contributions:

- We abstract the CSMA/CA backoff algorithm to a static game that models a single round of the media access procedure.

- We derive an *exact* condition based on the relationship between the cardinalities of the players' action sets that would make it possible to design a static game which exhibits a *unique* Nash equilibrium corresponding to a pre-specified full-support distribution profile.

- If the condition on the cardinalities of the players' strategies is not satisfied, we prove that it is impossible to create a game that has a unique full-support Nash equilibrium.

- When the condition is satisfied, we demonstrate how, based on the number of available actions for each player, to design a game that has a unique Nash equilibrium which corresponds to backoff scheme compliance in wireless networks.

- We propose a new backoff scheme, named XVBEB, that allows to deduce the backoff values of the participants based on the timeline of the channel access events (which is rarely possible in IEEE 802.11).

- We demonstrate how to perform sample validation on the backoff value choices of the participating stations in order to detect greedy misbehavior.

- We study the performance of XVBEB in a variety of aspects, such as saturation throughput, packet loss and packet delay, and show by simulations that it is similar or superior to IEEE 802.11.

  The results in Chapter 3 have been published in [GNS06] and [GNS08]. The work in Chapter 4 has been published in [GNS09]. The results in Chapter 5 have been published in [GN11] and in Chapter 6 in [GNA11].

1.5 Thesis outline

The rest of this thesis is organized as follows. In Chapter 2 we discuss some of the work related to our areas of research. In Chapter 3 we introduce a game-theoretic framework for an abstract version of the medium access contention resolution procedure and design games based on the number of players and their strategies that have a unique Nash equilibrium corresponding to cooperative behavior of the stations in wireless networks. In Chapter 4, we generalize these results by providing an exact condition under which it is possible to design such games. In Chapter 5 we propose XVBEB, a new backoff procedure, and illustrate how to detect misbehaving nodes when XVBEB is used. The performance of XVBEB is evaluated and compared against IEEE 802.11 in Chapter 6. Finally, some concluding remarks are made in Chapter 7.

Chapter 2

Related Work

There are three main research areas closely related to our work: game-theoretic and mechanism design approaches to ensure cooperation in wireless networks, selfish misbehavior detection and prevention in medium access schemes and performance evaluation of data link layer protocols. We survey the relevant literature in each of these three areas in the reminder of this chapter.

2.1 Game-theoretic and mechanism design approaches to accomplish cooperation in wireless networks

Game theory [Gib92, OR96] focuses on the interactions between individuals in competitive and cooperative situations. It aims to model and analyze the individual decision making in fundamentally strategic situations, where the outcome for the individuals not only depends on their decisions but also on what the other player will choose as a strategy. Two major categories are defined: *static* and *dynamic* games. In static games, all players make their moves simultaneously, whereas in dynamic the agents make their decisions based on the history of the game.

MacKenzie et al. [MW01] were the first to tackle the cooperation issue on the data link layer using game theoretic techniques. However, they analyzed a very limited model of Slotted Aloha assuming that each user knows how many backlogged packets there are in all other nodes. In [AEAJ03] the results in [MW01] are improved by analyzing a model of Slotted Aloha where nodes are not aware of other nodes' backlogged packet. It is shown that as the arrival probabilities increase, the behavior of the nodes becomes more aggressive resulting in deterioration of the system throughput. Also, the authors show that adding additional cost to the packet transmission could be used to improve the performance.

A game theoretic approach to analyze the problem in CSMA/CA protocols has been proposed in [CGAH05]. It is assumed that there are N static nodes willing to send data to N receivers (one per node) within the same communication range. The nodes always have packets (of the same size) to send. The presence of MAC layer authentication is another assumption. The players are assumed to be rational, and they try to maximize they payoff (throughput). Bianchi's model [Bia00] is used to measure the throughput and the access probabilities. The authors show, using both simulation and analysis, that in a game with single cheater the selfish node maximizes its utility (throughput) by minimizing his CW. Further, they look at a static game where all agents are cheaters. They show that there exist an infinite number of Nash equilibria and that normally the system will converge to a point where the nodes will receive zero payoffs. Another result is the existence of a Pareto optimal point of operation which is not a Nash equilibrium point. Using the theory of dynamic games, the authors design a distributed algorithm, and, by introducing a penalty function, they lead the cheaters to a desired Nash equilibrium. All nodes measure their own throughput and their neighbors' one. If someone's throughput is higher, this node is identified as misbehaving cheater. The punishment P_i for a misbehaving node should not affect any other player's payoff which could be achieved by selectively jamming player i's packets. After being punished, a node should run an adaptive strategy, meaning that a node should gradually increase its CW. One constraint is that the players must not use the penalization mechanism while running the adaptive strategy. According to the proposed mechanism, this will lead to a new Nash Equilibrium point. Finally, it is shown that the network could be brought to the Pareto optimal point of operation using a simple gradient search mechanism. Every cheater uses a random timer to increase its CW thus intentionally deviating from the current Nash Equilibrium.

Chen et al. [CCHD07] provide a general game theoretic framework for medium access control protocols. The medium contention is defined as a random access game where players' utilities are functions of their channel access probabilities. Finally, they design new classes of MAC protocols in efforts to achieve superior performance over 802.11.

Mechanism design [Par01, DNP03] is a branch of game theory that has been used to provide cooperation incentives in wireless networks mainly on the network layer. This field is concerned with the *design* of games in which the equilibrium strategy for all players represents a desired social outcome. In game theory, in general we know the strategies and the utilities available to each player, and the aim is to analyze the outcome for a given game. In mechanism design, on the other hand, we know the desired outcome, and the goal is to design utility function for the players such that their actions will represent the desired outcome.

One kind of mechanism that has been studied extensively is the VCG mechanism named after Vickrey [Vic61], Clarke [Cla71], and Groves [Gro73]. The typical property of the VCG based mechanism is that truth-telling is the dominant strategy for every player. Ad hoc-VCG [AE03] is a reactive routing protocol, which uses mechanism design techniques and is based on the VCG second best sealed bid auction. The network is represented as a directed graph where each has a weight representing the energy that a node has to spend in order to forward a packet on this edge. The mechanism calculates the shortest path based on energy cost. Using the VCG mechanism, a payment scheme is developed which stimulates the nodes to report their real costs. Two models are proposed. In the source model, the sender is willing to pay a premium to the intermediate nodes along the minimum cost path in addition to their true cost, and in the central-bank model, only the real cost is paid and a central authority maintains an account for each node. During the route discovery phase, the intermediate nodes append their types (forwarding costs) to the route request packets. Once the destination receives all the packets, it constructs the underlying graph, and after calculating the shortest path, it forwards a route reply packet, which is signed and contains the payment for each node, along this path. In the source model, during the data transmission, the sender will attach the payments to each data packet. In the central-bank model, the receiver records the amount of money the sender owes, which is eventually synchronized with the central authority. If a link along the path fails, a broken link message is sent to the source along the inverse path, and the sender initiates new route discovery. One of the main drawbacks of this algorithm is that some nodes may receive bigger amounts than what they normally should, which is termed as *overpayment*.

Sprite [ZCY03] is a system that provides incentive to mobile nodes to cooperate at the network layer using game theoretic tools to determine payment and charges. The source pays the intermediate nodes for the service they provide. Each node reports the packets it has forwarded to a central authority called Credit Clearance Service (CCS). Upon switching to a backup power and fast connection, each node uploads fingerprints of all forwarded messages called receipts. The authors show that each node is motivated to report its receipts honestly. Although this paper is motivated by algorithmic mechanism design, the information held by each player is not totally private, so this work does not fit exactly into the mechanism design framework.

The mechanism design problem for dynamic systems is termed *online* mechanism design. In [FP03], the authors consider the problem of designing mechanisms for problems when agents arrive and depart over time. They show how the results of the mechanism design field can be extended to the online problem. A specific example is examined where wireless access is shared among transient users who have to pay for the service. The wireless network can serve only limited number m of nodes simultaneously. Each agent has a valuation, and a VCG pricing scheme is developed such that it is in each player's interest to report its highest valuation. The scheme allows a node to claim later arrival time hoping that the price will drop due to subsequent departures or arrivals of other users. The authors show that when the valuations remain constant (over time), the online auction is equivalent to a series of $(m+1)$'st price auctions. The main problem in the online version is how to calculate the pricing in a timely fashion.

None of the strategies above seek to provide incentives to the wireless stations to follow the protocol specifications. Our approach is to design a utility scheme such that the unique best strategy for all players would be protocol compliance.

2.2 Selfishness detection and prevention for medium access protocols

As discussed in the previous section, the game-theoretic techniques have been rarely used to prevent selfish behavior at the medium access layer. There has been, however, considerable interest in the problem of selfishness detection and prevention at this layer. The approaches taken thus far fall into two general categories: protocol modification and reputation-based (punishment) schemes. The reputation-based schemes aim to detect misbehaving nodes and sometimes isolate them from the network activity, which is less desirable especially in ad-hoc environments, where isolating some nodes could result in a partitioned network.

2.2.1 Protocol modification schemes

Konorski [Kon01] and [Kon02] suggested new backoff algorithms resilient to selfish behavior. Stations send packets in bursts. The competition for channel access goes through several elimination and reaction burst cycles until a winner is elected who resumes its packet transmission. The proposed packet scheduling policies aim to converge the network to a fair and efficient Nash equilibrium.

A scheme trying to detect selfish misbehavior in IEEE 802.11 is proposed in [KV04]. The suggested solution modifies the 802.11 protocol specifications, assuming that the receivers are well-behaving nodes. In 802.11 the sender has the responsibility to choose its backoff value; instead, the authors assign this role to the receiver, which encapsulates this value in the CTS packet. If the sender tries to deviate from the assigned value, the receiver will detect this behavior and will add a penalty to the next backoff value, which will increase the possibility of detecting misbehavior. When the deviation reaches a certain threshold, the node is identified as misbehaving.

Lolla et al. [LLK+06] proposed a solution for the backoff value deduction problem in IEEE 802.11. Due to the nature of IEEE 802.11, in the presence of collisions it is impossible to know what are the backoff value choices of the participants. To overcome this problem, each station must include information in the RTS/CTS packets about the state of its pseudo-random sequence generator, which will allow the other nodes to estimate a sequence of expected future backoff values of the transmitting node and later compare whether the observed behavior complies with the expected sequence.

2.2.2 Detection schemes

The watchdog scheme [MGLB00] detects misbehaving nodes using a passive acknowledgment scheme. A node B, after forwarding a packet on behalf of node A to a node C, will expect C to retransmit the packet further. Due to the broadcast nature of the wireless links, in most cases B will overhear when C relays the packet to D thus allowing detection of misbehavior. The main weakness of this approach is that there are situations when B will not overhear the packet retransmission (collisions, different transmission ranges, etc). The pathrater component combines knowledge of misbehaving nodes with link reliability to choose reliable paths.

In efforts to overcome the watchdog's weaknesses, Djenouri et al. [DB05] suggest a two-hop active acknowledgment scheme. This method does not rely on passive ACKs; rather, node D will send back an encrypted message to B confirming that C has forwarded the packet. An obvious drawback of this scheme is the generated overhead. To overcome this problem, the authors propose a random two-hop ACK scheme, where ACKs are only required on randomly selected packets.

CORE [MM02] is a reputation-based scheme which extends watchdog using three different types of reputations: subjective, indirect, and functional. Subjective reputation is based on the node's direct observations, indirect is provided by other nodes, and functional is calculated from subjective and indirect reputations with respect to various functions.

DOMINO [RHA04] is a system which aims to detect MAC layer misbehavior while trying to remain transparent to the network operations. DOMINO could be implemented for example on an access point to monitor the behavior of the participants. It periodically collects nodes' behavior data, which is analyzed to detect potential misbehavior. DOMINO's measurements are based on several metrics as it tries to address several misbehaving issues such as scrambling the frames of other stations, NAV oversizing and backoff manipulation. The main drawback in terms of the backoff manipulation detection component is that it does not work in the presence of collisions, as it is impossible to make deductions for the station's backoff values.

Sequential probability ratio test (SPRT) is used in [RLC06] to detect misbehavior based on the throughput degradation monitored at a normally behaving station.

Another statistical approach is developed in [RBK05] using minimax robust detection approach. The performance of DOMINO and SPRT is compared in [CRB09]; in addition, the authors propose a more realistic framework for the SPRT test.

We propose a minor modification to IEEE 802.11 called XVBEB that allows us to deduce the backoff values of a wireless station even in the presence of collisions. XVBEB differs from IEEE 802.11 only in the way the nodes choose their backoff values. We also show how to determine whether the station is misbehaving based on its backoff value choices.

2.3 Performance evaluation of data link layer protocols

Saturation throughput of IEEE 802.11 networks was thoroughly analyzed using Markov chains for the first time in [Bia00]. Bianchi showed that as the channel offered load increased, the throughput increased to a certain maximum value, but then decreased to stabilize at the saturation value. Under the key approximation that each packet collides with constant and independent probability, the backoff procedure in IEEE 802.11 is modeled as a Markov stochastic process to obtain the transmission probability of a node as a function of the collision probability and the size of the contention window. Finally, a formula for the saturation system throughput is derived as a function of the transmission probability and the number of nodes, which enables the calculation of the value of the contention window to optimize the system throughput providing information for the number of participating nodes is available.

Much of the work that followed focused on enhancing the model presented in [Bia00]. In [WPL+02], the authors incorporated in the model the fact that a packet is dropped after several retransmission attempts, as defined by the short or the long retry counters in IEEE 802.11. In contrast, Bianchi's model incorporates a behavior where a packet stays in the queue until it is successfully transmitted.

Wang et al [WCLH05] broadened the model to mixed (IEEE 802.11b and IEEE 802.11g) networks. They proposed a hybrid Markov chain to evaluate the saturation throughput in heterogeneous IEEE 802.11 environments.

In [ZA02] the busy medium conditions that invoke the backoff algorithm are incorporated into the the Markov chain. In addition, an analytical model for delay analysis again based on the Markov chain model.

He et al. [HP06] extended the model to multihop networks using 3-dimensional Markov chains. It is assumed that the nodes are randomly situated according to a two-dimensional Poisson distribution with density as a parameter.

A fair backoff algorithm has been proposed in [FBW02], where each station continuously estimates its throughput and the aggregate throughput of the other nodes in its range. The station adjusts its contention window based on a fairness index based on its own throughput and the throughput of its neighbors.

In [MN07], the authors present an alternative backoff scheme aiming to reduce the number of collisions by choosing uniformly at random from the second half of the contention window range (instead of the entire backoff range) in the lower backoff levels. It is also claimed that this backoff procedure provides better performance in terms of packet delivery variation.

All of the performance evaluation work in listed this section is based on the backoff scheme using the uniform distribution used in IEEE 802.11. We, however, model and evaluate the performance of the XVBEB scheme and compare it against the performance of IEEE 802.11.

Chapter 3

On Games that Induce Unique A Priori Specified Nash Equilibria

In this chapter, we introduce a game-theoretic framework to analyze medium access protocols, more specifically the CSMA/CA backoff procedure. We first note that the medium access contention backoff procedure, in its full generality, corresponds naturally to realizing a *dynamic* game; the nodes can (and do) modify their actions in response to the outcome of previous rounds. We begin by studying a simpler abstraction: games that model *a single round* of the media access problem.

Thus, a static version of the cooperation problem in wireless networks is modeled as a strategic game played by non-cooperating, rational players (the stations). Our objective is to design a game which exhibits a *unique*, *a priori* specified mixed-strategy Nash equilibrium. In the context of the simplified media access problem, the game, if correctly implemented, would correspond to nodes choosing backoff times randomly from a given range of values, according to the given distribution, which would ensure protocol compliance. We consider natural variations of the problems concerning the number of actions available to the players and show that it is possible to design such a game when there are at least two players that each have the largest number of possible actions among all players.

Indeed, IEEE 802.11 can be abstracted as k stations (the players) competing for access to the shared wireless medium using a backoff protocol where the j^{th} node *should* choose a backoff value *uniformly at random* from a range given $[1, n_j]$ (the contention window). Our goal is to design the corresponding game, *i.e.* to specify utility functions for the players that would induce a *unique* mixed strategy Nash equilibrium which corresponds *exactly* to each player faithfully following the protocol, *viz.* choosing a backoff value uniformly at random. We stress here that it is not difficult to construct a game with a mixed strategy Nash equilibrium that corresponds to the uniform distribution (or indeed, any other distribution); the challenge lies in ensuring that this equilibrium is *unique* and not just one among many possible equilibria, so that rational play automatically leads to protocol compliance.

Hence, we start with the presumption that we are given an *a priori* distribution profile α^* (for example, the uniform distribution in the case of IEEE 802.11). We wish to *design* a strategic game that realizes *exactly* this distribution as its unique mixed-strategy Nash equilibrium. In this chapter, we show that this is possible when there exist at least two players with the largest number of actions; we arrive at this result by generalizing the construction of a game achieving a desired equilibrium distribution among players with exactly the same number of actions.

3.1 Preliminaries

For any fixed positive integer m, let $[1, m]$ denote the set of integers $\{1, 2, \ldots, m\}$. We shall be concerned with two such sets that arise in our strategic games:

- A finite ordered set of $k \geq 2$ players, $P = [1, k]$.

- A finite set of $n_j \geq 1$ possible actions (or strategies), $A_j = [1, n_j]$, for each player $j \in P$.

We use the terminology **profile** for an ordered tuple that is typically indexed by an index set such as P. Following standard game-theoretic notation, an **outcome** of the game is represented by an *action profile*, $s = (i_j)_{j \in P}$, with the interpretation that every player $j \in P$ performs the corresponding action $i_j \in A_j$ in the outcome. The space of all possible outcomes is denoted by S.

A **utility function** is a function $u : A_1 \times A_2 \times \ldots \times A_k \to \mathbb{R}$ that associates the real value $u(s)$ with the action profile s. Every player has its own utility function. Collectively, the *utility function profile*, $(u_j)_{j \in P}$ is interpreted as follows: for any action profile s, the corresponding utility profile for the players is simply $(u_j(s))_{j \in P}$. We assume rational players that play independently (without any collusion) but seek to maximize their respective utilities, *i.e.* a player will always prefer an action $a \in A_j$ over some other action $b \in A_j$ if the corresponding utility is strictly higher.

We briefly review the notion of Nash equilibria for our games; for details, the reader is referred to Osborne and Rubinstein [OR96]. Given an action profile s, we denote by s_{-j} the partial profile containing the actions in s for all players except player j. For any player j and any partial profile s_{-j}, the set

$$B_j(s_{-j}) = \{a \in A_j : u_j(s_{-j}, a) \geq u_j(s_{-j}, b) \text{ for all } b \in A_j\}$$

is the set-valued **best-response function** for player j. A **pure strategy Nash equilibrium** is a specific action profile

$$s^* = (a_j^*)_{j \in P}$$

such that all the individual actions in s^* are *simultaneously* best responses for the players with respect to the corresponding partial action profiles. More formally, it is the case that for every $j \in P$:

$$u_j(s^*) \geq u_j(s^*_{-j}, b) \quad \text{for every } b \in A_j$$

where (s^*_{-j}, b) is the action profile obtained from s^* by replacing the component action s_j^* with the action b. Intuitively, players cannot gain any utility by *unilaterally* changing their equilibrium actions.

Not all finite games necessarily have pure-strategy Nash equilibria. However, they must have **mixed strategy Nash equilibria** which generalize pure-strategy Nash equilibria. For a player $j \in P$, a **mixed strategy**, α_j, is a *discrete probability distribution* over its action set A_j. One interpretation of a mixed strategy is that the player j chooses any action $a \in A_j$ independently with the corresponding probability $\alpha_j(a)$. In particular, note that every outcome (*i.e.* action profile) of the game corresponds to a degenerate mixed strategy in which every player assigns probability

1 to its action in the outcome.

Collectively, the mixed strategies of all the players constitute a *distribution profile*, $\alpha = (\alpha_j)_{j \in P}$ with the following interpretation of utilities:

- Player j's utility for any particular pure strategy $a \in A_j$ is the expected value of the utility function u_j conditioned on the event that player j chooses strategy a. Let $U^j_\alpha(a)$ denote this expected value.

- Player j's overall utility for distribution profile α is given by

$$u_j(\alpha) = \sum_{a \in A_j} \alpha_j(a) U^j_\alpha(a) \quad (1)$$

We say an action $a \in A_j$ is in the *support* of a mixed strategy α_j for player j if $\alpha_j(a) > 0$. Furthermore, we say that $\alpha = (\alpha_j)_{j \in P}$ is a *full-support* distribution profile if for every player $j \in P$, the support of the distribution α_j is the entire action set A_j, *i.e.* $\alpha_j(a) > 0$ for all $j \in P, a \in A_j$. In this thesis, we will be exclusively interested in full-support distribution profiles as actions that have zero probability in an equilibrium profile could as well be omitted from consideration.

A *mixed-strategy Nash equilibrium* is a special distribution profile, $\alpha^* = (\alpha^*_j)_{j \in P}$, with the property that a player *cannot* increase its (expected) utility by unilaterally changing its own distribution in the profile. In other words, every player's mixed strategy at equilibrium is a best response to the mixed strategies of the other players. We have assumed a finite set of actions for each player. This allows us to use a very useful alternative characterization of a mixed-strategy Nash equilibrium α^*:

We make extensive use of an alternative characterization of any *full-support* Nash equilibrium:

Lemma 3.1.1. *A distribution profile, $\alpha^* = (\alpha_j^*)_{j \in P}$, is a full-support Nash equilibrium if and only if for every player P_j, all its actions have exactly the same expected utility under α^*.*

We do not provide a proof of this characterization; the interested reader is referred to Lemma 33.2 in [OR96] for details.

3.2 Designing games with identical player strategies

We first consider the situation where players have the same set of actions, $A = [1, n]$. We will use the index set $P = [1, k]$ for the players[1]. Suppose that we have an *a priori* known full-support distribution profile $\alpha^* = (\alpha_j^*)_{j \in P}$. We are interested in the following general question: is it possible to design a strategic game with a *unique* Nash equilibrium that is given by the profile α^*? In what follows, we will construct such a game.

For ease of description, we will treat both the index sets P and A as being *circularly ordered*, *i.e.* with player $k+1$ being interpreted as player 1, with action $n+1$ being interpreted as action 1 and so on. We design our game with the following property:

[1] In principle, players need not have exactly the same set of actions; what matters is that they have the *same number* of possible actions.

> The utility function for player $j \in P$ depends only on its own actions and those of its predecessor, player $j-1$.

This property allows us to present the game using an abbreviated version of the usual strategic form of presentation. Kearns *et al.* study a graphical representation of games where each player is represented by a node and a utility matrix, and the utility to a player i is affected only by the actions of player i and its neighbors in the underlying undirected graph [KLS01]. The game presented in this section is a graphical game but for a *directed* simple cycle on k nodes/players numbered from 1 through k: for every node/player i, there is a directed edge from i to node/player $(i+1)$ with $k+1$ interpreted as 1.

The utility function u_j for each player $j \in P$, can be represented concisely by a two dimensional matrix M_j with n rows and n columns. The interpretation of this matrix is as follows: $M_j(a, b)$ is the value of the utility function u_j when applied to *every action profile* s in which player $j-1$ performs action b and player j performs action a. Thus, one thinks of the rows of M_j as being indexed by the pure strategies of player j and the columns of M_j as being indexed by the pure strategies of player $j-1$.

For ease of description, the entries in matrix M_j can be specified over two steps. Let I_n be the identity matrix with n rows and columns. Consider the following matrix, V_n, obtained from I_n by shifting down (circularly) the rows of I_n:

$$V_n := \begin{bmatrix} 0 & \dots & 0 & 1 \\ 1 & \dots & 0 & 0 \\ & \dots & & \\ 0 & \dots & 1 & 0 \end{bmatrix} \tag{2}$$

For every player $j \in P$, an intermediate matrix $\hat{M}_j$ is defined as follows:

$$\hat{M}_j = \begin{cases} V_n & \text{if } j = 1 \\ I_n & \text{otherwise} \end{cases} \tag{3}$$

Now, let $\alpha^* = (\alpha_j^*)_{j \in P}$ be the desired unique mixed strategy equilibrium profile. Then, the utility matrix M_j for player $j \in P$ is defined as follows. Recall that the columns of M_j correspond to actions of the previous player $j - 1$ in the circular ordering of P. For any pair of actions $a, b \in A$, we have

$$M_j(a, b) = \hat{M}_j(a, b)/\alpha_{j-1}^*(b) \tag{4}$$

In other words, we obtain M_j from $\hat{M}_j$ by *scaling* each entry by the reciprocal of player $(j - 1)$'s column probability for that column. Note that the matrices are well-defined since we have assumed that α^* is a full-support distribution profile and therefore, the probability in the denominator of (4)'s right-hand side is always non-zero. We will now establish that the game defined above has a *unique* Nash equilibrium where player j chooses *exactly* the corresponding desired mixed strategy α_j^*.

Consider any mixed strategy, $\alpha = (\alpha_j)_{j \in P}$, for the game. Under this mixed strategy, player j's expected payoff for an action a is easily shown via (4) to be:

$$U^j_\alpha(a) = \begin{cases} \alpha_k(a-1)/\alpha^*_k(a-1) & \text{if } j = 1 \\ \alpha_{j-1}(a)/\alpha^*_{j-1}(a) & \text{otherwise} \end{cases} \tag{5}$$

Specifically, for the case when $\alpha = \alpha^*$, the right hand side is identically equal to 1 for *all actions of all the players* thus establishing that every player has equal payoffs for all its pure actions under distribution profile α^*. Thus, α^* is indeed a mixed strategy Nash equilibrium for the game. It remains to show that this equilibrium is unique. We start with a useful definition specific to our game.

Definition Let $\alpha = (\alpha_j)_{j \in P}$ be a mixed strategy profile that *differs* from α^*. For a given action a and player j, let $r_j(a) = \alpha_j(a)/\alpha^*_j(a)$. We say that action a is *α-deficient* for player j if $r_j(a) < 1$.

Lemma 3.2.1. *Suppose that the profile $\alpha = (\alpha_j)_{j \in P}$ is a mixed strategy Nash equilibrium for the game. Then, the following implications hold:*

(A) *If action a is α-deficient for player k, then $\alpha_1(a+1) = r_1(1) = 0$.*

(B) *For $1 \leq j < k$, if action a is α-deficient for player j, then $\alpha_{j+1}(a) = r_{j+1}(a) = 0$.*

Proof. Let α be a Nash equilibrium for the game. To prove the first implication (Lemma 3.2.1(A) above), assume that the hypothesis holds. Both α_k and α^*_k being probability distributions, $\sum_{b \in A} \alpha_k(b) = 1 = \sum_{b \in A} \alpha^*_k(b)$ and from this it

	Players			
Actions	1	2	...	k
a				$\odot$
$a+1$	0			

(A)

	Players						
Action	1	2	...	j	$j+1$	...	k
a				$\odot$	0		

(B)

Figure 6: Implications for r values in Lemma 3.2.1

follows that since $r_k(a) < 1$, then there must be another action $b \neq a$ for which $r_k(b) > 1$.

Applying (5) above with $j = 1$, we conclude that under the mixed strategy α, player 1 will have a strictly larger payoff for playing the pure strategy $b + 1$ as compared to playing the pure strategy $a + 1$. Consequently, action $a + 1$ cannot be in the support of the equilibrium strategy α_1 for player 1, and hence, $\alpha_1(a+1) = 0$ (which, in turn, implies that $r_1(a+1) = 0$). An almost identical argument works for the second part of the lemma except that we use (5) for the case when $1 < j \leq k$. Figure 6 is a schematic illustration of these implied dependencies among relevant r values for the players. □

Theorem 3.2.2. *The game outlined above is a* k*-player,* n*-strategy game that has the unique mixed strategy Nash equilibrium given by the full support distribution profile* $(\alpha_j^*)_{j \in P}$.

Proof. We have already shown that α^* is a Nash equilibrium for the game. To establish uniqueness, we will show that assuming a different equilibrium profile, $\alpha \neq \alpha^*$, yields a contradiction. Figure 6 (based on Lemma 3.2.1) provides the intuition for this: it shows that if an action a is α-deficient for a player j then so is action a for player $j+1$, except in the case when $j = k$ and then it is action $a + 1$

that is α-deficient for player 1.

More formally, let $\alpha \neq \alpha^*$. Then there must be some player j for whom there is an action a that is α-deficient. If player j is someone other than player k (*i.e.* where $1 \leq j < k$), then Lemma 3.2.1(B) implies that $\alpha_{j+1}(a) = 0$. In fact, we can apply Lemma 3.2.1(B) to obtain that $r_j(a) < 1$ implies $a_{j+1}(a) = 0$ and therefore $r_{j+1}(a) = 0 < 1$. By the same reasoning and by repeatedly applying Lemma 3.2.1(B), we obtain that $\alpha_i(a) = 0, \ \forall i \in \{j+2, k\}$. Thus we deduce that player k must have an α-deficient action if α differs from α^*.

Without loss of generality, let a be an α-deficient action for player k such that action $a+1$ is *not* α-deficient for player k, *i.e.* with $r_k(a+1) \geq 1$. Now, Lemma 3.2.1(A) applies, and we get $\alpha_1(a+1) = 0$. Thus, action $(a+1)$ is α-deficient for player 1 and by applying Lemma 3.2.1(B) in succession $(k-1)$ times, we conclude that $\alpha_k(a+1) = 0$ (see Figure 6). This contradicts our earlier assertion that action $a+1$ is not α-deficient for player k. Thus, contrary to assumption, α cannot differ from α^*; the game exhibits the unique Nash equilibrium profile α^*. □

We note that Theorem 3.2.2 can be easily specialized to the case that is relevant for the single round version of the medium access control problem, with all backoff values in the range $[1, n]$ and the desired distribution being the discrete uniform distribution for all players.

3.3 Designing games with non-identical player strategies

In this section, we consider games where the players do not have the same number of strategies available to them, but we still wish to achieve a target distribution profile that is a unique Nash equilibrium with full-support component distributions.

We first show how such a game can be designed if the players can be partitioned into groups where each group contains at least two players having the same number of actions. More generally, we show that it suffices to have at least two players that have the maximum number of actions among all players; under this condition, a given profile is realizable as the unique Nash equilibrium of an appropriately designed game.

From now on, we will assume that when a given distribution profile is to be realized, we limit the set of actions for any player to be exactly those actions that are in the support of the component that corresponds to the player's distribution. A simple corollary of Theorem 3.2.2 gives us the following result.

Theorem 3.3.1. *Consider a set of players* P *that can be partitioned into subsets* $P_1, P_2, \ldots, P_m$ *where* $|P_j| > 1$ *for all* $1 \leq j \leq m$*. If the set of strategies for all players in subset* P_j *is* $[1, n_j]$*, then for any given full-support, distribution profile* α^**, there exists a game whose unique Nash equilibrium is the profile* α^**.*

Proof. We note that the case when the number of groups m equals 1 is the case handled by Theorem 3.2.2. More generally, let $|P_1| = k_1 > 1$. Then we create utility matrices for the players in set P_1 according to the k_1-player, n_1-strategy game in Theorem 3.2.2. Similarly we create utility matrices for the players in each subset

P_j. Thus the utility for any player in P_j depends only on a single other player within the same subset P_j; the game is essentially partitioned into disjoint games - one for each subset of players, P_j. The topology of the graph corresponding to this game is a set of m disjoint cycles, each cycle corresponding to a set of players P_j. It is straightforward to see that the game represented by these utility matrices realizes the target profile as its unique Nash equilibrium. □

The conditions in the above theorem can be relaxed. We show that so long as there are at least *two* players with the (same) *largest* number of strategies, we can create a game corresponding to any *a priori* given, full-support distribution profile α^*. Our basic idea is to create utility matrices so that player j's utilities depend on the actions chosen by player $j-1$ and player k.

Consider the players arranged in non-decreasing order of the number of actions available to them. Let n_j be the number of actions available to player j. Then $n_{k-1} = n_k$; the last two players have the same number of actions. For the remaining players, we will make the simplifying assumption that for all $j \in [1, k-2]$, $n_j < n_{j+1}$. It will be obvious from the construction how this assumption can be relaxed [2]. The game itself is specified over two stages starting with unscaled utility matrices which will subsequently be scaled appropriately in a second stage. For convenience, we will assume that $n_0 = 0$ henceforth.

In the first stage, we will represent the utilities for j as simple unscaled matrices with player j's actions represented by the rows. Recall that for any $n \geq 1$, I_n is the identity matrix with n rows and n columns. The utility matrices are described

[2] Alternatively, if there are two or more players that have the same number of strategies, we can deal with this set of players in isolation using Theorem 3.3.1.

below:

- Player 1's utilities only depend on player k's actions; the utility matrix (unscaled) is:

$$\hat{M}_1 = [V_{n_1} \mid 0]$$

where V_{n_1} is the identity matrix with its rows shifted down once (circularly). The 0 sub-matrix corresponds to actions $n_1 + 1, \ldots, n_k$ of player k.

- Player k's utilities only depend on player $(k-1)$'s actions; the utility matrix (unscaled) is:

$$\hat{M}_k = I_{n_{k-1}}$$

Note that $n_{k-1} = n_k$.

- For every other player j (hence, $2 \le j \le (k-1)$), the utilities depend both on player k as well as the previous player $(j-1)$. We represent the utilities as separate $(n_j \times n_{j-1})$ matrices for each of the actions $1, \ldots, n_k$ of player k. The matrices are divided into three groups; each matrix has an *upper sub-matrix* consisting of the first n_{j-1} rows and a *lower sub-matrix* consisting of the remaining $(n_j - n_{j-1})$ rows:

– For player k's action $a \in [1, n_{j-2}] \cup [n_j + 1, n_k]$, the matrix is:

$$\hat{M}_j^a = \left[\begin{array}{cccc} \multicolumn{4}{c}{I_{n_{j-1}}} \\ \hline 0 & 0 & \dots & 1 \\ & & \dots & \\ 0 & 0 & \dots & 1 \end{array}\right]$$

Every row in the lower sub-matrix is identical, and equals $[0,\ 0, \dots,\ 1]$, the last row of the identity sub-matrix.

– For player k's action $a \in [n_{j-2} + 1, n_{j-1}]$, the matrix is:

$$\hat{M}_j^a = \left[\begin{array}{cccc} \multicolumn{4}{c}{I_{n_{j-1}}} \\ \hline x_j & x_j & \dots & 1 + x_j \\ & & \dots & \\ x_j & x_j & \dots & 1 + x_j \end{array}\right]$$

Every row in the lower sub-matrix is identical, and equals $[x_j,\ x_j, \dots,\ 1 + x_j]$ for a value $x_j > 0$ to be determined later.

– Let $y_j > 0$ be a value to be determined. For action $(n_{j-1} + i)$ of player k, with $i \in [1, n_j - n_{j-1}]$, the corresponding matrix is:

$$\hat{M}_j^{n_{j-1}+i} = \left[\begin{array}{c} I_{n_{j-1}} \\ \hline C_{i,j} \end{array}\right]$$

where $C_{i,j}$, the lower sub-matrix, has as its ith row, the row vector

$$[-(1 + y_j),\ -(1 + y_j), \dots,\ -(1 + y_j),\ -y_j],$$

and whose remaining rows are all identically equal to the row vector

$$[-y_j, \ -y_j, \ldots, \ -y_j, \ 1-y_j]$$

As before, we obtain the actual utility matrices by scaling the above matrix entries by the reciprocals of the α^*-probabilities of the actions of the relevant players that influence any given entry. Thus, for instance, the scaled matrix M_j^a for any player $j \in [2, k-1]$, is obtained from the corresponding unscaled matrix $\hat{M}_j^a$ by multiplying each entry in column b by

$$\frac{1}{\alpha_{j-1}^*(b)\alpha_k^*(a)}$$

and so on. The scaled utility matrices define our game. The topology of the graph corresponding to this game is a directed cycle on k nodes, with additional edges from node k to every node in $[2, k-2]$.

Suppose that the players use a distribution profile α for their mixed strategies. As usual, let $r_j(a) = \alpha_j(a)/\alpha_j^*(a)$ be the ratio of the actual probability to the desired one for action a by player j. Some more notation comes in handy when describing various expected payoffs. Let $B_j = [n_{j-1}+1, \ n_j]$ denote the jth *block* of actions (recall that $n_0 = 0$). For any player $m \geq j$, we let

$$R_m^j = \sum_{a \in B_j} r_m(a)$$

denote the sum of the r_m values over the B_j-actions. Also, for any player j, the sum of its ratios over *all* its actions is given by

$$R_j = \sum_{a \in [1, n_j]} r_j(a).$$

Let us calculate the expected payoffs for player j when the players use mixed strategy profile α. Then, the payoffs are as follows.

1. For player 1, the expected payoff for action $a \in [1, n_1]$ is

$$U^1_\alpha(a) = \begin{cases} r_k(a-1) & \text{when } 1 < a \leq n_1 \\ r_k(n_1) & \text{when } a = 1 \end{cases} \tag{6}$$

2. For player k, the expected payoff for action $a \in [1, n_k]$ is

$$U^k_\alpha(a) = r_{k-1}(a) \tag{7}$$

3. For every other player $j \in [2, k-1]$, it follows from the construction above that for an action $a \in [1, n_{j-1}]$, the identity sub-matrix (the upper sub-matrix) determines the expected payoff which is simply

$$U^j_\alpha(a) = r_{j-1}(a)R_k \tag{8}$$

since the sub-matrix is repeated for all actions of player k. Next, consider the payoff for action $n_{j-1} + i$ of player j; this action corresponds to the ith row of each of the lower sub-matrices in the three groups. The respective contributions from the three groups of matrices appear below on separate lines in the expression for the expected payoff:

$$
\begin{aligned}
U^j_\alpha(n_{j-1}+i) = r_{j-1}(n_{j-1})[R_k - R_k^{j-1} - R_k^j] \\
+ R_k^{j-1}[x_j R_{j-1} + r_{j-1}(n_{j-1})] \\
- y_j R_{j-1} R_k^j - R_{j-1} r_k(n_{j-1}+i) + R_k^j r_{j-1}(n_{j-1})
\end{aligned}
\tag{9}
$$

We now proceed to show that for appropriate values of x_j and y_j in the matrices above, the profile α^* is the unique Nash equilibrium for this game. Note that if the players use mixed strategy profile α^*, then every ratio $r_j(a)$ equals 1 and hence, by construction, the expected payoffs (under strategy α^*) for players 1 and k also equal 1 regardless of the action played.

For player $j \in [2, k-1]$, the payoff for any action in the upper sub-matrices is equal to $R_k = n_k$ from Equation (8) since all ratios are 1. Observing Equation (9), we can see that the contributions from all three groups of lower sub-matrices are independent of the action $n_{j-1}+i$ when the ratios are equal to 1; the net payoff, on simplification, can be seen to be

$$
U^j_{\alpha^*}(n_{j-1}+i) = n_k + x_j n_{j-1}(n_{j-1} - n_{j-2}) - y_j n_{j-1}(n_j - n_{j-1}) - n_{j-1}
$$

Hence, equating the payoff for the upper sub-matrix actions to the right hand side of the above equation gives us the following necessary and sufficient relationship between x_j and y_j *for* α^* *to be a Nash equilibrium*:

$$
x_j(n_{j-1} - n_{j-2}) = y_j(n_j - n_{j-1}) + 1 \tag{10}
$$

We can always choose $x_j, y_j > 0$ to ensure that Equation (10) holds, *e.g.* when

$x_j = 1$ and $y_j = (n_{j-1} - n_{j-2} - 1)/(n_j - n_{j-1})$.

Having established that α^* is a Nash equilibrium profile for our game for appropriate choices of x_j and y_j values as above, we now turn our attention to showing that the equilibrium is unique. We approach this in a spirit similar to that in Section 3.2, *i.e.* we first show that it suffices to consider distributions that differ in probability from the given distribution α^* for some actions of player k, and then show that this will lead to a contradiction.

Assume that our game has a Nash equilibrium α that differs from α^*. Recall that by definition, the action a for any player j is α-deficient if and only if the ratio $r_j(a) = \alpha_j(a)/\alpha_j^*(a)$ is less than 1.

Lemma 3.3.2. *Suppose that the profile $\alpha = (\alpha_j)_{j \in P}$ is a mixed strategy Nash equilibrium for the game. For $1 \leq j < k$, if action a is α-deficient for player j, then $\alpha_{j+1}(a) = 0$.*

Proof. The proof is very similar to that of Lemma 3.2.1(B). If action a is α-deficient, then there must be another action b that is not α-deficient for player j. Hence, the expected utility to player $j+1$ for action b will dominate the utility for action a via Equation (8) above. Hence, if α is an equilibrium profile, it will assign zero probability to action a for player $j+1$. □

Now, repeated applications of Lemma 3.3.2 allow us to conclude that a purported Nash equilibrium α that differs from α^* must witness some α-deficient action a for player k. In turn, this implies that player k has at least one action b for which $r_k(b) > 1$. Let A_d be the proper subset of $[1, n_k]$ that contains all the α-deficient actions for player k. We denote by $\bar{A_d}$, the complement of A_d in the set $[1, n_k]$.

Recall that $B_j = [n_{j-1}+1,\ n_j]$ is the jth block of actions (with $n_0 = 0$ tacitly). We have two exclusive (and exhaustive) cases to consider:

1. Within some block B_j of player k's actions, there is at least one action from each of the sets A_d and $\bar{A}_d$. Without loss of generality, let a and $a+1$ be a pair of consecutive actions (circularly within block B_j) such that $a \in A_d$ and $a+1 \in \bar{A}_d$. Then

$$r_k(a) < 1 \leq r_k(a+1)$$

by definition. Let us examine the difference in payoffs between actions $a+1$ and a for player j. From Equation (9), we observe for all actions within block B_j, only the contributions from the third group of utility matrices for player j differ. In fact, for consecutive actions like a and $a+1$, it is only the matrices corresponding to actions a and $a+1$ for player k that differ in their contribution. Upon simplification, we see that

$$\begin{aligned} U^j_\alpha(a) - U^j_\alpha(a+1) &= R_{j-1}[r_k(a+1) - r_k(a)] \\ &> 0 \end{aligned}$$

since R_{j-1} is positive and $r_k(a+1) > r_k(a)$ by assumption. Consequently, if α is a Nash equilibrium profile as claimed, it will yield $\alpha_j(a+1) = 0$. By repeatedly applying Lemma 3.3.2, we obtain the fact that $\alpha_k(a+1) = 0$ which contradicts the assumed non-deficiency of action $a+1$ for player k.

2. Every block of actions for player k either contains only actions from A_d or only actions from $\bar{A}_d$. Then there must be consecutive blocks B_{j-1} and B_j (in

circular order of the blocks) such that block B_{j-1} contains only A_d-actions and block B_j contains only $\bar{A}_d$-actions or vice-versa. Without loss of generality, consider the first possibility. Then by assumption, action n_{j-1}, the last action in block B_{j-1}, is deficient while action $n_{j-1}+1$, the first action in block B_j is not deficient. We now compare the expected payoffs for player j for these two actions. Observing Equation (9), we see that while the first group of matrices do not contribute to any difference in payoffs, the latter two groups do provide non-zero contributions. Since block B_{j-1} is entirely deficient for player k, it must be the case that

$$\begin{aligned}
R_k^{j-1} &= \sum_{b \in B_{j-1}} r_k(b) \\
&< \mid B_{j-1} \mid \\
&= (n_{j-1} - n_{j-2})
\end{aligned}$$

Similarly, $R_k^j \geq (n_j - n_{j-1})$ and $r_k(n_{j-1}+1) \geq 1$ since block B_j is assumed to be wholly non-deficient.

Putting these inequalities together, we can simplify and show that for action $a = n_{j-1}$

$$\begin{aligned}
U_\alpha^j(a) - U_\alpha^j(a+1) &= R_{j-1}[y_j R_k^j + r_k(n_{j-1}+1) - x_j R_k^{j-1}] \\
&> R_{j-1}[y_j(n_j - n_{j-1}) + 1 - x_j(n_{j-1} - n_{j-2})] \\
&= 0
\end{aligned}$$

where the last step above follows directly from Equation (10) that holds for

Actions	Players j	$j+1$	...	k
$n_{j-1}+1$	$\star$	$\star$	...	$\star$
...	...	...	...	...
n_j	$\star$	$\star$	...	$\star$

Block B_j with $1 \leq j \leq k-1$

Figure 7: Dependencies for r values in various blocks

the chosen values of x_j and y_j. Again, we conclude first that $\alpha_j(a+1) = \alpha_j(n_{j-1}+1) = 0$ and hence, that repeated applications of Lemma 3.3.2 imply $\alpha_k(n_{j-1}+1) = 0$. This violates our assumption that action $n_{j-1}+1$ is non-deficient for player k.

A similar argument works as well for the symmetric case where every B_j-action is deficient and every B_{j-1} action is not; we will not repeat the details. An illustration of ripple-effect of an α-deficient action causing further deficiencies is given in Figure 7; the two parts of the figure respectively show the dependencies for the action block B_j (with $1 \leq j \leq k-2$) and action block B_k.

We have thus established the following result:

Theorem 3.3.3. *Suppose we are given* k *players with action sets* $[1, n_j]$ *for every player* j *such that* $n_1 < n_2 < \ldots < n_{k-1} = n_k$. *Then given any full support distribution profile* α^* *for this collection of players and actions, there is a game whose unique Nash equilibrium is* α^*.

It is easy to see that some simple extensions to the construction described in this section (using techniques akin to those used in the proof of Theorem 3.3.1) can yield a game for the case where possibly multiple players have action set $[1, n_j]$

for any j; the game will have an *a priori* distribution as the only possible Nash equilibrium.

Chapter 4

A Tight Characterization of Strategic Games with a Unique Equlibrium

In Chapter 3 we sought to design a game with a *unique*, pre-specified Nash equilibrium. In particular, we posed the following basic question: given a set of players and their action sets as above, and given a *full-support* distribution profile α^* (viz. one that associated a positive probability with every action of every player), under what conditions is it possible to design a strategic game whose only Nash equilibrium is α^*?

In Chapter 3 we were able to answer this question partially. We showed that when there are at least 2 players that have the maximum number of actions among all the players, i.e. when k, the number of players, is at least 2 and $n_{k-1} = n_k$, then we can construct a game with the desired unique Nash equilibrium. The game-theoretic framework for the the medium access contention resolution scheme represents an abstracted, *snapshot* version of the backoff procedure. In IEEE 802.11, when nodes initiate the backoff procedure, they all have the same number of strategies - the size of the minimum contention windows. However, the stations double their contention windows when they collide, so eventually there will be a situation where the $n_{k-1} = n_k$ condition will not be satisfied. For example, $n_{k-1} < n_k$ when there is only one node that has to choose its backoff values from the maximum contention window.

In this chapter, we answer the question whether it is always possible to design such games. We build on the results in Chapter 3 to identify the *exact* condition based on the relationship between the cardinalities of the players' action sets that would make it possible to design a static game which exhibits a *unique* Nash equilibrium corresponding to a pre-specified full-support distribution profile. Moreover, when such a strategic game is possible, we illustrate how to explicitly construct the utility functions for all the players to achieve uniqueness.

Our main result is the following theorem:

Theorem 4.0.4. *For any given full-support distribution α^* on the action sets, there exists a game such that α^* is the unique Nash equilibrium for the game if and only if the cardinalities of the action sets satisfy*

$$\sum_{i=1}^{k-1} n_i \quad \geq \quad n_k + (k-2). \tag{11}$$

We prove the necessary and sufficient condition in the theorem in Sections 4.1

and 4.2 respectively. For instance, the theorem asserts that if three players P_1, P_2 and P_3 have, respectively, 2, 3 and 5 actions in their action sets, then no given, full-support distribution profile over these action sets can be a unique full-support equilibrium for any game. On the other hand, if P_3 has only 4 actions, then such a game is indeed possible. Note that the assumption of full-support in our results is critical because otherwise, any actions that have zero probability in a desired equilibrium profile could as well have be omitted from consideration from the very outset.

4.1 Games without a unique equilibrium

Theorem 4.1.1. *Consider a game framework (with* k *players etc. as defined earlier) in which the action sets satisfy*

$$\sum_{i=1}^{k-1} n_i \quad < \quad n_k + (k-2) \tag{12}$$

Suppose that $\alpha^* = (\alpha_i^*)_{i \in P}$ *is a full-support Nash equilibrium profile for a game* G *in this framework. Then* G *has other full-support equilibria that are distinct from* α^**.*

Proof. We apply Lemma 3.1.1 to player P_k, the player with the largest number of actions, n_k, in its action set. As per the lemma, every action for player P_k has the same expected utility under the joint distribution given by the partial distribution profile α^*_{-k}. Equivalently, we can think of the probabilities in the partial profile as being *fixed constants* and the equilibrium distribution α^*_k as being *a solution* of a system of linear equations with n_k variables, $\{p_l : \ 1 \leq l \leq n_k\}$, that denote

P_k's probabilities for its respective actions. The system consists of the following equations:

1. For each $i \neq k$, there will be exactly $(n_i - 1)$ equations that assert the equality of the expected utility of all of player P_i's actions.

2. An additional equation
$$\sum_{1 \leq l \leq n_k} p_l \;=\; 1$$
asserts that the variables form a probability distribution.

In all, the system has n_k variables and

$$\begin{aligned} m &= (\sum_{i=1}^{k-1} n_i) - (k-1) + 1 \\ &= (\sum_{1=1}^{k-1} n_i) - (k-2) \end{aligned}$$

equations. By hypothesis, $n_k > m$ and hence, the system is under-specified and must have an infinite number of solutions: after all, α_k^* is a known solution.

Let $\beta = (\beta_l)_{l \in A_k}$ be one such solution distinct from α_k^*. By convexity, it follows that there must exist a *full-support* solution $\gamma = (\gamma_l)_{l \in A_k} \neq \alpha_k^*$ that is a convex combination of the solutions α_k^* and β. It now follows that γ, together with the partial distribution profile α_{-k}^*, is a full-support Nash equilibrium for the game. This contradicts the presumed uniqueness of α^*.

□

4.2 Constructing games with a unique equilibrium

In this section, we establish the other half of the characterization. Without going into details, our approach to proving this result can be summarized as follows. We will first design a game in which the players' utilities are prescribed only based on the action set cardinalities, $\{n_i : i \in P\}$. Next, the utilities are fully specified by *scaling* them appropriately using the distribution α^*. The resulting game will then have α^* as a full support Nash equilibrium. We will establish uniqueness by an indirect argument as follows. Suppose that the game has another full-support equilibrium distinct from α^* and hence, there is some player that obtains different utilities for the same action under the two distributions. We will show that this leads to a contradiction either in the assumption of full-support or in the validity of Lemma 3.1.1.

We begin our construction by observing that since the action set cardinalities are ordered in non-descending order, inequality (16) implies that there is a well-defined *largest index* L where $1 \le L \le k-1$ satisfies the inequality:

$$\sum_{i=L}^{k-1} n_i \quad \geq \quad n_k + (k-1) - L, \tag{13}$$

Further, this index L can be used to construct a table of *overlapped* actions for the players. Each player's action set corresponds to a *contiguous interval of rows* in the arrangement shown in Figure 8. Actions for different players that are in the same row going across the table, are said to be *aligned*. In particular:

- The arrangement shown has n_k rows corresponding to player P_k's actions.

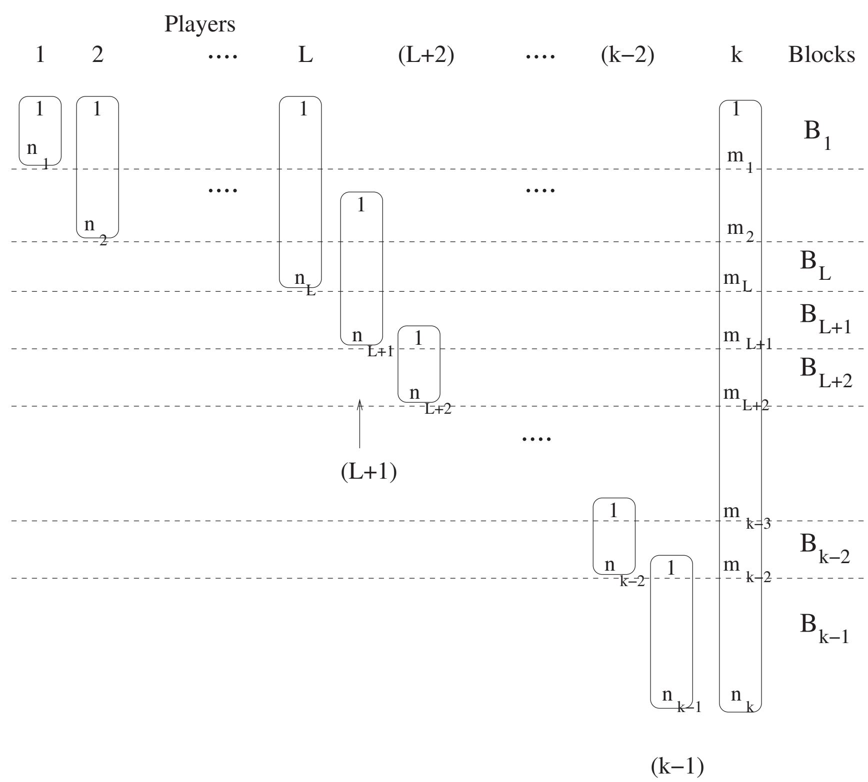

Figure 8: Action Overlaps and Blocks

- Column i (for $1 \leq i \leq L$) contains actions for player P_i in rows 1 through n_i in that column.

- Column $(k-1)$ contains actions for player P_{k-1} in an interval of rows that ends in row n_k of the table. In other words, the i^{th} action from the end for P_{k-1} is aligned with the i^{th} action from the end for P_k for all $1 \leq i \leq n_{k-1}$.

- For every remaining player P_j (with $j \in [L+1, k-2]$), the actions of P_j form an interval of rows so that the *only* overlap of actions between P_j and P_{j+1} is between the *last action* n_j of P_j and the *first action* of P_{j+1}.

- For $1 \leq j \leq k-1$, let m_j denote the index of player P_k's action that is aligned with the last action, n_j, of P_j. It is easy to verify from the table that

$$m_j = \begin{cases} n_j & \text{for } 1 \leq j \leq L \\ n_k & \text{for } j = k-1 \\ m_{j+1} - n_j + 1 & \text{for } L+1 \leq j \leq k-2 \end{cases} \tag{14}$$

  For convenience, we will let $m_0 = 0$. As Figure 8 suggests, the indices m_j for $1 \leq j \leq k-1$ partition P_k's actions into contiguous intervals. The interval $[1 + m_{j-1}, m_j]$ is defined to be the **block $\mathbf{B_j}$** of P_k's actions.

4.2.1 Utilities

Our game is defined so that for any individual player, its non-zero utilities *depend on* specific actions of other players, and the action overlaps and blocks shown in Figure 8 play a central role in this dependence:

- P_1's utilities only depend on block B_1 actions of P_k.

- P_k's utilities depend on specific actions of the players P_L through P_{k-1}.

- For every remaining player P_j, $2 \leq j \leq k-1$, the utilities for P_j only depend on actions of its predecessor player, P_{j-1}, and actions of P_k.

We will specify these utilities in abbreviated form. For instance, consider P_1's utility described above: specifically, P_1's utility for any action $a \in [1, n_1]$ is non-zero only if P_k simultaneously also chooses a unique action $f(a) \in B_1$ in the outcome; the actions of the remaining players do not matter to P_1. A compact representation of P_1's utilities, in this instance, is a two-dimensional matrix with n_1 rows (corresponding to P_1's actions) and n_1 columns (corresponding to block B_1 actions for player P_k) with non-zero values for entries indexed by $(a, f(a))$ for all $a \in [1, n_1]$. Note that all other outcome combinations have zero utility for P_1, e.g. outcomes in which P_k chooses actions that are not in block B_1,

For each player, we will first specify - in abbreviated form - *unscaled* utilities that only depend on the action set cardinalities, $\{n_i : i \in P\}$, and more specifically, on the table shown in Figure 8. These utilities can then be easily *scaled* according to the given distribution α^* to complete the construction.

Four specific kinds of matrices occur in our construction so it is worthwhile to fix some notation for them. Let n be a positive integer. Then, $\mathbf{I_n}$ denotes the n-dimensional identity matrix; $\mathbf{V_n}$ is the (cyclic) permutation matrix obtained by shifting down (circularly) the rows of the identity matrix; and $\mathbf{T_n}$ and $\mathbf{E_n}$ are, respectively, the row vectors $[1, 1, \ldots, 1]$ (all ones) and $[0, 0, \ldots, 0, 1]$ (zeroes with a single trailing one entry).

Utilities for P_1

Only player P_k's actions in block $B_1 = [1, n_1]$ influence P_1's utility. Specifically, the utility sub-matrix for P_1 is given by V_{n_1} (see the notation above) where the columns correspond to actions in block B_1 of player P_k. Intuitively, P_1 depends cyclically on P_k's actions in block B_1, viz. action a has non-zero utility for P_1 if and only if P_k chooses action $(a - 1)$ in the outcome (with $n_1 + 1$ interpreted cyclically as 1). The final, scaled utility in the outcome is obtained by dividing its value by the α^* probability of P_k's action in the outcome.

Utilities for P_j, $j \in [2, k-1]$

P_j's utility depends both on some actions of its *immediate predecessor*, P_{j-1}, and some actions of player P_k. There are two disjoint action intervals of P_j's actions for which this happens:

1. Consider the initial prefix of P_j's actions that overlaps with actions of P_{j-1}. For every action of player P_k, the abbreviated utility sub-matrix is the identity matrix I with its rows and columns corresponding, respectively, to the overlapping action intervals of P_{j-1} and P_j. Note that the dimensions of this matrix depend on j as can be seen from Figure 8:

    - for $2 \leq j \leq L$, the number of rows is n_{j-1},
    - for $j = L + 1$, the number of rows is

    $$n_{L+1} + n_L - m_{L+1},$$

    - for $L + 2 \leq j \leq k - 1$, since P_j and P_{j-1} overlap in just one action, the identity matrix reduces to a single 1 entry (for that combination of aligned actions).

In any such outcome where P_j's action is aligned with P_{j-1}'s action, the scaled utility is obtained by dividing the unscaled utility by the α^* probability of the latter action.

2. The remaining suffix of P_j's actions overlaps with block B_j of P_k's actions. Consider any action q of P_j from this suffix. Then, the utility for P_j for choosing action q depends on the actions of P_{j-1} and P_k in the outcome. In abbreviated form, we can describe this as a *combination* of the following row vectors of dimension n_{j-1}. Note that the columns of the vectors represent the actions of P_{j-1}, the predecessor player.

   (a) The vector E_n for *each one* of P_k's actions. The scaled form is obtained by dividing entries of the vector by the α^* probabilities of the corresponding column actions of P_{j-1}.

   (b) The vector $-T_n$ for the action of P_k that is aligned with action q of P_j. Denoting this action of P_k by $\hat{q}$, we obtain the scaled form of the utility by dividing each entry of the vector by $\alpha_k^*(\hat{q})$.

   (c) For some fixed chosen constant $x_j > 0$, the vector $x_j T_n$ for *each one* of P_k's actions in block B_{j-1}. The scaled form of the utility is obtained by dividing entries of the vector by the α^* probability of the corresponding action of P_k in block B_{j-1}.

(d) for the constant y_j satisfying the equation

$$x_j(m_{j-1} - m_{j-2}) = 1 + y_j(m_j - m_{j-1}), \tag{15}$$

the vector $-y_j T_n$ for *each one* of P_k's actions in block B_j.

The scaled form of the utility is obtained by dividing entries of the vector by the α^* probability of the corresponding action of P_k in block B_j.

Utilities for P_k

As mentioned previously, P_k's utilities depend on actions of all the preceding players P_L through P_{k-1}. The overlaps shown in Figure 8 define this dependence more precisely: any action of P_k *depends only on* the corresponding aligned action of a preceding player with the *largest index among such players*. Thus, all the utility sub-matrices for player P_k can be combined into a single compact representation: the *identity* matrix I_{n_k}, where the columns correspond to contiguous action intervals of *different* players. Referring to Figure 8, the columns of the (identity) utility matrix can be identified with players P_L through P_{k-1} as follows:

1. Let $d = m_{L+1} - n_{L+1}$. Then, columns 1 through d correspond to the action interval $[1, d]$ of player P_L since actions 1 through d for player P_k are aligned with those of P_L but not with the actions of players P_{L+1} through P_{k-1}.

2. Similarly, columns $d+1$ through $m_{L+1}-1$ of the identity sub-matrix correspond to the action interval $[1, n_{L+1} - 1]$ of player P_{L+1}.

3. For all j such that $L + 1 \leq j < k - 2$, the columns m_j through $m_{j+1} - 1$

correspond to the action interval $[1, n_{j+1} - 1]$ of player P_{j+1}.

4. The last n_{k-1} columns correspond to the actions of P_{k-1}.

In the scaled form, the utility is obtained by dividing each diagonal entry of the identity matrix with the α^* probability of the corresponding column action.

4.2.2 A complete example

Consider a game with three players P_1, P_2 and P_3, and suppose that the players have 2, 3 and 4 actions in their respective action sets. We will use the construction

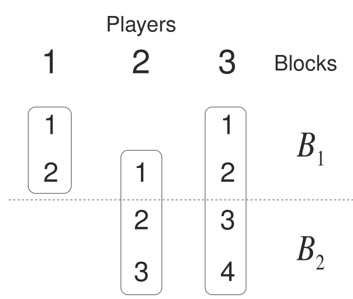

Figure 9: Action Overlaps and Blocks with 3 Players

outlined earlier to design a game where the desired Nash equilibrium α^* is the **uniform distribution** on the action sets of the players. From inequality (13), it follows that $L = 1$ and hence, the actions for the players will be aligned as shown in Figure 9. Note that there are two blocks of actions for player P_3, viz. block $B_1 = [1, 2]$ overlapping the two actions of P_1 and block $B_2 = [3, 4]$ overlapping actions $[2, 3]$ of P_2.

Player P_1's non-zero utilities for its actions are described in abbreviated form by by the submatrix, V_2, whose columns correspond to P_3's action block B_1. The complete strategic form for P_1's utilities is shown in Figure 10 as a sequence of three identical matrices that correspond to the three actions of player P_2: the row player is P_1 while the column player is P_3 with the row/column labels being their respective actions. Note that P_1's utilities are zero-valued for action block B_2 of player P_3, and the non-zero entries are scaled by a factor of 4 since they depend on actions of P_3, each of which is to be chosen with equal probability $1/4$.

$$
\begin{array}{c}
\quad\ \ \mathbf{1}\ \ \mathbf{2}\ \ \mathbf{3}\ \ \mathbf{4} \\
\begin{matrix}\mathbf{1}\\ \mathbf{2}\end{matrix}\begin{pmatrix} 0 & 4 & 0 & 0 \\ 4 & 0 & 0 & 0 \end{pmatrix} \\
\mathbf{1}
\end{array}
\qquad
\begin{array}{c}
\quad\ \ \mathbf{1}\ \ \mathbf{2}\ \ \mathbf{3}\ \ \mathbf{4} \\
\begin{matrix}\mathbf{1}\\ \mathbf{2}\end{matrix}\begin{pmatrix} 0 & 4 & 0 & 0 \\ 4 & 0 & 0 & 0 \end{pmatrix} \\
\mathbf{2}
\end{array}
\qquad
\begin{array}{c}
\quad\ \ \mathbf{1}\ \ \mathbf{2}\ \ \mathbf{3}\ \ \mathbf{4} \\
\begin{matrix}\mathbf{1}\\ \mathbf{2}\end{matrix}\begin{pmatrix} 0 & 4 & 0 & 0 \\ 4 & 0 & 0 & 0 \end{pmatrix} \\
\mathbf{3}
\end{array}
$$

Figure 10: P_1's utilities

For the strategic representation of player P_2's utilities, we choose the constant $x_2 = 1$ and substitute it in Equation (15) to obtain $y_2 = 0.5$ (since m_0, m_1 and m_2 are respectively 0, 2 and 4). Using these constants, the representation is shown in the four matrices in Figure 11 that correspond to the actions of player P_3, with P_2 and P_1 being the row and column players respectively. The first two matrices correspond to actions in block B_1 while the next two matrices correspond to actions in block B_2. We will describe two of the rows in the matrices to illustrate the construction.

Consider, for instance, the second rows in the third and fourth matrices in Figure 11, i.e. the utility vectors when P_3 choosing actions 3 and 4 respectively, P_2 chooses action 2, and where P_1's actions are the columns. Both the matrices correspond to block B_2. The second row of the third matrix is the weighted sum of the component vectors $E_2 = [0, 1]$ (from part (a) of the construction), $-T_2 = [-1, -1]$ (from part (b)) and $-y_2T_2 = [-0.5, -0.5]$ from part (d) of the construction. In particular, vector (a) is scaled by a factor of 2 (by dividing each entry by 1/2, the probability of each action of P_1); vectors (b) and (d) are each scaled by 4. The resulting weighted sum is $[-6, -4]$. Likewise, the second row of the fourth matrix can be shown to be the weighted sum of the component vectors $E_2 = [0, 1]$ (scaled by a factor of 2) and $-y_2T_2 = [-0.5, -0.5]$ scaled by a factor of 4; the result is the vector $[-2, 0]$.

$$
\underset{\mathbf{1}}{\begin{array}{c} \\ \mathbf{1} \\ \mathbf{2} \\ \mathbf{3} \end{array}\begin{array}{c} \begin{array}{cc} \mathbf{1} & \mathbf{2} \end{array} \\ \begin{pmatrix} 0 & 2 \\ 4 & 6 \\ 4 & 6 \end{pmatrix} \end{array}}
\qquad
\underset{\mathbf{2}}{\begin{array}{c} \\ \mathbf{1} \\ \mathbf{2} \\ \mathbf{3} \end{array}\begin{array}{c} \begin{array}{cc} \mathbf{1} & \mathbf{2} \end{array} \\ \begin{pmatrix} 0 & 2 \\ 4 & 6 \\ 4 & 6 \end{pmatrix} \end{array}}
\qquad
\underset{\mathbf{3}}{\begin{array}{c} \\ \mathbf{1} \\ \mathbf{2} \\ \mathbf{3} \end{array}\begin{array}{c} \begin{array}{cc} \mathbf{1} & \mathbf{2} \end{array} \\ \begin{pmatrix} 0 & 2 \\ -6 & -4 \\ -2 & 0 \end{pmatrix} \end{array}}
\qquad
\underset{\mathbf{4}}{\begin{array}{c} \\ \mathbf{1} \\ \mathbf{2} \\ \mathbf{3} \end{array}\begin{array}{c} \begin{array}{cc} \mathbf{1} & \mathbf{2} \end{array} \\ \begin{pmatrix} 0 & 2 \\ -2 & 0 \\ -6 & -4 \end{pmatrix} \end{array}}
$$

Figure 11: P_2's utilities

Finally, P_3's utilities are defined in abbreviated form by the identity matrix I_4 whose rows correspond to P_3's actions and whose columns, in sequence, to action 1 of P_1 followed by actions 1 through 3 of P_2. The equivalent strategic representation of P_3's utilities is shown in Figure 12 where the two matrices correspond to P_1's actions and the row and column players are P_3 and P_2 respectively. We note that the first row of the first matrix is scaled by a factor of 2 (corresponding to the two equi-probable actions of P_1) and the last three rows in both matrices are scaled by 3 (corresponding to the three equi-probable actions of P_2). It is easy to see that all actions, regardless of the player, have an expected utility of 1.

4.2.3 Analysis of the game

We now prove that the defined game has a unique, full-support Nash equilibrium distribution given by α^*. We start by proving in Lemma 4.2.1 that α^* is indeed a

$$
\begin{array}{c} \\ \mathbf{1} \\ \mathbf{2} \\ \mathbf{3} \\ \mathbf{4} \end{array}
\begin{array}{c} \begin{array}{ccc} \mathbf{1} & \mathbf{2} & \mathbf{3} \end{array} \\ \begin{pmatrix} 2 & 2 & 2 \\ 3 & 0 & 0 \\ 0 & 3 & 0 \\ 0 & 0 & 3 \end{pmatrix} \\ \mathbf{1} \end{array}
\qquad\qquad
\begin{array}{c} \\ \mathbf{1} \\ \mathbf{2} \\ \mathbf{3} \\ \mathbf{4} \end{array}
\begin{array}{c} \begin{array}{ccc} \mathbf{1} & \mathbf{2} & \mathbf{3} \end{array} \\ \begin{pmatrix} 0 & 0 & 0 \\ 3 & 0 & 0 \\ 0 & 3 & 0 \\ 0 & 0 & 3 \end{pmatrix} \\ \mathbf{2} \end{array}
$$

Figure 12: P_3's utilities

Nash equilibrium for the specified game; a sequence of subsequent lemmas (Lemmas 4.2.3 to 4.2.10) will establish that it is unique.

Lemma 4.2.1. *The distribution α^* is a Nash equilibrium for the specified game.*

Proof. We show that under α^*, each player gets the same utility from all its pure actions. Recall that the utility of any action a for player P_j is the expected value (under the joint product distribution for the players) of the sum of the utilities accrued from all distinct non-zero utility (sub)matrix entries corresponding to action profiles in which P_j chooses action a.

Since the reciprocals of the α^* probabilities were used to scale the entries in our construction, it is easy to see that while taking expectations, these probabilities (of dependent actions) cancel out and hence, the utility values are simply obtained by summing over the relevant unscaled utilities in expectation.

1. For players P_1 and P_k, the unscaled utilities are simply entries in an appropriately constructed identity matrix (Figures 10 and 11). A simple calculation shows that all pure actions for players P_1 and P_k have the same expected utility 1.

2. Consider player P_j where $2 \leq j \leq k-1$. From the construction in the previous section, any action of P_j that is aligned with an action of its predecessor P_{j-1} gets expected utility 1 for choosing this action, which corresponds to the first row of four matrices in Figure 11 in Example 1. Otherwise, the action has expected utility given by the summation of four terms (obtained from the four contributing parts in the construction in subsection 4.2.1).

   Consider action q of player P_j and let $\hat{q}$ be the action of P_k that is aligned with q. Then, part (a) of the construction has expected utility

$$\begin{aligned}\sum_{b \in [1, n_k]} \alpha_k^*(b)\alpha_{j-1}^*(n_{j-1}) \cdot \frac{1}{\alpha_{j-1}^*(n_{j-1})} &= \sum_{b \in [1, n_k]} \alpha_k^*(b) \\ &= 1\end{aligned}$$

   while part (b) contributes expected utility

$$\begin{aligned}\alpha_k^*(\hat{q}) \sum_{b \in [1, n_{j-1}]} \alpha_{j-1}^*(b) \cdot \frac{-1}{\alpha_k^*(\hat{q})} &= -\sum_{b \in [1, n_{j-1}]} \alpha_{j-1}^*(b) \\ &= -1.\end{aligned}$$

   Thus, the first two parts cancel out in expectation. Meanwhile, the choice of constants x_j and y_j in parts (c) and (d) of the construction implies that the expected utility from part (c) is

$$\begin{aligned}\sum_{b \in B_{j-1}} \sum_{c \in [1, n_{j-1}]} \alpha_k^*(b)\alpha_{j-1}^*(c) \cdot \frac{x_j}{\alpha_k^*(b)} &= \sum_{b \in B_{j-1}} x_j \\ &= x_j(m_j - m_{j-1})\end{aligned}$$

and the expected utility from part (d) is

$$\begin{aligned}\sum_{b\in B_j}\sum_{c\in[1,n_{j-1}]} \alpha_k^*(b)\alpha_{j-1}^*(c)\cdot\frac{-y_j}{\alpha_k^*(b)} &= \sum_{b\in B_j} -y_j \\ &= -y_j(m_{j+1}-m_j).\end{aligned}$$

Thus, using Equation (15), we conclude that all four contributions for the expected utility of P_j for action q sum to 1. In all cases, therefore, a pure action for player P_j accrues the same expected utility 1.

From Lemma 3.1.1, we conclude that α^* is indeed a Nash equilibrium of the game. □

We now argue by contradiction that α^* is the only equilibrium for the game. Consider any fixed distribution profile α over the given domain of action sets, and *assume that $\alpha \neq \alpha^*$ is also a Nash equilibrium for the game*. For any player P_j and any action $a \in [1, n_j]$, we define the ratio $r_j(a) = \alpha_j(a)/\alpha_j^*(a)$ that quantifies the relative difference between the probabilities assigned to action a by two distributions. We say that action a is *deficient* for P_j if $r_j(a) < 1$ and *unsupported* for P_j if $\alpha_j(a) = r_j(a) = 0$. Note that the definition of deficiency in the subsequent argument uses the assumed distribution α implicitly.

Our argument proceeds in essentially three steps. We first show that if any player has a deficient action, then the deficiency *propagates forward* to P_k, viz. that P_k must also have a deficient action. Next, we prove that any deficient, block B_j action for player P_k implies that the entire block of B_j actions cannot be in the support of α_k, the distribution for P_k's actions. In other words, each block consists either entirely of unsupported actions, or entirely of non-deficient actions for player P_k.

As a final step, we show that it is impossible for P_k to have the property described in the previous sentence, i.e. simultaneously having an completely unsupported block and a block containing only non-deficient actions leads to a contradiction. As a consequence, we can conclude that the distribution α cannot differ from α^* anywhere, and hence that α^* is unique for the game.

A simple observation is recorded here for future use:

Lemma 4.2.2. *For any player P_j, there is an action a such that $r_j(a) < 1$ if and only if for some other action $b \neq a$, it holds that $r_j(b) > 1$.*

Proof. This follows easily from the fact that α_j and α_j^* are both probability distributions summing to 1. □

Forward Propagation

Lemma 4.2.3. *For any $j: \ 1 \leq j \leq L-1$, if an action a is deficient for P_j then $\alpha_L(a) = 0$.*

Proof. A similar result was proved in Chapter 3, but we will reprise it here for completeness. Note that the actions of P_j form an initial prefix of the actions of P_{j+1} in the given range for j. Hence, for the given action a, player P_{j+1}'s expected utility for action a is equal to $r_j(a) < 1$ (since a is deficient for P_j by assumption). Then, by Lemma 4.2.2, there must be an action $b \neq a$ for P_j such that $r_j(b) > 1$. Since the expected utility of P_{j+1} for action b equals $r_j(b)$, it implies that action a for P_{j+1} has strictly smaller expected utility than action b for P_{j+1}. Under the claimed equilibrium profile α, action a must therefore be unsupported for P_{j+1}. A transitive application of the same argument will lead us eventually to the conclusion that $\alpha_L(a) = 0$. □

Lemma 4.2.4. *Consider player P_k's utility for some action c and suppose that it depends only on the corresponding aligned action c_j^k for the nearest preceding player P_j with $L \leq j < k$. If c_j^k is deficient for P_j, then $\alpha_k(c) = 0$.*

Proof. For the given actions c (of P_k) and c_j^k (of P_j), it follows that P_k's expected utility for c is given by $r_j(c_j^k)$. This latter quantity is less than one by assumption that c_j^k is deficient for P_j. We will now show that there is another action b of P_k such that P_k's expected utility for b equals or exceeds one. By appealing to the equilibrium property of distribution α, we can conclude that $\alpha_k(c) = 0$.

Indeed, the desired action b will be one of P_k's actions in the interval $[m_{k-2}, m_{k-1}]$. This interval overlaps exactly with all the actions of player P_{k-1} and hence, the expected utility is just $r_{k-1}(b_{k-1}^k)$ (recall that b_{k-1}^k is the corresponding aligned action of P_{k-1}). By Lemma 4.2.2, there must be an action among P_{k-1}'s actions which is not deficient; we let b_{k-1}^k be one such action. □

So far, we have established that most of the forward dependencies propagate deficiencies along the aligned actions. The only remaining forward dependencies that we need to address are:

1. for each $j : L + 1 \leq j \leq k - 2$, the dependence of P_{j+1}'s utility for action 1 on P_j's action n_j, and
2. the dependence of P_{L+1}'s utilities for each of its actions in the interval that overlaps with P_L's actions (see Figure 1).

Consider the first of these dependencies. We show that if action n_j for P_j is deficient, then that causes the corresponding aligned action m_j of P_k to be unsupported. In turn, this implies that the *entire block* B_j is unsupported.

Lemma 4.2.5. *For* $j : L + 1 \leq j \leq k - 2$*, if action* n_j *is deficient for* P_j*, then some action in the range* $[m_{k-2}, m_{k-1}]$ *is unsupported for* P_k*.*

Proof. If action n_j is deficient for P_j, then there exists an action $b < n_j$ with $r_j(b) > 1$ (by Lemma 4.2.2). Note that action b of P_j defines the expected utility of the corresponding aligned action b_k^j of P_k via a forward dependency. Hence, the expected utility of action b_k^j is $r_j(b)$ and since α is an equilibrium, this means that every supported action of P_k has expected utility greater than or equal to $r_j(b)$, and hence, greater than one.

On the other hand, there exists some action a of P_{k-1} such that $r_{k-1}(a) \leq 1$. From this, we conclude that the corresponding aligned action $a_k^{k-1} \in [m_{k-2}, m_{k-1}]$ has expected utility less than $r_j(b)$ which implies, via equilibrium considerations, that a_k^{k-1} in the desired range is unsupported for P_k. □

The following notational abbreviation is used in calculating utilities. For any player P_j,

$$R_j = \sum_{a \in [1, n_j]} r_j(a)$$

is the sum of its r_j values over all its actions.

Lemma 4.2.6. *For* $j : L + 1 \leq j \leq k - 1$*, consider block* B_j *and an action* a *in the block. If either* $j = k - 1$ *(the last block) or* $a = m_j$ *(the last action in the block), and* a *is unsupported for* P_k*, then the entire block* B_j *is unsupported.*

Proof. Suppose that action $a = m_j$ is unsupported in block B_j, and assume that action $1 + m_{j-1}$ *is* supported for P_k. Consider the corresponding aligned actions

n_j and 2 for player P_j. The difference in expected utilities for these actions can be shown to be:

$$\begin{aligned} U^j_\alpha(n_j) - U^j_\alpha(2) &= R_{j-1}(r_k(1+m_{j-1}) - r_k(m_j)) \\ &> 0 \end{aligned}$$

where the last inequality follows from the assumption above. Consequently, action 2 must be unsupported for P_j since it is dominated by action n_j. By Lemma 4.2.4, action $1+m_{j-1}$ is unsupported for P_k. The same argument, used inductively, allows us to show that each action in block B_j is unsupported.

In the special case of the last block B_{k-1}, the argument holds for an arbitrary initial action a that is known to be unsupported in the block. This is because the forward deficiency propagation has already been established for that entire block via Lemma 4.2.4, whereas there is no direct way to prove that a deficiency in action n_j for P_j propagates to the next aligned action 1 for P_{j+1}. □

The preceding two lemmas can be combined as follows.

Lemma 4.2.7. *For* $j:\ L+1 \leq j \leq k-1$*, if action* n_j *is deficient for* P_j*, then all the blocks* $B_j,\ B_{j+1}, \ldots, B_{k-1}$ *are unsupported for* P_k*.*

Proof. We proceed by backward induction on the sequence of blocks. Consider block B_{k-1}; we know from Lemma 4.2.5 that if n_j is deficient, then either m_{k-2} is unsupported or some action in block B_{k-1} is unsupported (meaning the entire block B_{k-1} is unsupported by Lemma 4.2.6). We show that in both cases, all the actions in $[m_{k-2}, m_{k-1}]$ are unsupported. Assume to the contrary. There are two possibilities: either the entire block B_{k-1} is unsupported and action m_{k-2} is not or action m_{k-2} is unsupported but the entire block B_{k-1} is supported.

Assume first that block B_{k-1} is unsupported and action m_{k-2} is not. Let us compare the utilities for actions 1 and 2 of P_{k-1}. For every action of P_k, the utility of action 1 of P_{k-1} is equal to the vector E_n for each one of P_k's actions. On the other hand, action 2 of P_{k-1} is aligned with the first action in block B_{k-1} and all actions in the block have zero probability. Hence, from the row vector definition of utilities, it follows that action 2 of P_{k-1} has non-zero contributions only from parts (a) E_n from each one of P_k's actions and (c) $x_j T_n$ for each one of P_k's actions in block B_{k-2}. By assumption, m_{k-2} is supported and being part of block B_{k-2}, provides a strictly positive contribution to the utility of action 2. Thus, action 2 dominates action 1 in utility and hence, action 1 must be unsupported. Applying Lemma 4.2.4, we conclude that action m_{k-2} is unsupported, a contradiction.

Similarly, if m_{k-2} is unsupported and the entire block B_{k-1} is supported, by Lemma 4.2.6 it follows that the entire block B_{k-2} is unsupported. It is easy to observe from the row vector definition of utilities that in this case action 1 of P_{k-1} dominates its action 2, and, by Lemma 4.2.4 P_k's action $m_{k-2}+1$ is unsupported, which again is a contradiction.

We have shown that if n_j is unsupported for P_j, then action m_{k-2} as well all actions in B_{k-1} are unsupported for P_k. Applying Lemma 4.2.6, we get the basis case for our induction: viz. all of block B_{k-2} is unsupported. The inductive argument now mimics the reasoning in the previous paragraph to show that blocks B_{k-3}, $B_{k-3}, \ldots, B_j$ will all be unsupported. □

We now verify that any deficiency, for an action of player P_L that overlaps with an action of P_{L+1}, propagates forward to the aligned action of P_k and thence to the whole block containing that action. Observe that there may be several action blocks B_j, with $j \leq L$, that overlap with the interval $[d+1, n_L]$ - the range of P_L's action aligned with corresponding actions of P_{L+1}.

Lemma 4.2.8. *Let a be an action of P_L in the range $[d+1, n_L]$. If a is deficient for P_L then the corresponding aligned action of P_k given by a_k^L is unsupported.*

Proof. By Lemma 4.2.2, there must be another action $b \neq a$ such that $r_L(b)$ is greater than 1. If b also lies among the actions in the overlap range, viz. $[d+1, n_L]$, then it follows that b's aligned action for P_{L+1} dominates a's aligned action for P_{L+1} and consequently, that latter action is unsupported for P_{L+1}. By Lemma 4.2.4, the action a_k^L is unsupported.

Otherwise, all the actions of P_L in the overlap range are deficient, and hence by Lemma 4.2.2, there must be an action in the range $[1, d]$ for P_L with ratio greater than 1. We now have a situation that is very similar to the one analyzed in Lemmas 4.2.5, 4.2.6 and 4.2.7; without repeating all the details, we can conclude in a like manner that every block of P_k, overlapping with the range of actions $[d+1, n_L]$ for player P_L, is not supported in this latter case. □

The preceding sequence of results collectively assert that forward deficiencies propagate from *any* player's deficient action to the corresponding aligned action of P_k (Figure 13).

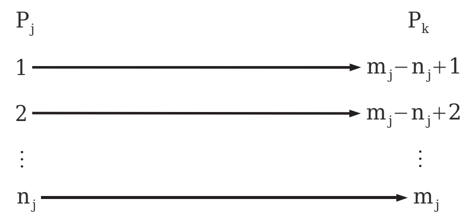

Figure 13: Forward Propagation of Deficiencies

Backward Propagation

We next show that every block B_j of player P_k is either completely unsupported or is completely non-deficient. Lemma 4.2.6 already establishes part of this assertion; we now establish it by showing that the proof of Lemma 4.2.6 goes through in full generality.

Consider any block B_j with $1 \leq j \leq k-1$: this block corresponds to the action interval $(m_{j-1}, m_j]$ for player P_k.

Lemma 4.2.9. *It is impossible to have both deficient and non-deficient actions for player P_k in block B_j.*

Proof. Assume to the contrary and without loss of generality, let action a in B_j be such that a is deficient for player P_k but $a+1$ (interpreted circularly within the block B_j) is not. Consider the corresponding aligned actions a_j^k and $1 + a_j^k$ for P_j. The difference in expected utilities for these actions are, by definition:

$$\begin{aligned} U_j^\alpha(a_j^k) - U_j^\alpha(1 + a_j^k) &= R_{j-1}(r_k(a+1) - r_k(a)) \\ &> 0 \end{aligned}$$

where the inequality follows from the assumption above. Consequently, action

$1 + a_j^k$ must be unsupported for P_j since it is dominated by action a_j^k. Deficiencies, therefore, propagate backward as shown in Figure 14. *The forward propagation argument implies - in all cases - that action* $a+1$ *is unsupported, and hence, deficient for* P_k. This contradicts our assumption regarding action $a+1$ for P_k.

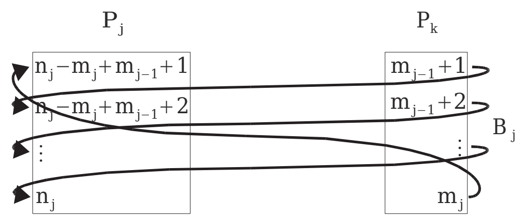

Figure 14: Backward Propagation of Deficiencies

□

Note that we needed to develop all the machinery in the previous subsection for the italicized statement in the last paragraph to hold unconditionally. To summarize thus far, we have now shown that either block B_j contains only deficient actions or that it contains only non-deficient ones.

Lemma 4.2.10. *Every action of player* P_k *is non-deficient.*

Proof. Suppose player P_k has a deficient action. Then without loss of generality, it follows from Lemma 4.2.9 that there must be two consecutive blocks B_{j-1} and B_j (with the subscripts interpreted circularly in the range $[1, k-1]$) such that all actions in B_{j-1} are deficient and all actions in B_j are non-deficient.

In particular, action m_{j-1} (the last one in block B_{j-1}) is deficient, while action $m_{j-1}+1$ (the first action in B_j) is non-deficient. Consider the corresponding aligned (consecutive) actions a and $a+1$ for player P_j, i.e. a_k^j, the action of P_k aligned with action a of P_j, is identically equal to m_{j-1}. We now examine the difference in utilities for player P_j between actions a and $a+1$.

The utility of action $a+1$ can be seen as a set of row vectors, which can be partitioned into three subsets. The first subset corresponds to the actions of player P_k in block B_{j-1}, and is identically $[x_j, x_j, \ldots 1 + x_j]$ (comprising contributions from components labeled (a) and (c) in the definition of utilities). The second subset corresponds to the actions of player P_k in block B_j: the row vector corresponding to action $m_{j-1}+1$ is $[-1-y_j, -1-y_j, \ldots, -y_j]$ (comprising contributions from components (a), (b), and (d)) and all other row vectors in this subset are identically $[-y_j, -y_j, \ldots 1 - y_j]$ (comprising contributions from components (a) and (d)). Finally, the third subset of row vectors corresponds to all the remaining actions of player P_k and is identically $E_{n_{j-1}}$ (comprising contributions only from component (a)).

Recall that a is the last action of P_j that overlaps with player P_{j-1} and therefore its row vectors are all identically $E_{n_{j-1}}$ regardless of the actions of player P_k. Therefore, any difference in utility between action a and $a+1$ for player P_j is contributed entirely by the first two subsets of row vectors, corresponding to player P_k's actions in blocks B_{j-1} and B_j.

Let the sum of the r_k values over the action block B_j for player k be defined as:

$$R_k^j \;=\; \sum_{a \in B_j} r_k(a)$$

Similarly, R_k^{j-1} is the sum of the r_k values over the action block B_{j-1} for player k. Observe that since block B_{j-1} is entirely deficient for player k, it must be the case that

$$\begin{aligned} R_k^{j-1} &= \sum_{b \in B_{j-1}} r_k(b) \\ &< \mid B_{j-1} \mid \\ &= (m_{j-1} - m_{j-2}) \end{aligned}$$

Similarly, $R_k^j \geq (m_j - m_{j-1})$ and $r_k(m_{j-1} + 1) \geq 1$ since block B_j is assumed to be wholly non-deficient.

Putting these inequalities together, we can simplify and show that the required difference in utilities

$$\begin{aligned} U_\alpha^j(a) - U_\alpha^j(a+1) &= R_{j-1}[y_j R_k^j + r_k(m_{j-1}+1) - x_j R_k^{j-1}] \\ &> R_{j-1}[y_j(m_j - m_{j-1}) + 1 - x_j(m_{j-1} - m_{j-2})] \\ &= 0 \end{aligned}$$

where the last step above follows directly from (15) that holds for the chosen values of x_j and y_j.

The difference being positive, implies that action $a+1$ for player P_j is dominated in utility by action a. Hence, by Lemma 3.1.1, we conclude that action $a+1$ is unsupported for P_j. Forward propagation now ensures that the aligned action $m_{j-1}+1$ for P_k is also unsupported, which contradicts the assumption that action $m_{j-1}+1$ is non-deficient. □

We have established that all actions of P_k are non-deficient. By Lemma 4.2.2, all the ratios $r_k(\cdot)$ must be identically equal to 1. In other words, α_k coincides with its counterpart α_k^* in the desired Nash equilibrium profile.

Furthermore, if any of the remaining players P_j for $1 \leq j < k$ exhibit a deficient action, then the forward propagation results from the last subsection ensure that the corresponding, aligned action of P_k is deficient; we know that this is impossible courtesy Lemma 4.2.10 above. As a consequence, *every* component, α_j, coincides with its counterpart α_j^*.

Lemmas 4.2.1 to 4.2.10 establish Theorem 4.2.11.

Theorem 4.2.11. *If the cardinalities of the action sets satisfy*

$$\sum_{i=1}^{k-1} n_i \quad \geq \quad n_k + (k-2) \tag{16}$$

then for any given full-support distribution α^* on the action sets, it is possible to construct a game such that α^* is the unique Nash equilibrium for the game.

4.3 Discussion

All of the results presented so far in this thesis are based on game-theoretic techniques. The main disadvantage of the game-theoretic approaches is that they often involve complex, time-consuming and resource intensive techniques, which could obstruct the implementation of such schemes in the world of wireless communications where limited resources are always a concern and events occur within microseconds. Moreover, such methods are based on the game-theoretic assumption that the nodes are rational. In practice, however, it might happen that some nodes are greedy but not necessarily rational.

Finally, recall that the game-theoretic framework that we have developed is for an abstracted, single-round version of the backoff procedure. As previously mentioned, the nature of the medium access contention resembles a dynamic game. In dynamic games, a player's strategy specifies the actions the player will take at each stage, for each possible history of play thus far. A *subgame* is a piece of the game that remains to be played beginning at any point at which the complete history of the game is common knowledge among the players. A Nash equilibrium is *subgame-perfect* if the players' strategies constitute a Nash equilibrium in every subgame. Thus, subgame-perfect Nash equilibrium is a refinement of Nash equilibrium which eliminates noncredible threats.

The dynamic nature of the CSMA/CA backoff procedure could be captured, for example, as a repeated game. A repeated game is a game which consists in some number of repetitions of some base game (called a stage game). In the CSMA/CA context, a new stage (subgame) begins whenever a transmission occurs on the channel. All players make their moves simultaneously at each subgame and their actions are the choices of backoff values.

In a *finitely* repeated game (with any finite number of stages), if all stage games have a unique Nash equilibrium, the repeated game has a unique subgame-perfect outcome. Thus, to achieve unique subgame-perfect Nash equilibrium of the dynamic game, the utilities at each subgame can be distributed according to our static game model.

More precisely, for the players whose backoff counters are greater than zero the utilities at each stage can be implemented as dominant strategies , whereas for the nodes that have participated in the transmission attempt and must choose new backoff values, the utilities could be distributed according to the scheme presented in this chapter.

Note that on the top of the complexity of calculating the equilibrium in the static game, implementing such a repeated game would be difficult because the backoff counter state (or at least the choice of a backoff value of all stations) must be known to everybody, which is not possible when the uniform distribution is used, as specified in the IEEE 802.11 standard. Furthermore, the CSMA/CA backoff procedure can be looked at as an *infinitely* repeated game (as we do not know when the nodes will have no more data to transmit). Unfortunately, in the infinite-horizon case, even if all stage games have a unique Nash equilibrium, there might be subgame-perfect outcomes in which no stage's outcome is a Nash equilibrium.

Chapter 5

Selfishness Detection for Backoff Algorithms in Wireless Networks

Game-theoretic approaches are complex in nature. Furthermore, such mechanisms are often based on unrealistic assumptions, so their practical implementation might not be feasible. For example, the repeated game model mentioned in Section 4.3 requires that the backoff values of the participating nodes are known to all stations, which is generally impossible in the standard IEEE 802.11 backoff procedure. In this chapter we investigate more practical methods to detect selfish misbehavior on the data link layer.

As already discussed, in IEEE 802.11 the backoff procedure specifies that the participants should choose a backoff value uniformly at random from a given interval $[0, CW]$. We call this backoff procedure UVBEB (Uniform Value Binary Exponential Backoff). A misbehaving node might choose smaller backoff values more often than would be dictated by pure chance. Detecting this kind of misbehavior is far from obvious as it is not always possible to deduce the backoff values used by a wireless node.

Any scheme that requires the participants to delay transmission according to voluntarily chosen random backoff values is susceptible to selfish behavior. In this chapter, we study methods to *detect* such selfish behavior. There are two problems in detecting whether the node is following the backoff algorithm, namely, *backoff value deduction* and *sample validation*. Backoff value deduction concerns deducing the backoff values chosen by an observed node over a period of time, based on observations of transmissions and collisions over the medium. In the absence of collisions, it is easy to deduce the backoff values chosen by the observed node: simply count the number of empty slots between successive transmissions by the node. However, in the presence of collisions, and the absence of knowledge of the identity of colliding nodes, the problem of deducing the backoff value chosen by the node is far from obvious. Once the backoff values are known, the sample validation problem lies in detecting whether they are in fact valid samples drawn from the random distribution specified by the backoff procedure. We claim that both these problems are hard to solve for UVBEB, which makes it difficult to track down selfish nodes.

To overcome this obstacle, we propose a new backoff algorithm called XVBEB (eXtreme Value BEB), in which both backoff deduction and sample validation are easier to solve. In XVBEB, a node has only 2 choices of backoff value: 0 and CW. Given a specified probability q, a node chooses backoff value 0 with probability $1-q$ and backoff value CW with probability q. As in UVBEB, when a node encounters a collision, the value of CW is doubled up to a maximum value of CW_{max}, and upon successful transmission, the value of CW is reset to CW_{min}.

In this chapter, we analyze the behavior of XVBEB from the perspective of selfishness detection. First, we present an algorithm for backoff value deduction for the XVBEB protocol. In effect, we show how the backoff values of an XVBEB station can be derived from the number of empty slots between the station's two successive successful transmissions and the collision timeline for that time period. At the same time, we explain the difficulty of backoff value deduction for the UVBEB scheme. Second, we present a statistical test for sample validation, that determines with a desired degree of accuracy whether an XVBEB or a UVBEB node is behaving selfishly or if the deviation from the a priori specified distribution profile could be due to chance. We show that the sample size needed to perform the test to a desired degree of accuracy is more for UVBEB than for XVBEB in higher backoff stages. Together, the results show that selfishness detection is feasible for an XVBEB-based protocol, and can be performed more efficiently than for UVBEB .

5.1 Backoff value deduction

In this section we investigate whether it is possible to deduce the backoff values choices of a particular monitored node by observing the events occurring on the wireless medium. To analyze these events, we use the notion of *virtual slots*. As defined in [DV05], there are several types of virtual slots, depending on the access method. For example, in Basic access, there are five types of virtual slots: empty (all stations are backing off or idling), collision, data errors, ACK errors and successful transmission slots.

During channel contention, the number of collisions and the number of empty slots between two successive successful transmissions of a station are always known. Indeed, there are two possible outcomes following a communication attempt: failed or successful transmission. In the case of a successful attempt, the identity of the transmitting node is contained within the packet and becomes known to everyone within its transmission range. If the failure is due to a collision, however, there is no information about the identity of the colliding nodes. If an agent participates in a collision, it chooses a new backoff value; if not, it has to keep counting down after the collision virtual slot expires. Due to this limitation, in UVBEB it is almost always impossible to decompose the number of empty slots in a way to deduce the backoff value choices of a given station.

As an example, consider a simple 802.11 contention timeline as shown on Figure 15.

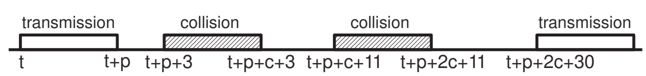

Figure 15: 802.11 contention timeline

A node being monitored starts transmission at time at time t for a duration of time p. Then, there are 3 empty slots followed by a collision slot at time $t + p + 3$ which lasts time c, followed by another collision after 8 empty slots. Finally, 19 empty slots after the second collision, the monitored node successfully transmits another packet. There might have been other types of virtual slots initiated by other nodes and which contained identity information, but we omit all frames in which the monitoring node had no implication. There are several possibilities for the node's backoff values depending on whether the station has participated in some of the collisions:

- The station has not participated in any of the collisions, meaning the node has a single backoff value of 30.
- The station has been involved in the first collision only, so its backoff values are 3 and 27.
- The node has contributed to the second collision only. In this case, 11 and 19 are its backoff values.
- The observed node has participated in both collisions. Here, the backoff values are 3, 8 and 19.

This example serves to illustrate that we cannot make any conclusions about the nodes' choices of backoff values in UVBEB. In fact, a deduction would only be possible if there were no collisions between two successful transmissions of the same node. With the XVBEB algorithm, however, it turns out it is always possible to deduce the backoff values of a station.

To illustrate how the number of empty slots can be uniquely decomposed to obtain the backoff values of an observed station, we examine all possible channel contention outcomes. Consider the contention tree shown on Figure 16. It illustrates all possible contention paths (for up to 6 successive collisions) following a successful transmission (the root node) provided the first backoff value choice of an XVBEB node is 0. The vertices represent transmission attempts, and the number at a vertex represents the total number of empty slots needed to get to the vertex. The number x/y at an arc indicates the node's backoff value x while the current size of the contention window was y. An observed node follows a path in the tree based on its choice of backoff values and whether or not it experiences a collision when it tries to transmit.

However, the observing authority does not know the exact path followed by a given node. Yet, it does know the number of idle slots between two successive successful transmissions and when collisions occurred (without knowing the identity of the colliding nodes). It turns out that this information along with the nature of the XVBEB procedure allows us to decompose the number of empty slots between a node's successful transmissions.

For example, suppose the number of idle slots between a nodes' two consecutive successful transmission attempts is 190 and there have been exactly 2 collisions in between. We can certainly conclude that the node has collided two times in a row with backoff values of $0, 63$, and 127.

Consider the scenario of 190 empty slots and 3 collisions. Here, some ambiguity may arise. For example, the observed station might have participated in all three collisions before succeeding with backoff values $0, 63, 127, 0$ or it might have participated in only two of the collisions with $0, 63$, and 127 as backoff values (some other nodes participated in the third collision). Fortunately, it is possible to distinguish between the 2 possibilities by observing the collision timeline: $0, 63, 127, 0$ implies a collision slot right before the successful transmission, whereas $0, 63, 127$ implies an empty slot before the second successful transmission. Similarly, if there were 5 or more collisions and 190 empty slots, the number of successive collision slots right before the transmission allow to deduct the backoff values. For instance, 3 collision slots indicate $0, 63, 127, 0, 0, 0$ backoff values. The decomposition as a sum

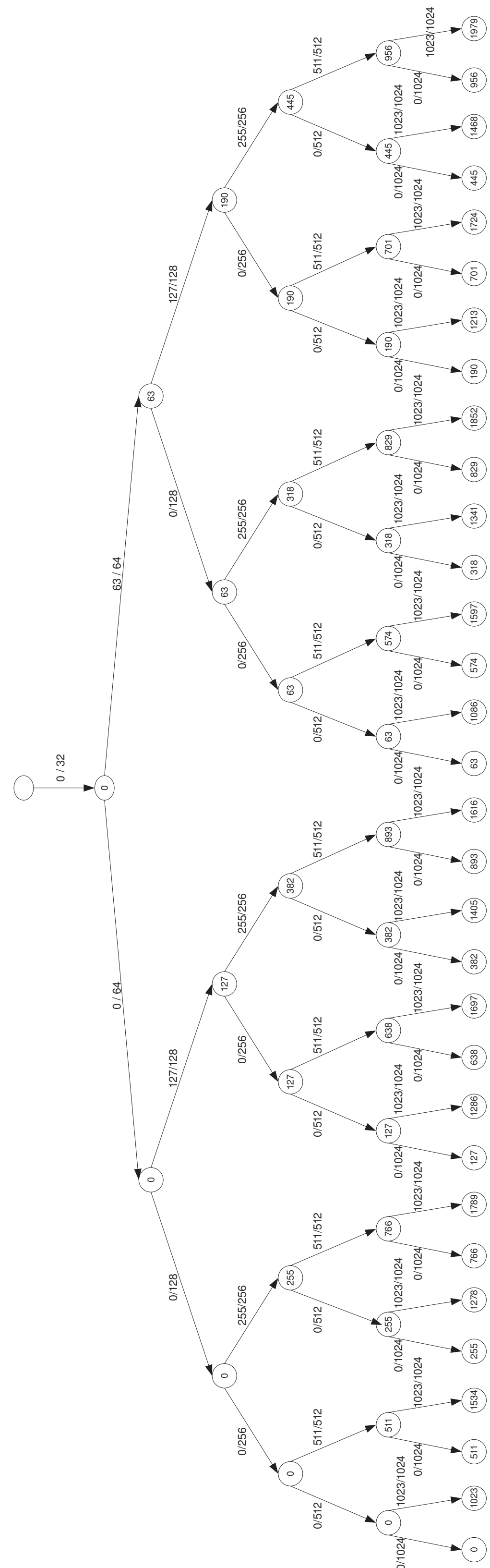

Figure 16: Contention tree

of powers of two in conjunction with the collision timeline guarantees the unique and correct deduction of the station's backoff values.

To summarize, our backoff value deduction scheme works as follows. Denote the number of empty slots between two successful transmissions from the same node as E. This number is decomposed to determine all possible paths that the node's choices could produce on the collision tree. In 802.11b for example, where $CW_{min} = 31$ and $CW_{max} = 1023$ (6 backoff stages), the decomposition of E is done by finding all possible solutions to Equation 17:

$$E = 31\nu_0 + 63\nu_1 + 127\nu_2 + 255\nu_3 + 511\nu_4 + 1023\nu_5$$

, where

- ν_i, $0 \leq i \leq 4$ is either 0 or 1, where 1 represents the possibility that a node opts for CW_i as a backoff value at stage i.
- ν_5, $0 \leq \nu_5 \leq \frac{E}{1023}$ is the number of times a node that is backing off at the last stage chooses its backoff value as CW_{max}.

This decomposition represents the shortest path to a vertex of the contention tree containing E. Further, the collision timelime is checked to determine whether other vertices containing E are reached with backoff value of zero . This ensures that that the number of empty slots is correctly decomposed to determine the node's backoff values.

5.2 Sample validation for XVBEB

We have already shown in Section 5.1 how to collect samples in a XVBEB network and explained why this is not possible with the UVBEB scheme. We will now investigate the sample validation problem for XVBEB. The problem is approached using the χ^2 *goodness-of-fit* test. We start by giving a general description of how to use the test and proceed by describing the application to XVBEB.

5.2.1 Goodness-of-tit test

The *Goodness-of-fit* χ^2 test is used to compare observed data with expected results and aims to determine whether the difference between the two is a result of chance or other factors. One can take the *null hypothesis* to be that there is a significant difference between the expected and the observed result. Alternatively, the null hypothesis could be that there is no significant difference between expectations and the observations. The χ^2 test is a test to verify the null hypothesis in either way.

Several steps are involved in conducting a χ^2 *goodness-of-fit* test: stating the hypotheses, defining the test parameters, analyzing the sample data and interpreting results:

- Hypothesis statement. Two hypothesis testing approaches exist. One approach is to form the null hypothesis H_0 as something that is the logical opposite of what the actual belief is. Once the observation data is gathered, the researcher's goal is to show that most likely H_0 is false, and, therefore, should be rejected. This is called *Reject-Support testing* (RS testing). The opposite approach is to accept as H_0 what the actual belief is and try to show that H_0 is true. That is called *Accept-Support testing* (AS testing).

For example, suppose that the purpose of a test is to determine whether a coin is fair. If the belief is that the coin is fair and RS testing approach is followed, H_0 would state that the coin is not fair and the goal would be to reject H_0 using the χ^2 test.

- Test parameters definition. To test a hypothesis against collected sample data, a parameter called *significance level* needs to be specified. The significance level of a test represents the maximum probability of mistakenly rejecting the null hypothesis. The lower the level, the less chances are that H_0 is rejected (stronger evidence is required to reject the null hypothesis). If one argues there is only one chance in a hundred this could have happened by coincidence, it implies a significance level of one percent ($\alpha = 0.01$). There is a trade-off associated with smaller significance levels because it increases the chances of failure to reject a false null hypothesis. Often, researchers choose significance levels equal to 0.01 or 0.05, but any value between 0 and 1 could be used.

- Analysis of the observed data. The analysis of the test results consist in calculating the following three values: the *degrees of freedom*, *test statistic* and the p-*value* associated with the test statistic. The *degrees of freedom* is equal to the number of levels of the categorical variable minus 1. In the coin flipping example, there are two categorical variables, but knowing that the number of heads is 42 out of 100 tosses, the number of tails is determined to be 58. Hence, there is one degree of freedom. Similarly, a fair six-sided dice problem has 5 degrees of freedom.

The *test statistic* X^2, also called Pearson's cumulative test statistic, which asymptotically approaches a χ^2 distribution and is calculated by the formula:

$$X^2 = \sum_{i=1}^{n} \frac{(O_i - E_i)^2}{E_i}$$

where O_i is the observed frequency, E_i is the expected frequency as stated in the null hypothesis and n is the number of the categorical variables. In the fair coin case, the test statistic is

$$X^2 = \frac{(42 - 50)^2}{50} + \frac{(58 - 50)^2}{50} = \frac{128}{50}$$

Finally, the p-*value* of the test is the probability that values bigger or equal to the test statistic could be observed in a χ^2 distribution and is defined as $p = 1 - cdf$ (cumulative distribution function). The cdf expresses he probability of having obtained a value less extreme than the parameter x. The cdf of the χ^2 distribution with k degrees of freedom is given by Equation 17:

$$CDF_c = \frac{\gamma(k/2, x/2)}{\Gamma(k/2)} \tag{17}$$

, where $\Gamma(k)$ is the Gamma function and $\gamma(k, x)$ is the lower incomplete Gamma function.

- Acceptance or rejection of the null hypothesis. Once the p-value for the test statistic is determined, it is compared against the significance level. If the value is greater than the significance level, the null hypothesis would not be rejected. If the p-value is smaller than the significance level, H_0 is rejected. In our coin flipping example, the p-value is 1 - 0.89 = 0.11, so we would conclude that the coin is fair even at significance level of 0.1.

In some situations, undesirable results might occur. There are two possible erroneous outcomes. Type I error (false positive) happens when H_0 is true, but the test claims it is false. The probability of committing Type I error is in fact the significance level α.

There exists another possible error a test could produce: the test could confirm the null hypothesis, whereas in reality it is false. This is called Type II or β-error (false negative). The possibility of committing Type II error is calculated using the *power of the test* and is denoted as β. The power of a test is the probability that the test would not accept untruthfully an alternative hypothesis and is equal to $1 - \beta$.

Researchers' goal should be to minimize both errors. As previously noted, there is a trade off between Type I and Type II errors. Table 1 summarizes the possible outcomes of a statistical test [KMW08]:

		True state of population	
		H_0	H_1
Conclusion	H_0	Correct Acceptance	Type II Error (β)
	H_1	Type I Error (α)	Correct Rejection

Table 1: Possible outcomes of a statistical test

The Type II error of a test is calculated using the power of the test. The power of a test is a function of the number of observations, the size of the effect in the population and the standards or criteria used to test statistical hypotheses:

- Number of samples. The most efficient way of increasing the power of a test is by increasing the number of observations.

- Size of the effect. The size of the effect is the magnitude of the expected results. The larger the effect size (larger deviation) the higher the power.

- Test parameters. Higher significance levels (i.e. the easier to reject H_0) increase the power of a test.

To calculate the exact power, a particular *alternative* hypothesis H_a (or a set of alternatives) has to be specified and the probability of accepting the null hypothesis if in fact the alternative had been evaluated as being truthful. To calculate the probability β of committing Type II error against the alternative hypothesis, a generalization of the χ^2 distribution is used, called *noncentral* χ^2 distribution [Fer96]. Designate the null hypothesis as a distribution $\gamma^0 = \{r_1^0, r_2^0, \ldots, r_k^0\}$ and the alternative as $\gamma^a = \{r_1^a, r_2^a, \ldots, r_k^a\}$. Let $\delta_j = \sqrt{N}(r_j^a - r_j^0)$ (where N is the number of samples). The *noncentrality parameter* λ of the noncentral χ^2 distribution is a function of the number of samples and is given by Equation 18.

$$\lambda = \sum_{j=1}^{k} \delta_j^2 / r_j^0 \tag{18}$$

For example, to calculate λ for a fair coin (0.5/0.5) against the alternative (0.4/0.6) for 100 tosses, Equation 18 writes as:

$$\lambda = \frac{100(0.4 - 0.5)^2}{0.5} + \frac{100(0.6 - 0.5)^2}{0.5} = 2 + 2 = 4$$

Once the noncentrality parameter λ is derived from Equation 18, it is substituted in Equation 19, which defines the cumulative distribution function of the noncentral χ^2 distribution (CDF_{nc}) and represents the power of the test against γ^a:

$$CDF_{nc}(x;\lambda;k) = \sum_{i=0}^{\infty} e^{\lambda/2}\frac{(\lambda/2)^i}{i!}CDF_c(x;k+2i) \tag{19}$$

where $CDF_c(x;k)$ is the cdf of the central χ^2 distribution for k degrees of freedom. Finally, the possibility of committing Type II error is approximated as $\beta = 1 - CDF_{nc}$.

Thus, the number of samples needed to perform the test is calculated numerically according to the desired acceptable Type I and II error levels and some predefined alternative behavior. First, the quantile of the central χ^2 is calculated for the specified α. The quantile function is the inverse of the cdf; it specifies the maximum value of the random variable for some given probability. Then, given the centrality quantile, the equation for the cumulative distribution function of the noncentral χ^2 is solved for λ to meet the desired Type II error level β. Once the value of λ is derived, the necessary number of observations is determined by Equation 18.

It needs to be mentioned that the sampling distribution of the test statistic that is calculated is only approximately equal to the theoretical chi-squared distribution. The approximation is inadequate when sample sizes are small, or the data is very unequally distributed. The approximation is poor when the expected cell counts are small. There are different rules of thumb of what the number of samples should be, with the most common (and conservative) one being that the expected cell frequency for each cell should be at least 1 ($Nr_i \geq 1$) and no more than 20% of the cells should have an expexted count of less than 5 [Ros04].

Hence, the number of samples needed to achieve certain power and confidence level should be the greater of the values calculated by Equation 18 and the number of samples needed to satisfy the χ^2 approximation.

5.2.2 Application to XVBEB

When XVBEB is used as a backoff procedure, the null hypothesis H_0 states that for backoff level i, the collected sample data is distributed according to $(1-q_i, 0, 0, \dots, 0, q_i)$ distribution over the $[0, CW_i - 1]$ range. Since any backoff value different than 0 or $CW_i - 1$ results in immediate detection of misbehavior, H_0 that needs be evaluated becomes simply $(1 - q_i, q_i)$ over the two values 0 and $CW_i - 1$.

Note that there are many ways a station can alter its distribution profile, so we focus our analysis on rational cheaters that aim to increase their throughput. The misbehavior is generalized as follows: in each backoff level i a cheater would increase the probability of choosing the backoff value 0 by a positive value ω_i and decrease the probability of choosing CW_i by that same amount. Thus the alternative hypothesis H_a becomes $(1 - q_i + \omega_i, q_i - \omega_i)$.

The ultimate goal is to accept or reject the null hypothesis that the nodes are behaving according to the backoff procedure. While doing this, we want to minimize *both* Type I (α) and Type II (β) errors: that is identifying normally behaving nodes as cheaters and vice-versa.

The non-centrality parameter for the XVBEB algorithm is shown in Equation 20.

$$
\begin{aligned}
\lambda &= \frac{N_i^{XVBEB}(1 - q_i + \omega_i - 1 + q_i)^2}{1 - q_i} + \\
&\quad + \frac{N_i^{XVBEB}(q_i - \omega_i - q_i)^2}{q_i} \\
&= \frac{N_i^{XVBEB}\omega_i^2}{q_i(1 - q_i)} \qquad (20)
\end{aligned}
$$

Hence, Equation 21 allows us to calculate the number of samples needed to detect selfish behavior:

$$
N_i^{XVBEB} = \frac{\lambda q_i(1 - q_i)}{\omega_i^2} \qquad (21)
$$

It is worth noting that the number of samples needed in the XVBEB case depends on the choice of q_i. More observations are needed to achieve the same power when q_i is close to 0.5 (worst case being $q_i = 0.5$). Almost three times fewer samples are needed when $q_i = 0.1$ compared to the $q_i = 0.5$ case.

To illustrate this result, we examine some particular cases. For simplicity, suppose the stations are required to choose according to the $(0.5, 0.5)$ distribution at all backoff stages and that three types of alternative behaviors are evaluated: $(0.6, 0.4), (0.75, 0.25)$ and $(0.9, 0.1)$ at three different error levels: $\alpha = \beta = 0.05$, $\alpha = \beta = 0.01$ and $\alpha = \beta = 0.001$.

Table 2 shows the numerically calculated values for λ given these error levels and one degree of freedom.

By substituting the values from Table 2 in Equation 21, we obtain the number of samples needed to detect each type of misbehavior, as shown in Table 3.

Note that the greedier the station becomes (the larger the effect size), the easier

$\alpha = \beta = 0.05$	$\alpha = \beta = 0.01$	$\alpha = \beta = 0.001$
12.9947	24.0313	40.7141

Table 2: Noncentrality parameter with one degree of freedom

	$\alpha = \beta = 0.05$	$\alpha = \beta = 0.01$	$\alpha = \beta = 0.001$
$(0.6, 0.4)$	325	601	1018
$(0.75, 0.25)$	52	96	163
$(0.9, 0.1)$	20	38	64

Table 3: Number of samples needed to detect selfish XVBEB nodes

it becomes to detect misbehavior.

Once the required samples are collected, it is straightforward to put the station to the χ^2 test and determine whether the station is misbehaving.

5.3 XVBEB and UVBEB comparison

In Section 5.1, we showed how to obtain samples for the XVBEB procedure and explained why it is rarely possible to do the same with the UVBEB scheme. In this section, XVBEB and UVBEB are compared against each other in terms of the number of samples needed to detect selfishness, *assuming* the backoff values of a monitored UVBEB node are somehow known.

In Section 5.2, the null hypothesis for XVBEB nodes was shown to be $(1-q_i, q_i)$ over the two values 0 and CW_i-1. In the UVBEB procedure, the expected distribution profile is uniform, so the null hypothesis H_0 would be that node is choosing its backoff values according to the probability distribution $(\frac{1}{CW_i}, \frac{1}{CW_i}, \ldots, \frac{1}{CW_i})$, where CW_i is the current size of the contention window for the i^{th} backoff stage.

In XVBEB we have only 1 degree of freedom, whereas in UVBEB there are different degrees of freedom at the different backoff stages (31 for the first backoff stage, 63 for the second, etc). Therefore, to compare the schemes, we propose a generalized cheating model that fits both procedures. The XVBEB selfish behavior described in Section 5.2 can be looked at as if a cheater assigns higher probability on the values of the first half of the contention window range and less on the second. The equivalent misbehavior for a UVBEB station is in each backoff level i to increase the probability of choosing each value in the first half of the backoff range by a positive value ϵ_i and decrease the probability of choosing each value in the second half by that same amount. Thus the alternative hypothesis H_a for the UVBEB scheme is that a node would choose each value in $[0..\lfloor(CW_i-1)/2\rfloor]$ with probability $\frac{1}{CW_i}+\epsilon_i$ and each remaining value with probability of $\frac{1}{CW_i}-\epsilon_i$.

The non-centrality parameter in XVBEB is given by Equation 20, whereas Equation 22 presents the expression for λ in UVBEB.

$$\begin{aligned}\lambda &= \frac{CW_i}{2}\frac{N_i^{UVBEB}(\frac{1}{CW_i}+\epsilon_i-\frac{1}{CW_i})^2}{\frac{1}{CW_i}}+\frac{CW_i}{2}\frac{N_i^{UVBEB}(\frac{1}{CW_i}-\epsilon_i-\frac{1}{CW_i})^2}{\frac{1}{CW_i}}\\ &= N_i^{UVBEB}\epsilon_i^2 CW_i^2 \end{aligned} \tag{22}$$

Thus, the number of samples needed to detect selfishness for the XVBEB and UVBEB procedure are given by Equation 21 and 23 respectively.

$$N_i^{UVBEB}=\frac{\lambda}{\epsilon_i^2 CW_i^2} \tag{23}$$

To compare the number of samples needed to detect selfishness, we look at a few particular examples. Again, we have to model the behavior in a way to be able to compare both schemes. We establish the correspondence between the parameters ϵ_i and ω_i in terms of the transmission probability τ, that is, they are chosen so as to achieve the same transmission probability. For simplicity, the models are compared in saturated conditions. The q_i parameter in the XVBEB algorithm is set to 0.5 at all backoff stages, which is shown in Chapter 6 to be equivalent to the UVBEB backoff in terms of saturation throughput. As noted previously, this is also the worst case scenario for the number of samples needed to detect selfishness. Solving numerically Bianchi's equation for the transmission probability [Bia00] of normally behaving UVBEB nodes yields the values for τ in Table 4, which is the same for the XVBEB mechanism with $q_i = 0.5$ as shown in [GNA11].

number of nodes	τ
3	0.0537218
5	0.0478464
10	0.0373051
20	0.0264229
30	0.0209678
40	0.0176494
50	0.0153917

Table 4: Values of τ in a system of well behaving nodes

For the purpose of stating the alternative hypotheses, the three degrees of cheating are defined as: low level cheaters increase their transmission probability τ by 10%, medium by 50% and high by 90%. The level of cheating represents the effect size: cheating becomes easier to detect (fewer samples are needed) as nodes become greedier and aim for higher transmission probabilities. To influence its transmission probability, a node following the UVBEB algorithm modifies its ϵ_i parameters; XVBEB nodes change their ω_i. Table 5 reflects the numerically calculated values of ϵ_0 needed for the nodes to increase their transmission probabilities by 10, 50 and 90 percent. The table shows the values of ϵ for the zero backoff stage. For simplicity, we assume that the ϵ_{i+1} values of the upper backoff stages are half the ϵ_i value of the previous backoff stage. Different ϵ assignments may lead to other possible cheating strategies, such as a mix of normal and selfish behavior. An example of such a mixed cheating strategy would be to behave normally ($\epsilon = 0$) in the lower backoff stages (e.g. $CW = 32, CW = 64$) and misbehave in the higher stages. A not very aggressive cheater might not mind waiting for 31 slots, but the idea of waiting 1023 slots would not seem highly attractive. Such behavior can be also specified as an alternative hypothesis and put to the χ^2 test.

number of nodes	ϵ_0 (low τ)	ϵ_0 (medium τ)	ϵ_0 (high τ)
3	0.00583862	0.0214084	0.0304224
5	0.00582102	0.0213439	0.0303308
10	0.00578986	0.0212294	0.030168
20	0.005758	0.0211123	0.0300017
30	0.005742	0.021054	0.0299189
40	0.00573257	0.0210189	0.0298689
50	0.00572593	0.0209949	0.0298349

Table 5: Values of ϵ required to increase τ as desired

The ω_i values can either be calculated numerically or expressed as function of ϵ_i by incorporating them into the XVBEB and UVBEB transmission probability equations as derived in Chapter 6 and [Bia00]. To obtain equal transmission probability, for all backoff stages ($i \in (0,5)$) they must satisfy:

$$\begin{aligned}(1-q_i-\omega_i)+(q_i-\omega_i)W_i &= \sum_{k=1}^{\frac{W_i}{2}} k(\frac{1}{W_i}+\epsilon_i)+\sum_{k=\frac{W_i}{2}+1}^{W_i} k(\frac{1}{W_i}-\epsilon_i) \\ &= \frac{W_i+1}{2}-\epsilon_i\frac{W_i^2}{4}\end{aligned}$$

Thus, the general link between ω_i and ϵ_i in terms of saturated transmission probability is given in Equation 24.

$$\omega_i = \frac{\epsilon_i W_i^2 + 4q_i W_i - 2W_i + 3 - 4q_i}{4W_i - 1} \tag{24}$$

In the $q_i = 0.5$ case, Equation 24 becomes:

$$\omega_i = \frac{\epsilon_i W_i^2 - 1}{4W_i - 1} \tag{25}$$

Table 6 shows the values of ω_0 calculated by Equation 25 needed for the nodes to increase their transmission probabilities by 10, 50 and 90 percent in the XVBEB case at the zero backoff stage.

number of nodes	ω_0 (low τ)	ω_0 (medium τ)	ω_0 (high τ)
3	0.048215701	0.176791948	0.251230142
5	0.048070359	0.176259303	0.250473703
10	0.047813037	0.175313755	0.24912929
20	0.047549935	0.174346735	0.247755974
30	0.047417806	0.17386529	0.247072206
40	0.047339933	0.173575432	0.246659303
50	0.047285099	0.173377239	0.246378529

Table 6: Values of ω required to increase τ as desired

Since the distribution profiles must remain valid (i.e. the probabilities should not be more 1 or less than 0), the ϵ_i values are constrained by $\epsilon_i < 1/32 = 0.03125$ and the ω_i values by $\omega_i < 0.5$. However, ϵ_i and ω_i should satisfy one additional requirement. Since $\omega_i > \omega_{i+1} \forall i \in (0, 4)$, the condition (as found in Chapter 6) for a unique solution of the transmission/collision probability system of equations is satisfied. It is easy to show that in the UVBEB procedure with the $\epsilon_i = 2\epsilon_{i+1}$ assignment, the system has a unique solution.

Tables 5 and 6 allow us to express the alternative hypotheses. For example, H_a for the first backoff stage and low level of cheating with 3 nodes would correspond to assigning $1/32 + 0.00583862$ on the first 16 backoff values and $1/32 - 0.00583862$ on the second half. Thus the corresponding alternative distribution profile would be $(0.03708862, \ldots, 0.03708862, 0.02541138, \ldots, 0.02541138)$.

Now that all parameters are established to define equivalent behavior in both XVBEB and UVBEB algorithms, as in Section 5.2, the number of samples needed is calculated for three different acceptable error levels: $\alpha = \beta = 0.001, 0.01$, and 0.05. The non-centrality parameter (λ) values corresponding to the degrees of freedom and error levels are numerically calculated in Table 7

The values in Tables 5, 6 and 7 allow us to calculate the number of samples required to remain within the acceptable error levels for the three degrees of cheating at the different backoff stages.

As it turns out that there is not much of a difference between the number of required samples to detect selfishness for different numbers of nodes, we only show the results for three nodes. Figures 17, 18 and 19 illustrate the volume needed to determine whether a node is misbehaving or not at low, medium and high degree of

DF	$\alpha = \beta = 0.001$	$\alpha = \beta = 0.01$	$\alpha = \beta = 0.05$
1	40.7141	24.0313	12.9947
31	83.3501	56.465	35.9491
63	104.601	72.3987	47.1527
127	134.246	94.6259	62.7991
255	175.8	125.806	84.7757
511	234.232	169.69	115.74
1023	316.568	231.577	159.442

Table 7: Noncentrality parameter for different degrees of freedom

cheating at $\alpha = \beta = 0.001$ precision levels. The values in Figures 18 and 19 reflect the fact that the number of observations needed as derived by Equation 18 is smaller than the number needed to satisfy the approximation rule. Only the numbers obtained from Equation 18 are shown in Figure 17 because the approximation condition is already satisfied. For example, at the zero backoff stage with error rates of 0.001, 64 samples are needed to detect high level of misbehavior for three nodes in UVBEB by Equation 18; however, the approximation would only be good if 160 samples have been collected, which is the same number needed to detect selfishness in a XVBEB node.

Finally, note that the number of samples needed to detect misbehavior in UVBEB mode drastically increases when CW increases. Table 8 illustrates the percentage of the time 10 competing nodes spend in the different backoff stages obtained by simulations. It is no surprise that the nodes spend most of their time in the first two backoff stages, so the time needed to collect the required number of samples at these stages is not a concern. On the contrary, the number of samples required drastically increases at the higher backoff stages for the UVBEB backoff

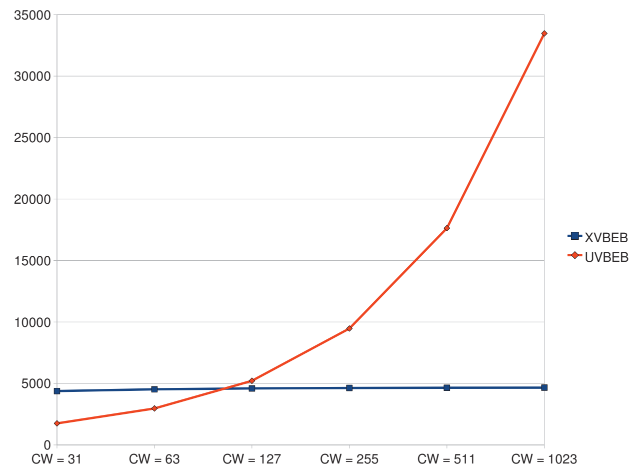

Figure 17: Number of samples, low degree of cheating

Figure 18: Number of samples, medium degree of cheating

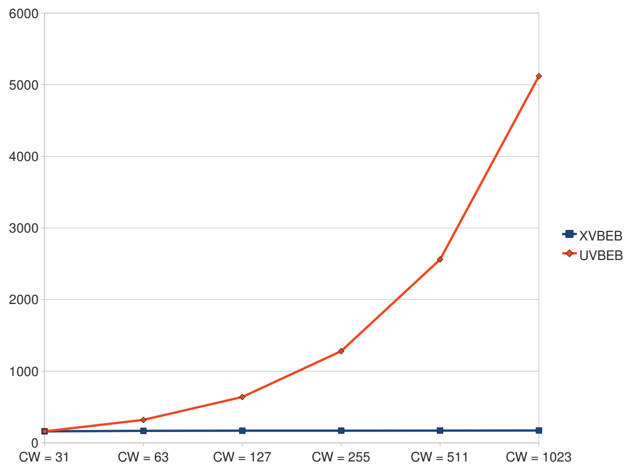

Figure 19: Number of samples, high degree of cheating

algorithm. This trend along with the fact that the nodes spend only small portion of their contention time at the higher backoff stages would make the sample collection process extremely time consuming for the UVBEB protocol.

Number of Attempts	UVBEB nodes	XVBEB nodes
1	72.0%	86.8%
2	20.0%	6.3%
3	5.5%	3.1%
4	1.7%	1.8%
5 or more	0.6%	2.0%

Table 8: Backoff stage profiles for 10 nodes

Chapter 6

Performance Evaluation of Backoff Algorithms for Medium Access in Wireless Networks

In Chapter 5, we defined an alternative backoff procedure for IEEE 802.11 stations to make possible the detection of selfish nodes. Yet, the gain in reliability would be negated if the procedure resulted in poorer use of the network resources. Therefore, we study the performance of the 802.11 MAC protocol using XVBEB as the backoff scheme and compare it against the classic IEEE 802.11 protocol, which uses UVBEB as a backoff scheme. For convenience, we call the modified protocol the XVBEB protocol, reiterating that the only difference between the XVBEB protocol and the 802.11 protocol is in the backoff scheme. We provide a theoretical analysis of the throughput of the XVBEB protocol in saturation conditions and prove that the throughput of our protocol with $q = 1/2$ exactly matches the throughput of the 802.11 protocol. We show that the value of q that maximizes the saturation throughput is a function of the number of the nodes in the network. In the absence of knowledge of number of nodes, there is no single value of q that maximizes the throughput for all network sizes. If the nodes have access to the number of nodes in the network, then we prove that it is possible to obtain an improvement over the optimal version of 802.11 in which contention window sizes can be changed as a function of the number of nodes in the network.

We validate our model with extensive simulations using ns-2. In fact, our protocol enjoys a higher throughput in simulations than the model predicts, both in the case when there is no knowledge of the number of nodes and the case when the number of nodes is known, for saturated CBR traffic. The pattern of access appears different for the two protocols; in our protocol, nodes display a limited amount of *channel capture* compared to 802.11; however, simulation results show that our protocol enjoys a high fairness index. We simulated both algorithms for VBR (video) traffic as well as VoIP traffic. In both cases, the XVBEB protocol (optimized and non-optimized versions) demonstrates a lower packet loss rate, packet delay, and packet delay variation than the 802.11 protocol for a variety of load conditions for different numbers of nodes.

6.1 Analytical modeling

In this section, we analyze the behavior of a node following the XVBEB protocol using a Markov model, similar to the model used in [Bia00]. In fact, we model a somewhat more general protocol, in which at a given backoff stage i, we choose to delay transmission with probability q_i. In other words, the probability of delaying transmission can be different in different backoff stages. We obtain the transmission probability τ of a node in a slot time, independently of details of the protocol such as time necessary to sense the channel, the access mechanism etc. We proceed to express the throughput as a function of the computed value τ. We assume that there are n stations in *saturation conditions*, that is, each station always has a packet for transmission immediately after it successfully transmits. Let p be the conditional collision probability, assumed to be constant and independent for all nodes, and let m be the maximum number of backoff stages, that is, $CW_{max} = 2^m CW_{min}$. We denote the backoff value in stage i by W_i. It follows that $W_0 = CW_{min}$ and $W_i = 2^i W_0$ for $0 \leq i \leq m$. Finally, we denote the probability of choosing the backoff value W_i in stage i to be q_i. Clearly the probability of choosing the backoff value 0 in stage i is then $1 - q_i$. The Markov chain corresponding to such behavior in saturated conditions is shown in Figure 20.

Let $b_{i,k}$ be the stationary distribution of the chain. When $1 \leq i \leq m-1$ we have:

$$
\begin{aligned}
b_{i,W_i-1} &= q_i \; p \; b_{i-1,0} \\
b_{i,W_i-2} &= q_i \; p \; b_{i-1,0} \\
\vdots \\
b_{i,1} &= q_i \; p \; b_{i-1,0} \\
b_{i,0} &= (1 - q_i + q_i) \; p \; b_{i-1,0}
\end{aligned}
$$

Hence, for $1 \leq i \leq m-1$, since $b_{i,0} = p \; b_{i-1,0}$,

$$\sum_{k=0}^{W_i-1} b_{i,k} = b_{i,0}(1 - q_i + W_i \; q_i) \tag{26}$$

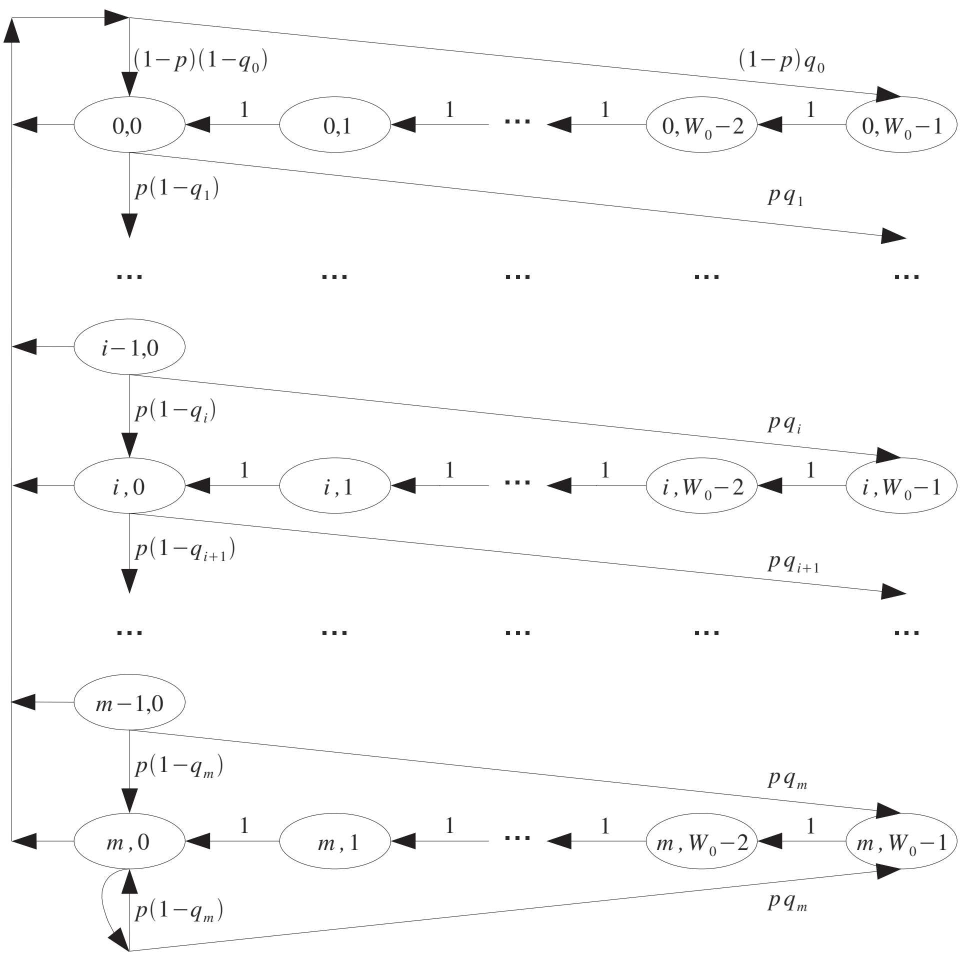

Figure 20: Markov chain for the XVBEB protocol

Similarly, for the first backoff stage $(i = 0)$

$$
\begin{aligned}
b_{0,W_0-1} &= q_0\ (1-p)\ \sum_{l=0}^{m} b_{l,0} \\
b_{0,W_0-2} &= q_0\ (1-p)\ \sum_{l=0}^{m} b_{l,0} \\
&\vdots \\
b_{0,1} &= q_0\ (1-p)\ \sum_{l=0}^{m} b_{l,0} \\
b_{0,0} &= (1 - q_0 + q_0)\ (1-p)\ \sum_{l=0}^{m} b_{l,0}
\end{aligned}
$$

Here again, because

$$b_{0,0} = (1-p)\ \sum_{l=0}^{m} b_{l,0}$$

we derive

$$\sum_{k=0}^{W_0-1} b_{0,k} = b_{0,0}\ (1 - q_0 + W_0\ q_0) \tag{27}$$

Finally, for the last backoff stage m, we have

$$
\begin{aligned}
b_{m,W_m-1} &= q_m\ p\ (b_{m-1,0} + b_{m,0}) \\
b_{m,W_m-2} &= q_m\ p\ (b_{m-1,0} + b_{m,0}) \\
&\vdots \\
b_{m,1} &= q_m\ p\ (b_{m-1,0} + b_{m,0}) \\
b_{m,0} &= (1 - q_m + q_m)\ p\ (b_{m-1,0} + b_{m,0})
\end{aligned}
$$

Since $b_{m,0} = b_{m-1,0}\ p + p\ b_{m,o}$

$$\sum_{k=0}^{W_m-1} b_{m,k} = b_{m,0}\ (1 - q_m + W_m\ q_m) \tag{28}$$

From equations 26, 27, 28 and the fact that $b_{i,0} = p^i.b_{0,0}$ and $b_{m,0} = \frac{p^m}{1-p}.b_{0,0}$, the normalization condition can be written as

$$\begin{aligned} 1 &= \sum_{i=0}^{m}\sum_{k=0}^{W_i-1} b_{i,k} \\ &= b_{0,0}\sum_{i=0}^{m-1} p^i\ (1 - q_i + W_i\ q_i) + b_{0,0}\frac{p^m}{1-p}\ (1 - q_m + W_m\ q_m) \end{aligned}$$

As in [Bia00], the stationary distributions of the chain allow us to express the transmission probability of a node τ as a function of q_i (Equation 29).

$$\tau = \frac{1}{(1-p)\sum_{i=0}^{m-1} p^i\ (1 - q_i + W_i q_i) + p^m(1 - q_m + W_m q_m)} \tag{29}$$

Clearly, the collision probability is given by:

$$p = 1 - (1-\tau)^{n-1} \tag{30}$$

Inverting Equation 30 to $\tau^*(p) = 1 - (1-p)^{\frac{1}{n-1}})$ allows to conclude that $\tau(p)$ is a continuous and monotone increasing function in $(0, 1)$ with extremes $\tau(0) = 0$ and $\tau(1) = 1$.

In contrast to [Bia00], the transmission probability in the XVBEB scheme (Equation 29) also depends on q_i. Thus, it cannot be claimed that $\tau(p)$ is decreasing in $(0, 1)$. In fact, it is easy to give a counterexample in which the function will not be decreasing. For two backoff stages, let $q_0 = 1/2$ and $q_1 = 1/8$. The transmission probability becomes $\tau = \frac{1}{(1-p)(1/2+W/2)+p(7/8+2W/8)}$, so $\tau(0) = \frac{1}{1/2+W/2}$ and $\tau(1) = \frac{1}{7/8+2W/8}$. Therefore, for $W \geq 2$, $\tau(0) < \tau(1)$.

By imposing certain conditions on q_i, however, we are able to ensure that function is non increasing in $(0, 1)$. Let $q_{i-1} \leq \frac{2W_{i-1}-1}{W_{i-1}-1} q_i$, $\forall i \in (1, m)$. Designate $\alpha_i = 1 - q_i + W_i\ q_i$ for each backoff level i. With these q_i values, we observe that $\forall i \in (1, m)$:

$$\begin{aligned}\alpha_{i-1} - \alpha_i &= q_{i-1}(W_{i-1} - 1) - q_i(2W_{i-1} - 1) \\ &\leq \frac{2W_{i-1} - 1}{W_{i-1} - 1} q_i(W_{i-1} - 1) - q_i(2W_{i-1} - 1) \\ &= 0 \end{aligned} \tag{31}$$

To prove that in Equation 29 $\tau(p)$ is non increasing, we need to show that $\frac{\partial \tau}{\partial p} \leq 0$ for $p \in (0, 1)$. The denominator of the partial derivative is always positive and the numerator N is:

$$\begin{aligned} N &= \alpha_0 - (1 - 2p)\alpha_1 - (2p - 3p^2)\alpha_2 - \ldots - ((m-1)p - mp^{m-1})\alpha_{m-1} - mp^{m-1}\alpha_m \\ &= (\alpha_0 - \alpha_1) + 2p(\alpha_1 - \alpha_2) + \ldots + (mp^{m-1})(\alpha_{m-1} - \alpha_m) \end{aligned}$$

By Equation 31, $N \leq 0$ for $p \in (0, 1)$, and therefore, the function is non increasing.

Since the extreme values $\tau(0) = \frac{1}{1-q_0+Wq_0} > 0$ and $\tau(1) = \frac{1}{1-q_m+2^m W q_m} < 1$, the system of Equations 29 and 30 has a unique solution.

By choosing $q_i = 1/2$ for all i in the range $0 \leq i \leq m$, and substituting $W_i = 2^i W$ in Equation 29, the expression for the transmission probability becomes the same as the one for UVBEB as found in [Bia00].

$$\begin{aligned}
\tau &= \frac{1}{(1-p)\sum_{i=0}^{m-1} p^i \, (1 - q_i + W_i \, q_i) + p^m \, (1 - q_m + W_m \, q_m)} \\
&= \frac{1}{(1-p)\sum_{i=0}^{m-1} p^i \, (1 - 1/2 + W_i/2) + p^m \, (1 - 1/2 + W_m/2)} \\
&= \frac{2}{(1-p^m) + (1-p)W\sum_{i=0}^{m-1}(2p)^i + p^m + W(2p)^m)} \\
&= \frac{2}{1 + W + pW\sum_{i=0}^{m-1}(2p)^i + p^m}
\end{aligned} \tag{32}$$

The expression for system throughput S has been derived in [Bia00]:

$$S = \frac{E}{T_s - T_c + \frac{\sigma(1-P_{tr})/P_{tr} + T_c}{P_s}} \tag{33}$$

where E is the average payload size, T_s is the average time the channel is sensed busy because of a successful transmission, T_c is the average time the channel is sensed busy because of a collision, P_{tr} is the probability that there is at least one transmission in the considered slot time, and P_s is the probability that a transmission occurring on the channel is successful and σ is the duration of an empty slot time. Since E, T_s, T_c are all constants depending on the access scheme (Basic Access or RTS/CTS, for example), the throughput is maximized when the following quantity is maximized. Let

$$M = \frac{P_s}{(1 - P_{tr})/P_{tr} + T_c/\sigma}$$

As M depends only on τ, and the transmission probability for the XVBEB scheme with probabilities $q_i = 1/2$ is the same as that of 802.11, the following somewhat surprising result follows:

Theorem 6.1.1. *The XVBEB protocol with probabilities* $q_i = 0.5$*, for* $0 \leq i \leq m$ *yields the same saturated system throughput as the 802.11 protocol.*

Next we study how changing the q_i probabilities influences the system throughput. One might ask the question whether there exist universal values of q_i such that the XVBEB protocol would yield better throughput than 802.11 for all numbers of nodes for fixed CW_{min} and CW_{max}. Figure 21 is a simple illustration of the numerically calculated system throughput for the XVBEB scheme with $q_i = 0.1, 0.25, 0.5, 0.75, 0.9$ for all backoff stages in an 1Mbps RTC/CTS enabled network with 3, 5, 10, 20 and 30 nodes. As expected, decreasing the q_i (assigning higher probabilities to the 0 backoff values) works better with smaller number of nodes while increasing the q_i helps with higher number of nodes.

To prove why no universal q_i values that improve the throughput regardless of the number of nodes exist, we examine the impact of changing the transmission probability on the system throughput. Let τ^* solve Equation 34:

$$(1 - \tau^*)^n - T_c\{n\tau^* - [1 - (1 - \tau^*)^n]\} = 0 \tag{34}$$

Lemma 6.1.2. *The expression* $M = \frac{P_s}{(1-P_{tr})/P_{tr}+T_c/\sigma}$ *is a decreasing function of* τ *in* $[\tau^*, 1]$ *and an increasing function in* $[0, \tau^*]$*.*

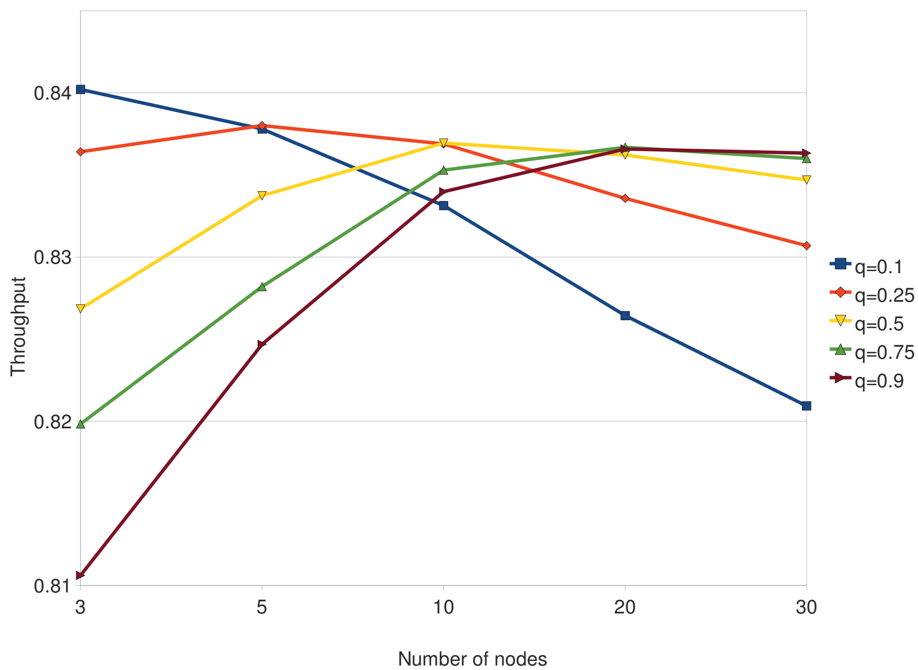

Figure 21: Calculated saturated throughput for different q_i

Proof. To prove that the expression is decreasing in $[\tau^*, 1]$, we need to look at the sign of the slope of the tangent line. The derivate of M with respect to τ is:

$$\frac{\partial M}{\partial \tau} = (1 - T_c^*)(1-\tau)^n - T_c^* n\tau + T_c^*$$

We need to show that $\frac{\partial M}{\partial \tau}(\tau^* + \epsilon) < 0$ for $0 < \epsilon < 1 - \tau^*$:

$$\begin{aligned}
\frac{\partial M}{\partial \tau}(\tau^* + \epsilon) &= (1 - T_c^*)(1 - \tau^* - \epsilon)^n - T_c^* n(\tau^* + \epsilon) + T_c^* \\
&= (1 - T_c^*)(1 - \tau^* - \epsilon)^n - T_c^* n(\tau^* + \epsilon) + T_c^* - \\
&\quad - (1 - T_c^*)(1 - \tau^*)^n + T_c^* n\tau^* - T_c^* \\
&= (T_c^* - 1)((1 - \tau^*)^n - (1 - \tau^* - \epsilon)^n) - T_c^* n\epsilon \\
&= (T_c^* - 1)\epsilon \sum_{k=0}^{n-1} (1 - \tau^*)^k (1 - \tau^* - \epsilon)^{n-1-k} - T_c^* n\epsilon \\
&< (T_c^* - 1)n\epsilon - T_c^* n\epsilon \\
&< 0
\end{aligned}$$

The proof that M is increasing of τ in $[0, \tau^*]$ is similar. □

Note that in the 802.11 protocol, the transmission probability depends only on the number of nodes and the contention window. In contrast, in the XVBEB protocol it also depends on q_i. Thus by fixing W and n, one could still influence τ, and, therefore, the system throughput. Lemma 6.1.2 allows us to establish the behavior of the system throughput for changing transmission probabilities.

Theorem 6.1.3. *For fixed number of nodes n and minimum contention window*

W the saturated system throughput S using a XVBEB profile increases if τ *is increased in* $[0..\tau^*]$ *or decreased in* $[\tau^*..1]$ *and vice-versa.*

Proof. As we already know, the system throughput S can be expressed as:

$$S = \frac{E}{T_s - T_c + \frac{\sigma(1-P_{tr})/P_{tr}+T_c}{P_s}} = \frac{E}{T_s - T_c + \sigma\frac{1}{M}}$$

By Lemma 6.1.2, S is an increasing function of τ in $[0, \tau^*]$ and a decreasing function in $[\tau^*, 1]$. □

It is now easy to show that there is no q_i assignment such that the XVBEB profile would produce better throughput than the uniform distribution regardless of the number of nodes for a given minimum contention window. Indeed, by observing Equation 29, we conclude that no matter how we change the q_i values, the transmission probability will either increase for any number of nodes or decrease no matter how many nodes are involved in a competition. By Theorem 6.1.3, increasing τ benefits the scenario where τ^* (obtained from Equation 34) is higher than the current transmission probability and vice versa. For example, in a 1Mbit RTS/CTS enabled network with 6 backoff stages τ^* for 3 nodes is 0.158557, whereas for 30 nodes it is less than one-tenth of that values: 0.0142753. In an XVBEB scheme with CW_{min}=32 and $q_i = 0.5\ \forall i \in [0..5]$, the transmission probability for 3 nodes becomes 0.0515231 and 0.0208665 for 30 nodes. Obviously, any changes to q_i that lead to the increase of τ would bring the transmission probability closer to τ^*, but, will on the other hand, make things worse for the 30 nodes network, which is the result observed in Figure 21.

6.2 Optimizing throughput

In this section we study the maximum achievable saturation throughput of the XVBEB protocol. In [Bia00], it was already shown that it is possible to compute the optimal transmission probability for a given number of nodes. Assuming the number of competing nodes is known, Bianchi showed that the optimal transmission probability is the solution to Equation 34: $(1-\tau^*)^n - T_c\{n\tau^* - [1-(1-\tau^*)^n]\} = 0)$. An interesting question is whether we can find an assignment of q_i to achieve a certain transmission probability (in turn to achieve a maximum throughput for given number of nodes). Due to the limitation $0 \leq q_i \leq 1$, it turns out this is not always possible if the size of the contention window stays fixed. For example, if we wanted to achieve system throughput of 0.83649 for thirty 1Mbps RTS/CTS enabled nodes, this corresponds to $\tau = 0.0142753$. Then using $CW_{min} = 32$, at least one q_i value would have to be bigger than 1 (if all $q_i = q$, then q would be 1.13526).

In [Bia00] it is shown that once the optimal transmission probability τ^* is calculated, the throughput can be optimized by finding the optimal minimum contention window W^* from the system of Equations 35 and 36:

$$\tau^* = \frac{2}{1 + W^* + p^*W^* \sum_{i=0}^{m-1} (2p^*)^i} \tag{35}$$

$$p^* = 1 - (1-\tau^*)^{n-1} \tag{36}$$

However, W^* is unlikely to be an integer, so in practice it needs to be rounded up to some value $\hat{W}$ as all the values in the backoff interval must be integers. In the

XVBEB scheme, the expression for the transmission probability also includes the distributions q_i (Equation 29). The easiest way to achieve the same throughput as the optimal 802.11 protocol follows directly from Theorem 6.1.1. To achieve the same throughput at the optimal 802.11, the XVBEB protocol is run with $q_i = 0.5$ and minimum contention window of $\hat{W}$. However, since the optimal contention window has been rounded up to an integer, the throughput in both uniform and XVBEB profiles will be slightly lower than the theoretical maximum. However, since in the XVBEB scheme the transmission probability also depends on the q_i values, it is possible to change them in a way to make up for rounding of the optimal value W^*. Let $W_i^* = 2^i W^*$ and $\hat{W}_i = 2^i \hat{W}$.

Theorem 6.2.1. *The saturated throughput in the XVBEB scheme with* $q_i^* = \frac{W_i^*-1}{2(\hat{W}_i-1)}$, $\forall i \in [0..m]$, *and minimum contention window* $\hat{W}$ *produces higher throughput than 802.11 with the same minimum contention window.*

Proof. The transmission probability of the XVBEB scheme is:

$$\tau_q = \frac{1}{(1-p_q)\sum_{i=0}^{m-1} p_q^i(1+(\hat{W}_i-1)q_i)+p_q^m(1+(\hat{W}_m-1)q_m)}$$

$$= \frac{1}{(1-p_q)\sum_{i=0}^{m-1} p_q^i(1+\frac{(\hat{W}_i-1)(W_i^*-1)}{2(\hat{W}_i-1)})+p_q^m(1+\frac{(\hat{W}_m-1)(W_m^*-1)}{2(\hat{W}_m-1)})}$$

$$= \frac{1}{(1-p_q)\sum_{i=0}^{m-1} p_q^i(\frac{W_i^*+1}{2})+p_q^m(\frac{W_m^*+1}{2})}$$

$$= \frac{2}{1+W^*+p_q W^*\sum_{i=0}^{m-1}(2p_q)^i}$$

such that $p_q = 1 - (1 - \tau_q)^{n-1}$. Bianchi showed that the system of Equations 35 and 36 has a unique solution in $[0..1]$; therefore, $\tau_q = \tau^*$. □

6.3 Simulation results

We now evaluate some aspects of both backoff approaches. To illustrate the differences between 802.11 and the XVBEB protocols, we first examine through simulations how the stations compete for access to the channel.

The transmission attempts of three competing nodes on a 1Mbps basic access channel over a period of 1 second is illustrated in Figures 22 and 23: the XVBEB protocol allows the nodes to send more successive packets, but they end up in the backoff procedure for more extended periods of time compared to the 802.11 protocol, where most often a node sends only one packet and then waits its turn to send subsequent packets. Intuitively, a node has a chance $q = 1/2$ in our experiments of being able to re-transmit immediately after a successful transmission in the XVBEB protocol, whereas in 802.11, it has only a $1/CW$ chance of immediate re-transmission.

To compare the performance of XVBEB and 802.11 the following aspects are evaluated in ns-2: saturation bandwidth, fairness (of the bandwidth), packet loss, delay and delay variation. Since the only difference between XVBEB and 802.11 is in the way the backoff values are selected, the single change in ns-2 to implement XVBEB involves the modification of the MAC timers.

Thus, four protocols are simulated:

- 802.11: all nodes behave according to the IEEE 802.11 standards.

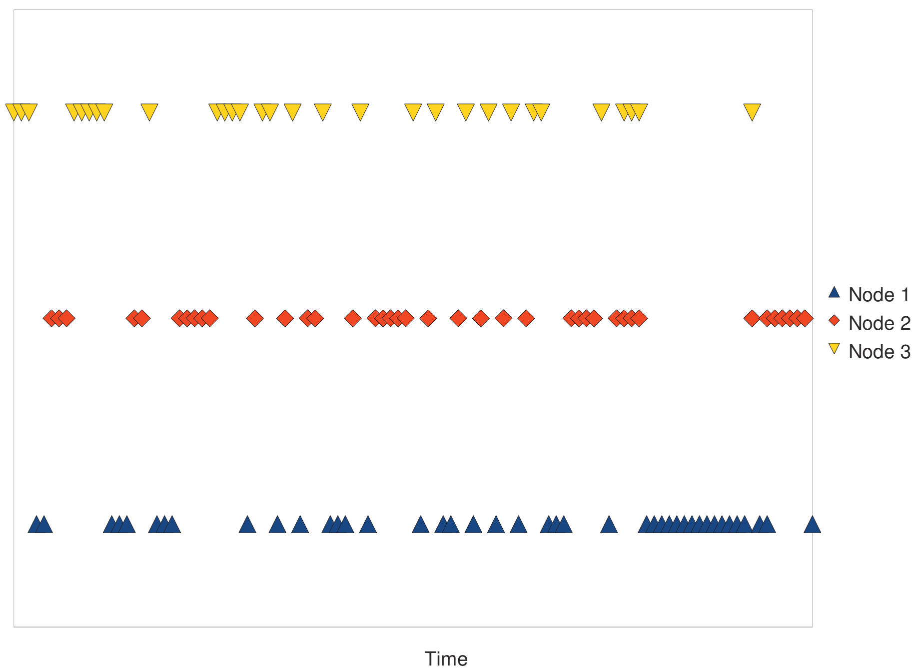

Figure 22: XVBEB channel access

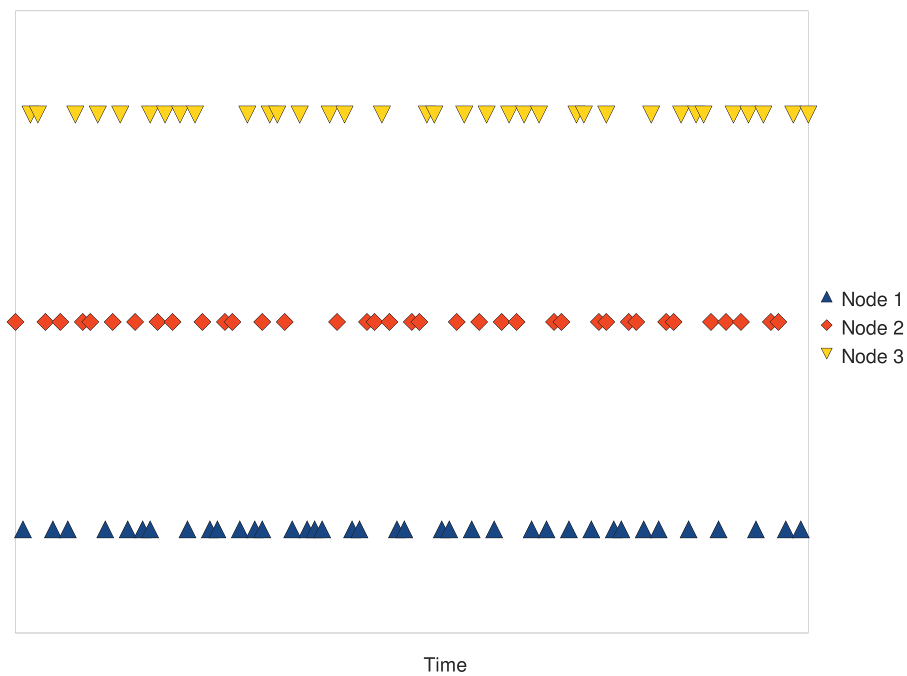

Figure 23: 802.11 channel access

- XVBEB : all nodes use the XVBEB approach with $CW_{min} = 32$ and $q_i = 1/2$.

- Optimal 802.11: all nodes choose randomly from 0 to $CW_{min} = \lfloor W^\star \rfloor$, where $W^\star$ is a function of the number of competing nodes.

- Optimal XVBEB : all nodes use the XVBEB approach, with $CW_{min} = \lfloor W^\star \rfloor$, where $W^\star$ is a function of the number of competing nodes, and using probability $q^\star$ as in Theorem 6.2.1.

The system parameters we use are as specified in the standard and are given in Table 9.

Parameters	1Mbps	11Mbps
packet payload	8184 bits	8184 bits
MAC header	272 bits	224 bits
PHY header	128 bits	72bits@1 + 48bits@2
ACK	112 bits + PHY	112 bits + PHY
RTS	160 bits + PHY	160 bits + PHY
CTS	112 bits + PHY	112 bits + PHY
Channel bit rate	1 Mbps	11 Mbps
Propagation delay	1 μs	1 μs
Slot time	50 μs	20 μs
SIFS	28 μs	10 μs
DIFS	128 μs	50 μs

Table 9: System parameters used for calculations

6.3.1 Saturation throughput

The values in Table 9 yield the following collision and successful transmission times: $T_c^{1MBasic} = 8713$, $T_s^{1MBasic} = 8982$, $T_c^{1MRTS} = 417$ and $T_s^{1MRTS} = 9568$. In the 11mbit case, the values are: $T_c^{11MBasic} = 911$, $T_s^{11MBasic} = 1130$, $T_c^{11MRTS} = 307$ and $T_s^{11MRTS} =$

1616. These values are substituted in Equation 33 to numerically calculate the expected saturation throughput in each scenario.

To evaluate the throughput via simulations in ns-2, an extra node is set as a sink that acts exclusively as a recipient to all data packets. Saturation conditions are ensured as each node is offered the exact same load, which is 1.5 times the channel bandwidth divided by the number of nodes. For example, in the case of three 1Mbps nodes, each node has an attached CBR agent generating packets at 0.5Mbps rate; in the case of five 11Mbps nodes, the CBR agents generate traffic at 3Mbps. In all graphs illustrating throughput results, the expected (calculated) system throughput is represented by dashed lines, whereas the actual simulation results are given by solid lines. To avoid UDP packet segmentation, we increase the maximum UDP packet size.

Figures 24 and 25 represent the simulation results for 1Mbps and 11Mbps channel for the 802.11 and the XVBEB protocols while Figures 26 and 27 illustrate the optimized 802.11 and XVBEB protocols (requiring knowledge of the number of nodes) in RTS/CTS enabled networks.

As illustrated, both regular and optimal XVBEB outperform 802.11, and the ns-2 saturated throughput simulation results for both XVBEB and 802.11 miss the expected theoretical calculations. This is likely due to several assumptions in the Markov chain model, such as the assumption that all nodes collide with same conditional collision probability or to some other model inaccuracies.

The same trend is observed with the basic access mechanism, as illustrated in Figures 28, 29, 30 and 31.

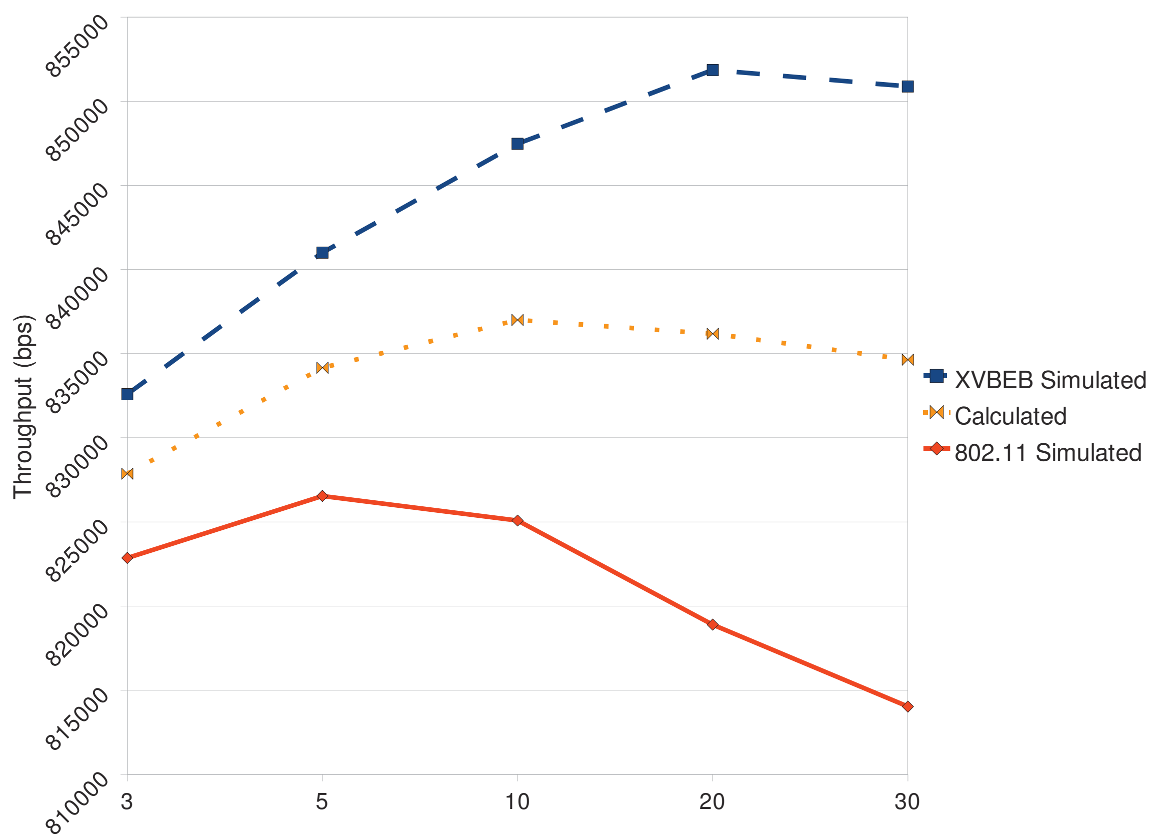

Figure 24: Saturated throughput, 1Mbps RTS/CTS access, regular protocols

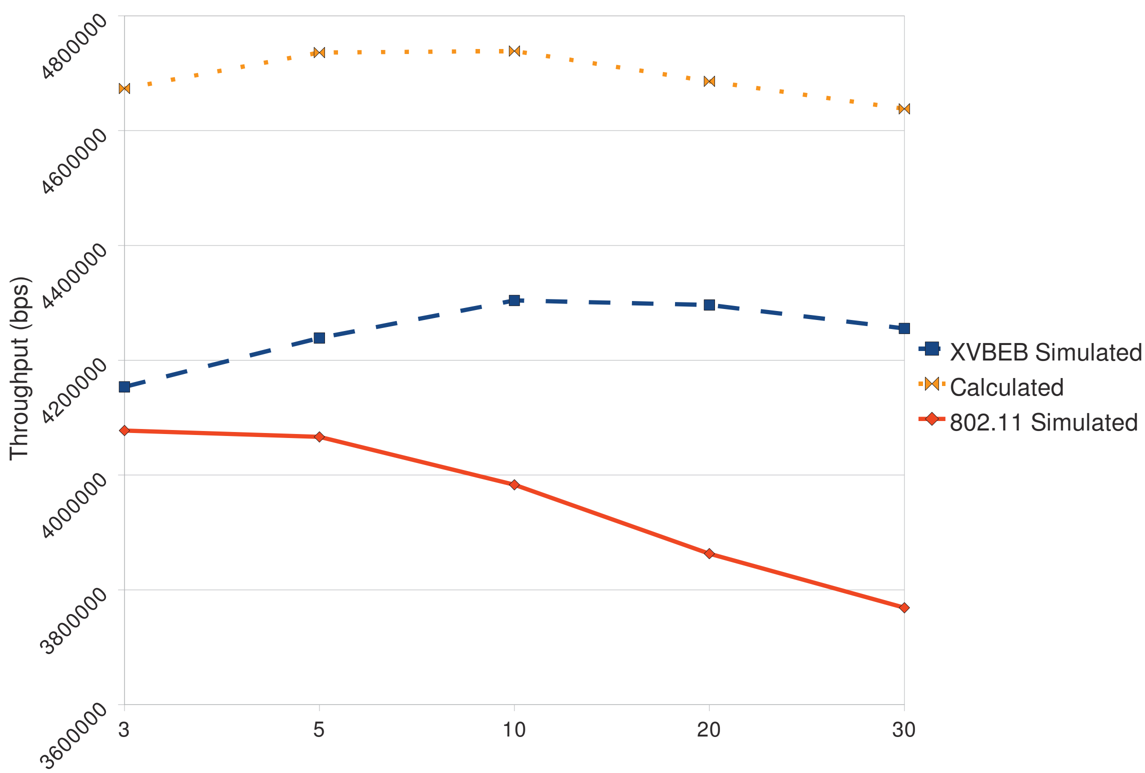

Figure 25: Saturated throughput, 11Mbps RTS/CTS access, regular protocols

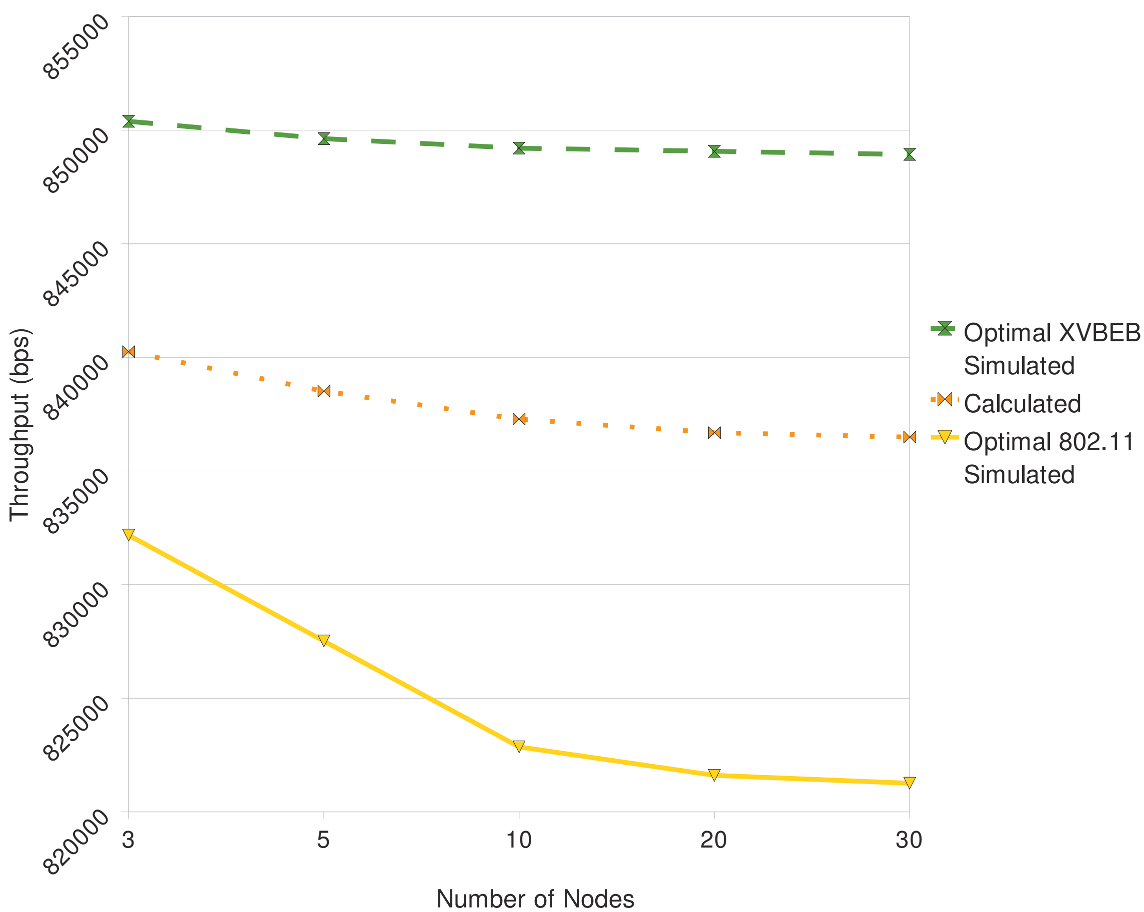

Figure 26: Saturated throughput, 1Mbps RTS/CTS access, optimized protocols

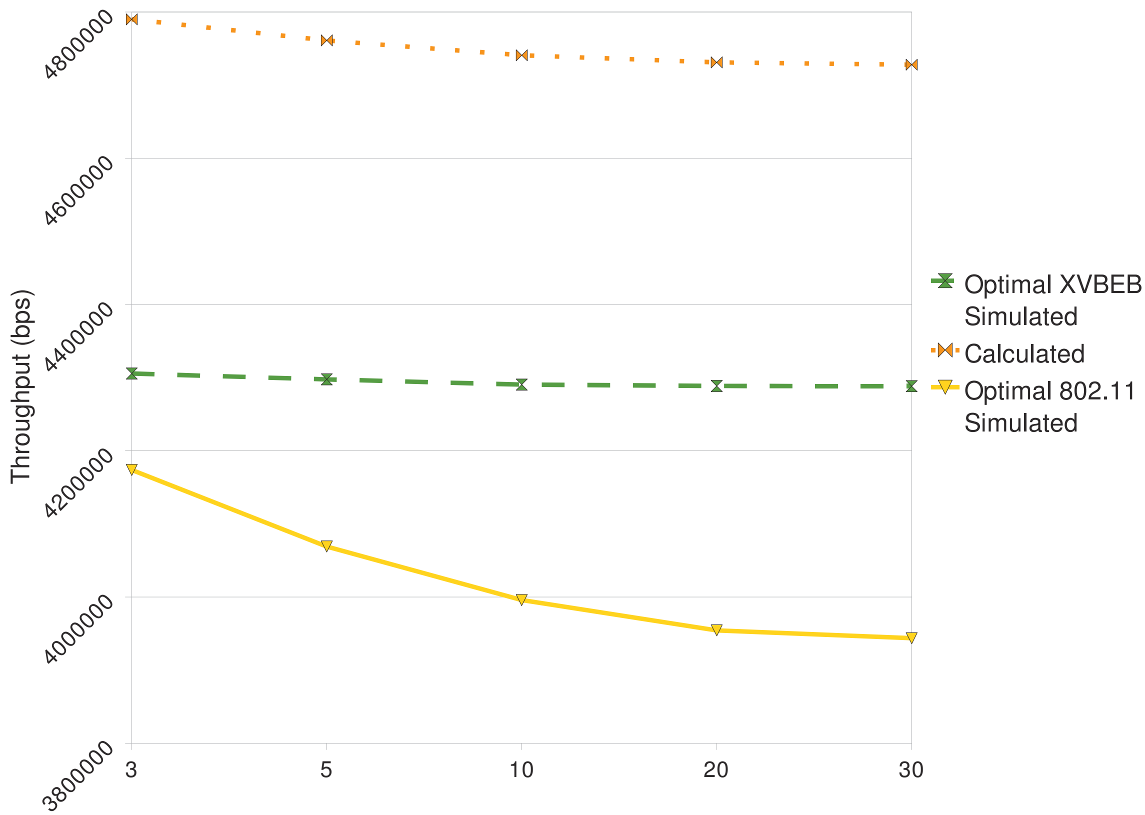

Figure 27: Saturated throughput, 11Mbps RTS/CTS access, optimized protocols

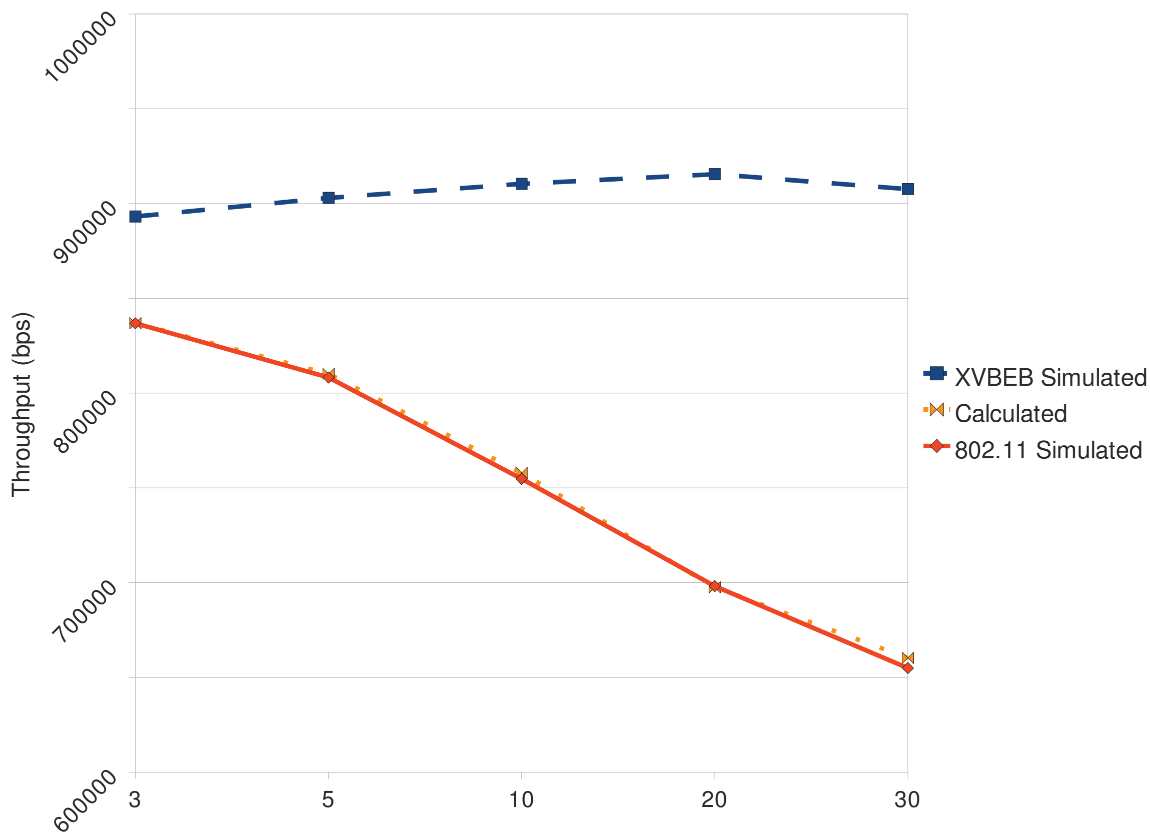

Figure 28: Saturated throughput, 1Mbps basic access, regular protocols

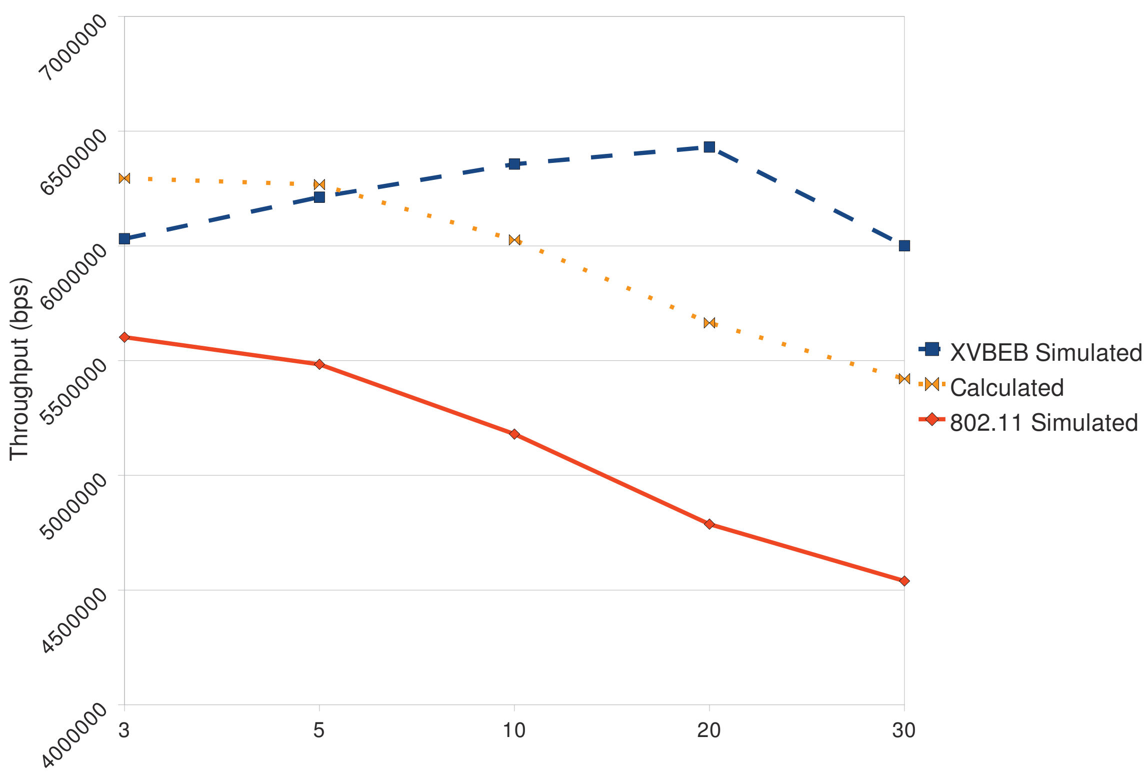

Figure 29: Saturated throughput, 11Mbps basic access, regular protocols

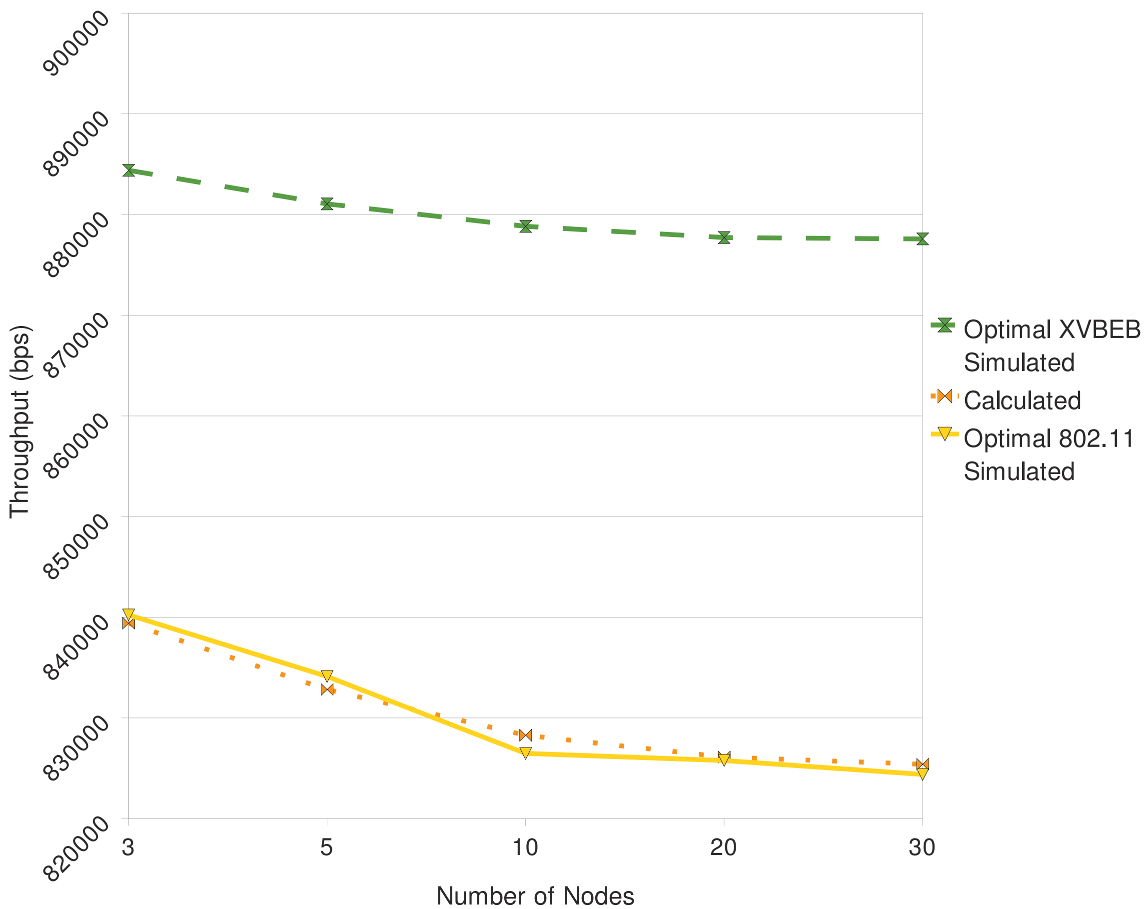

Figure 30: Saturated throughput, 1Mbps basic access, optimized protocols

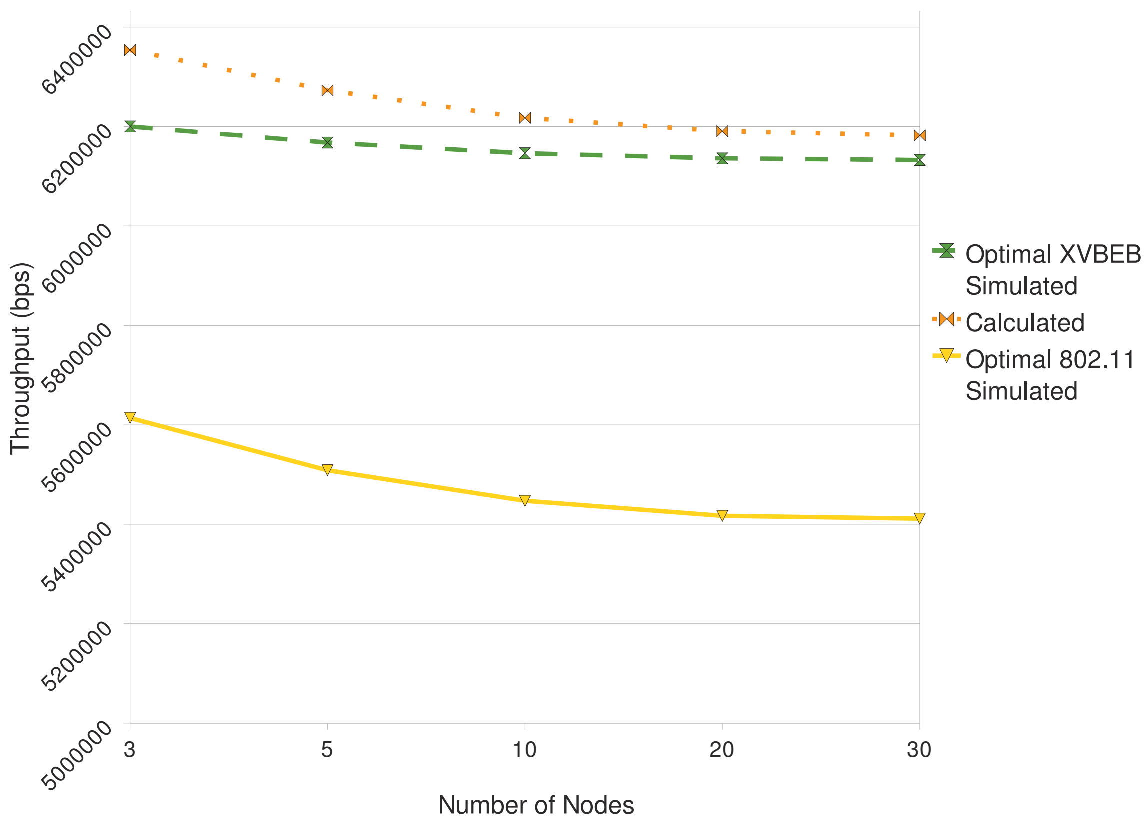

Figure 31: Saturated throughput, 11Mbps basic access, optimized protocols

6.3.2 Fairness index

To compare the fairness of the saturation throughput, Jain's fairness index [JCH98] is used:

$$J = \frac{(\sum_{i=1}^{n} x_i)^2}{n \sum_{i=1}^{n} x_i^2}$$

where n is the number of users and x_i is the throughput of the i^{th} connection. The value of J lies between 0 and 1, with 1 representing the best possible fairness.

Figures 32 and 33 exhibit the fairness index in 1Mbps and 11Mbps RTS enabled networks. The index is better for the optimal XVBEB compared to the optimal 802.11 protocol. The throughput fairness of the regular 802.11 is better than the regular XVBEB algorithm; however, this could be expected given the big improvement in performance of the XVBEB scheme. As with the saturation throughput, the trend is similar in basic access networks (Figures 34 and 35).

6.3.3 Packet loss

To analyze the performance in terms of packet loss, the behavior of the protocols is evaluated for video and voice traffic.

First, video traffic is simulated in ns-2 using the TES based MPEG4 model [ML]. All participating nodes send video to a sink at the frame rate. Two load scenarios are tested for streams with low, medium and high bit rates on an 11Mbit channel.

As illustrated in Figures 36, 37, 38, 39, 40 and 41, both the regular and optimal XVBEB algorithms perform better than both 802.11 protocols in terms of packet loss regardless of the offered load and the channel access method.

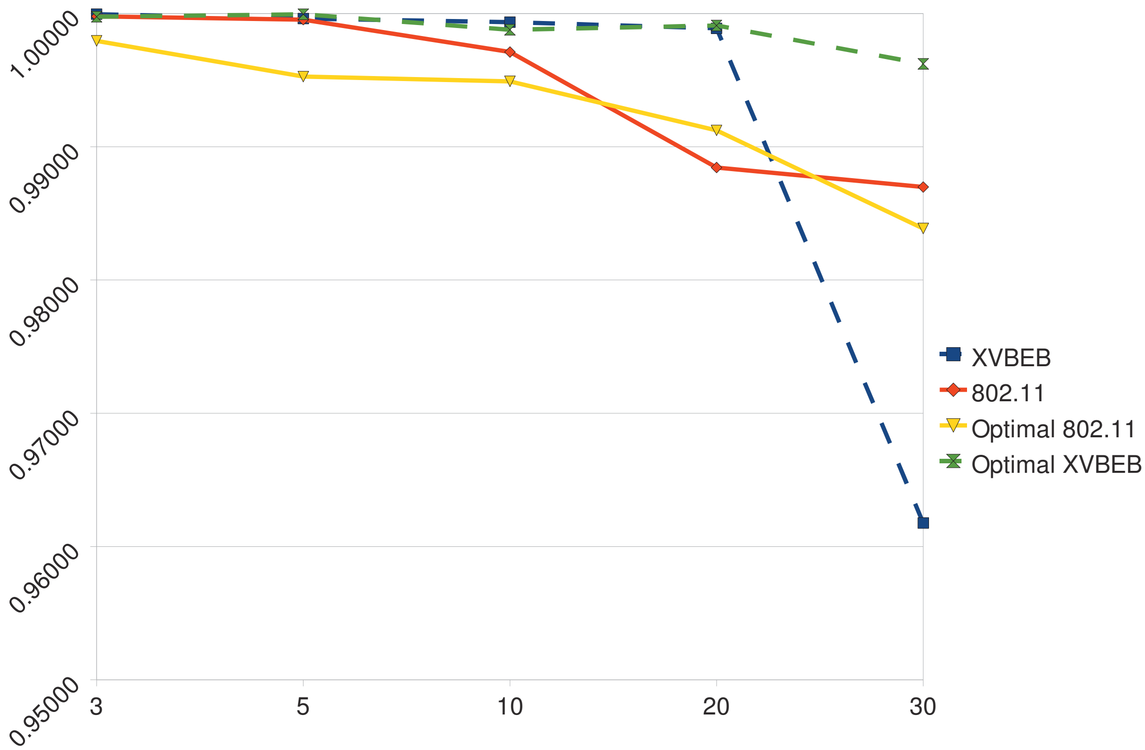

Figure 32: Fairness index, 1mb RTS

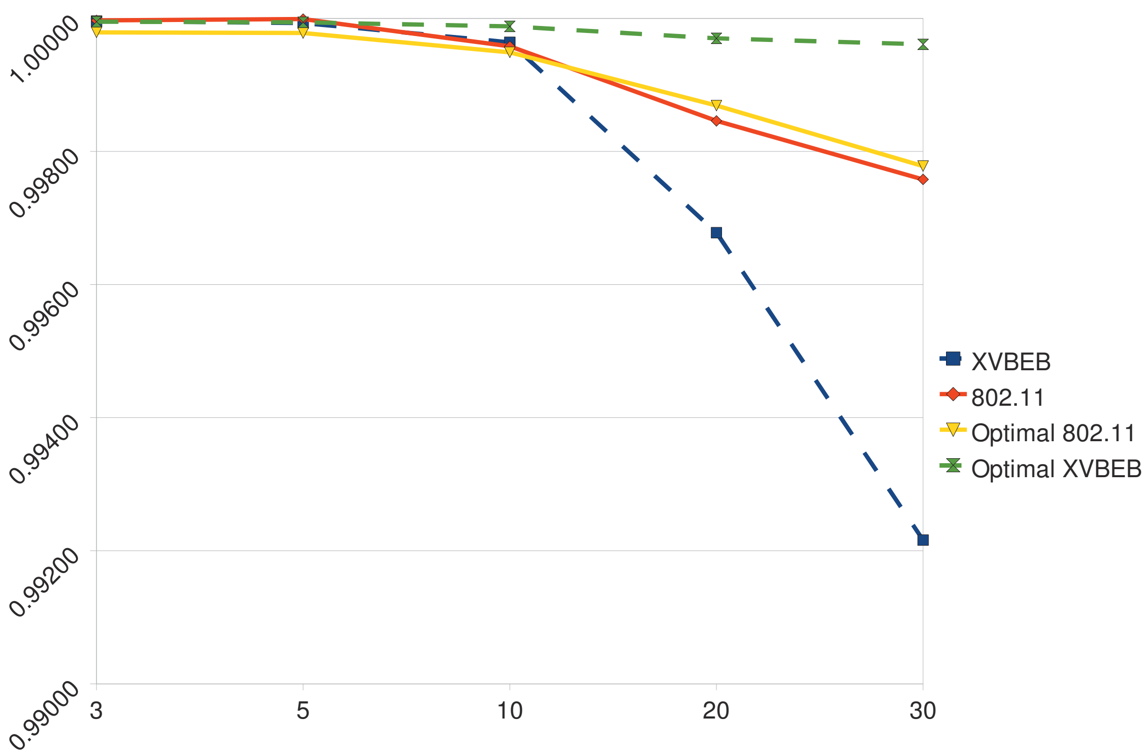

Figure 33: Fairness index, 11mb RTS

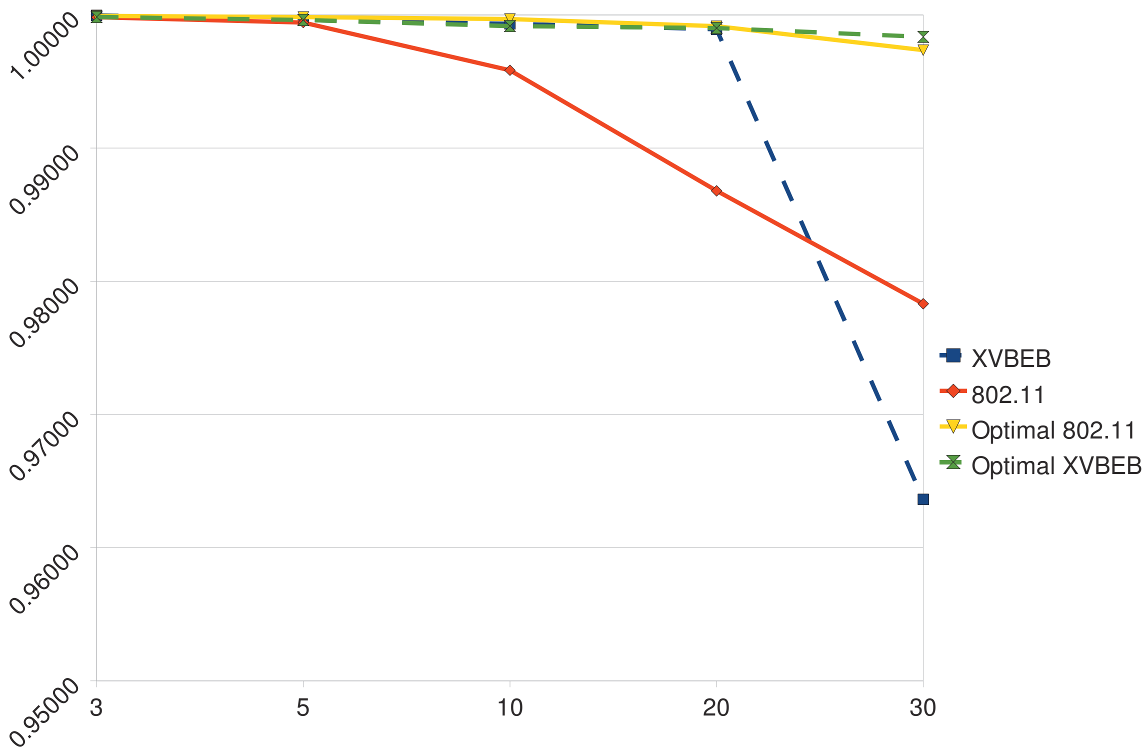

Figure 34: Fairness index, 1Mbps, basic access

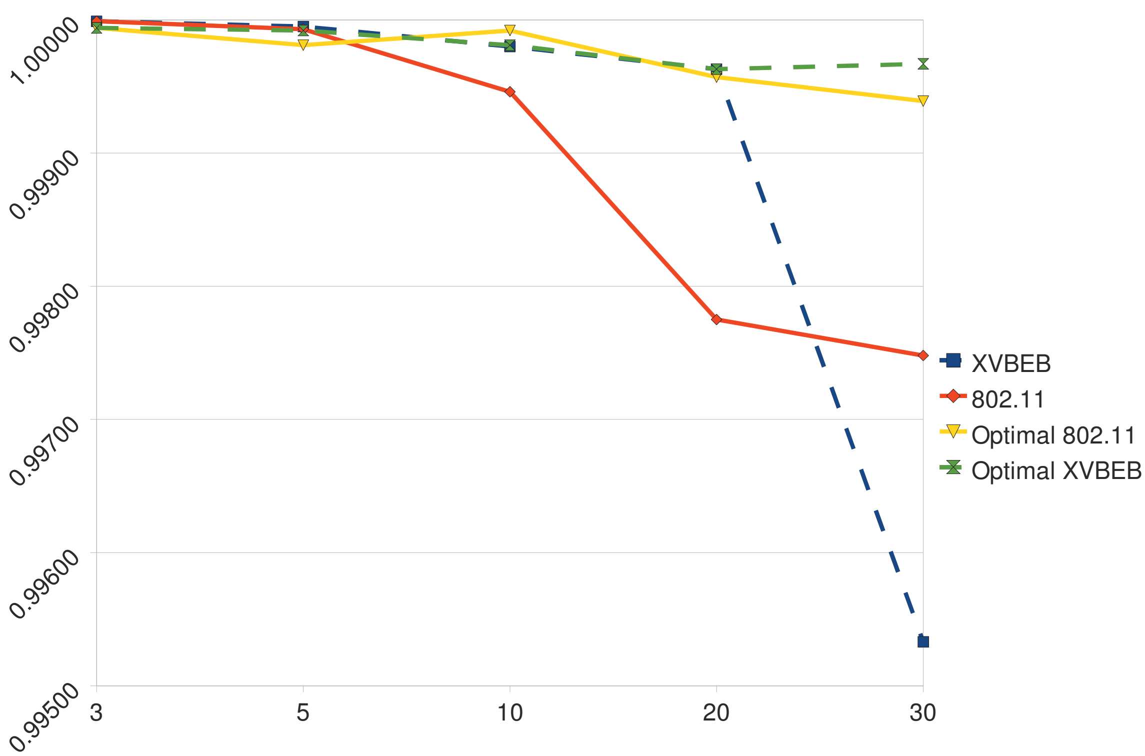

Figure 35: Fairness index, 11Mbps, basic access

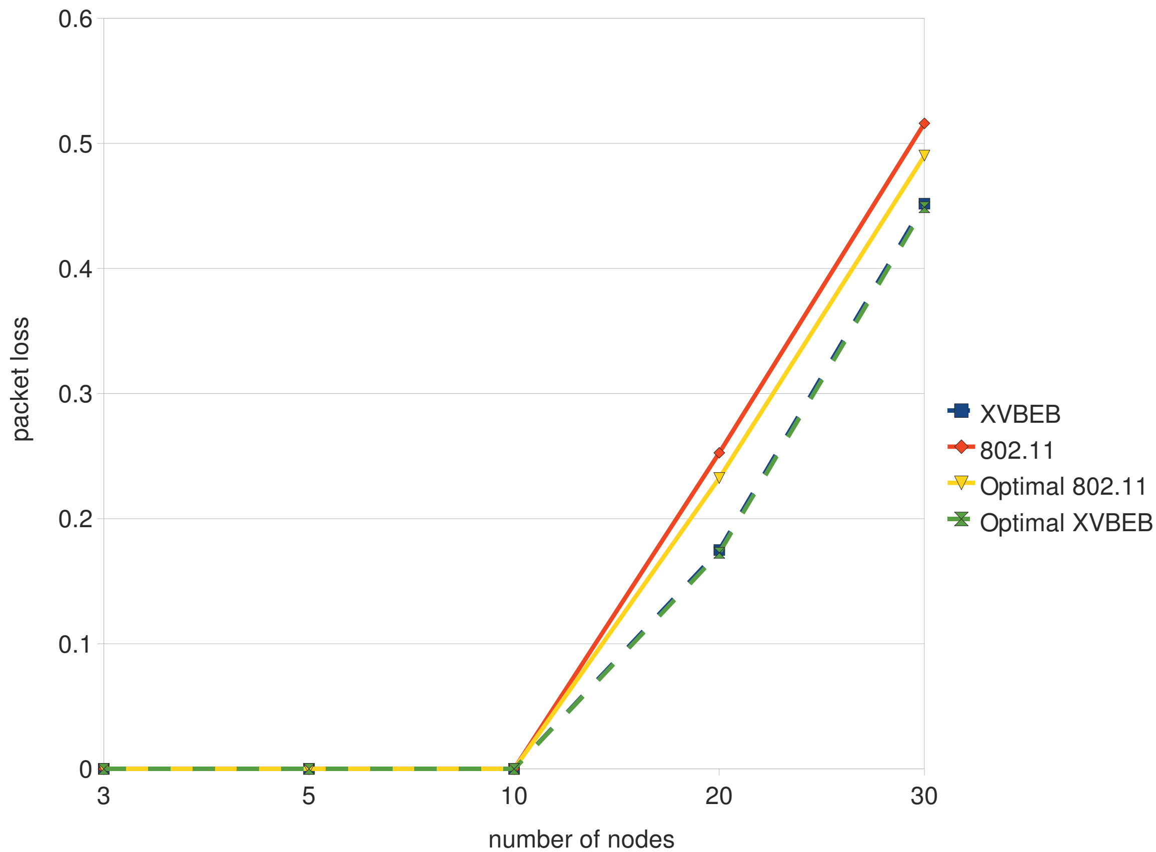

Figure 36: Packet loss ratio, low bitrate video, RTS/CTS

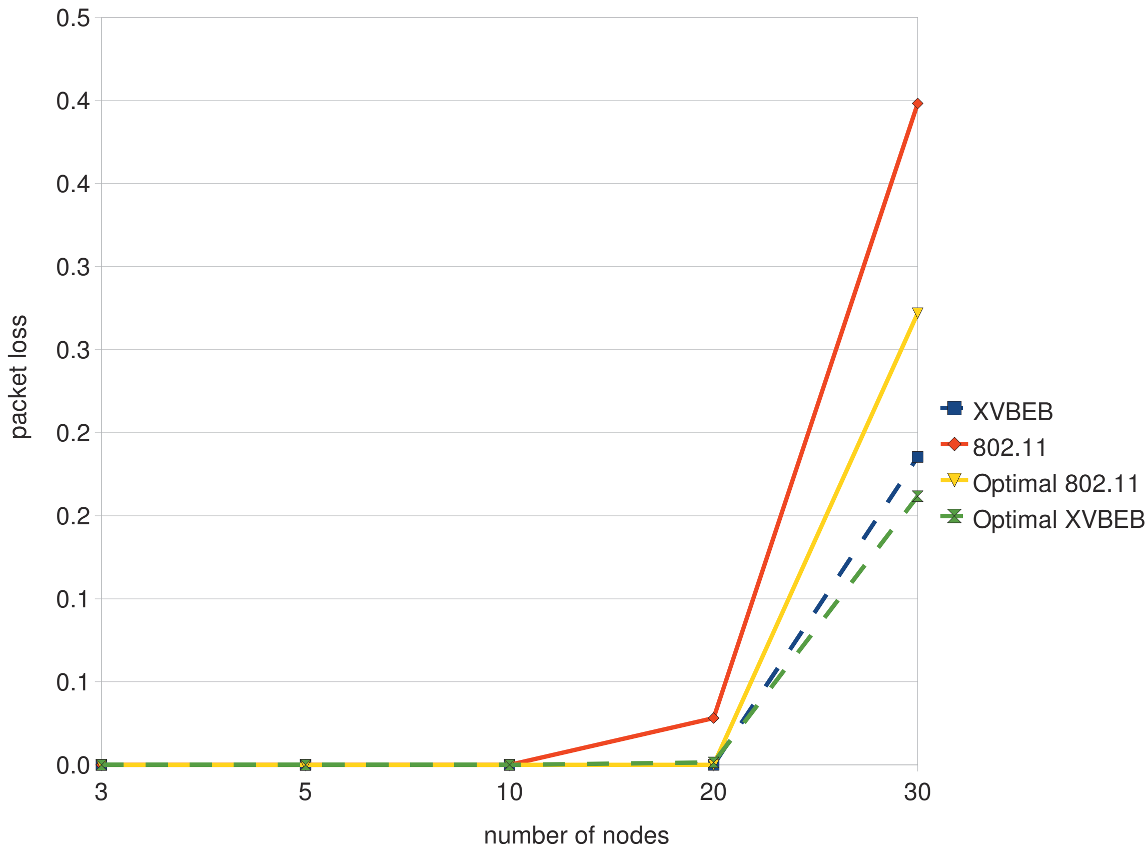

Figure 37: Packet loss ratio, low bitrate video, basic access

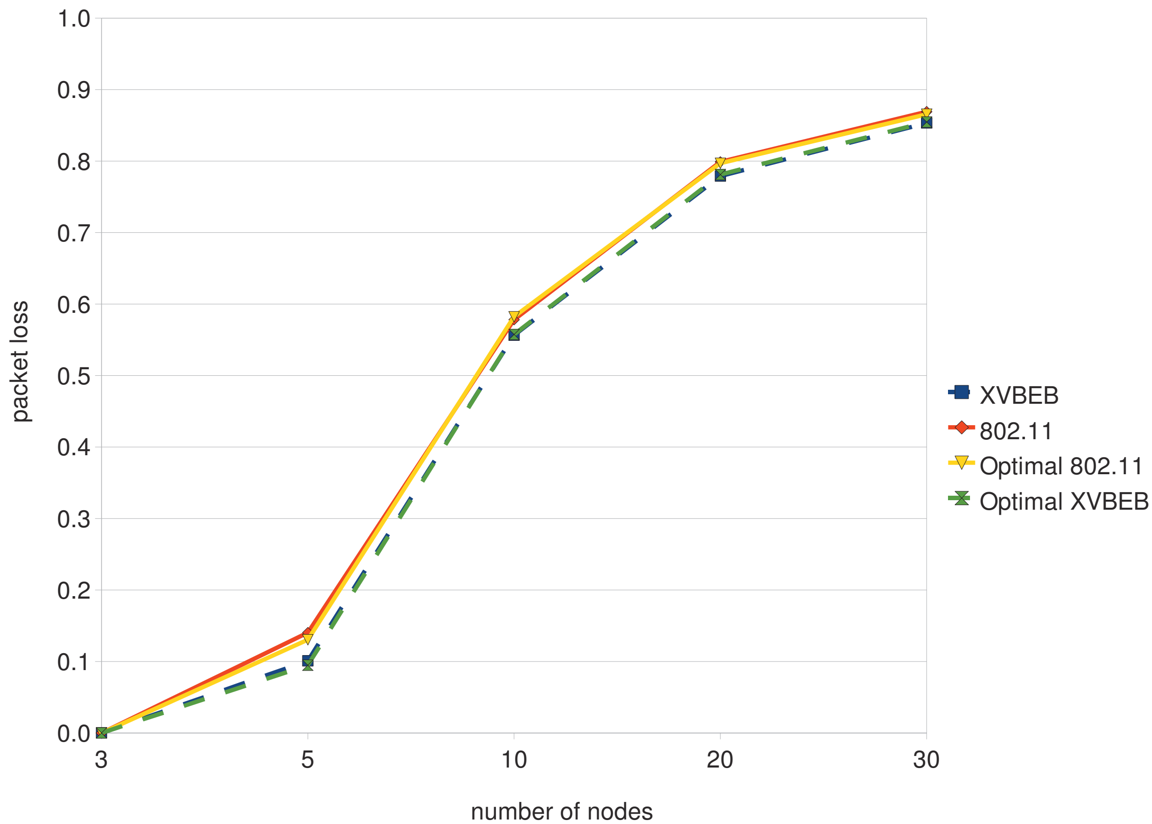

Figure 38: Packet loss ratio, medium bitrate video, RTS/CTS

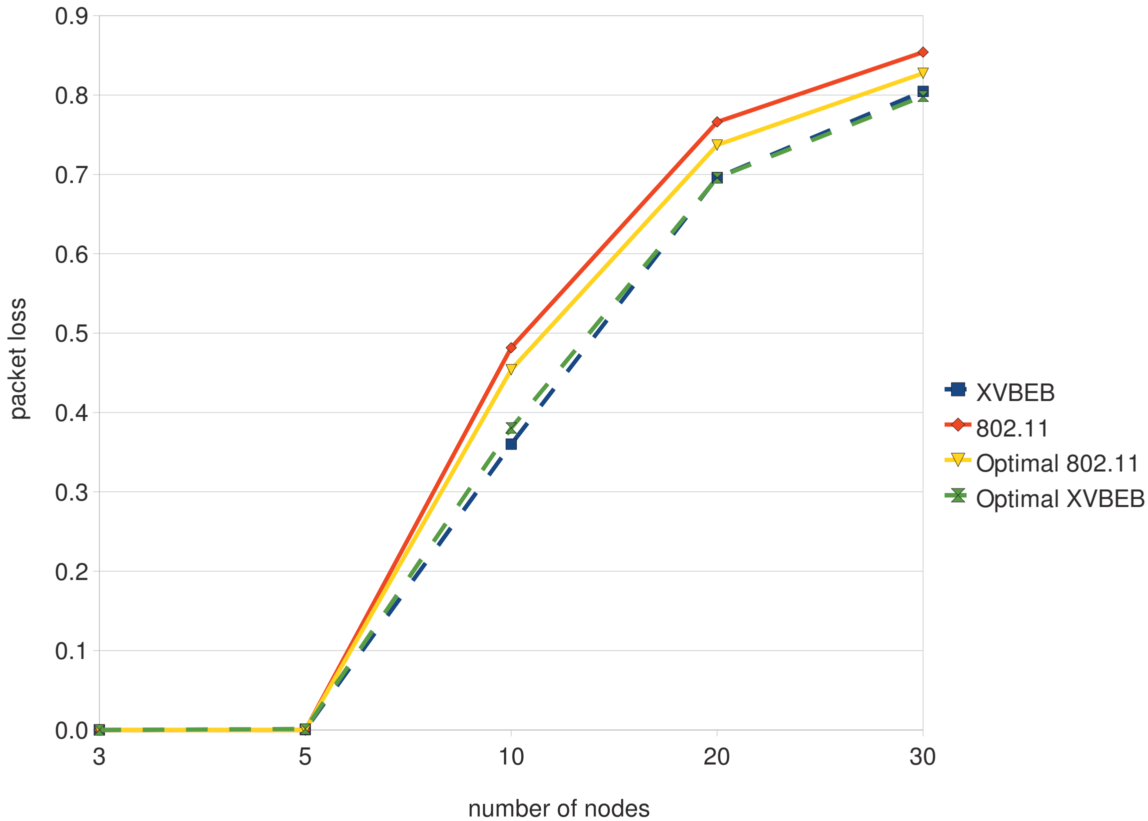

Figure 39: Packet loss ratio, medium bitrate video, basic access

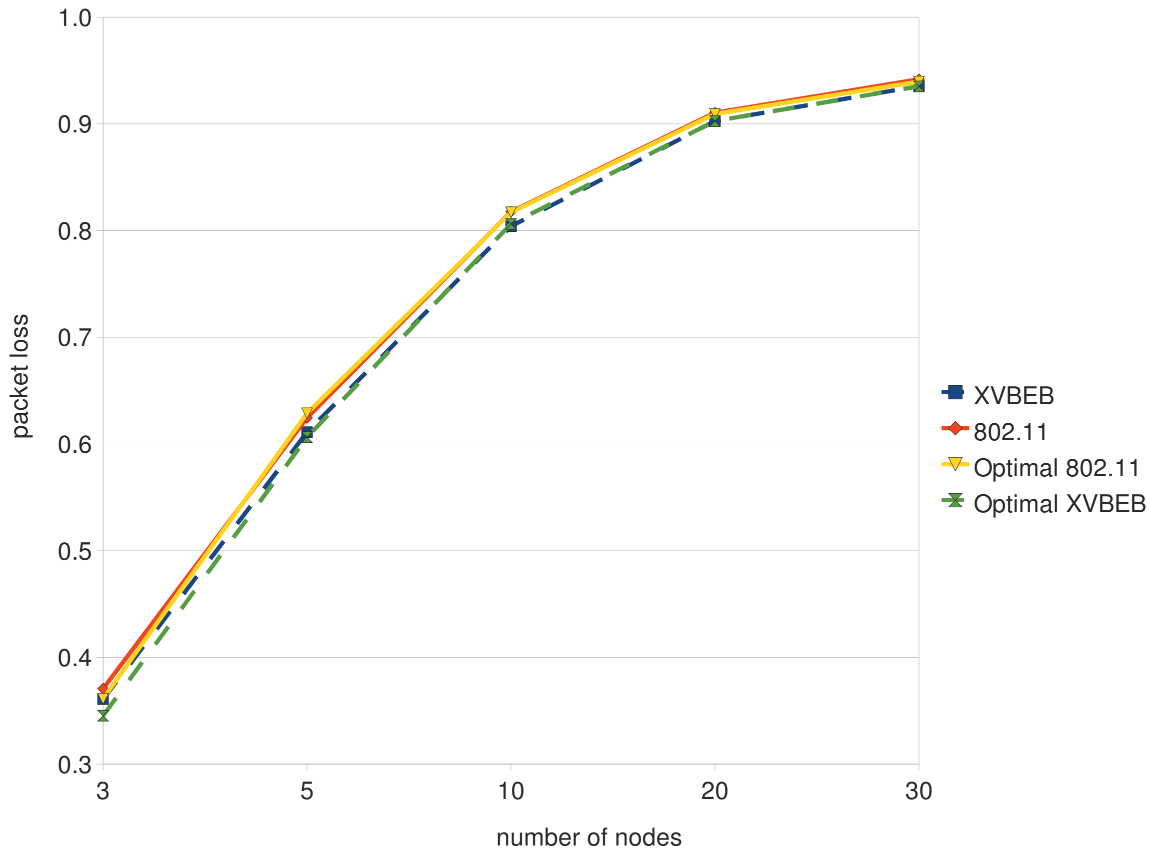

Figure 40: Packet loss ratio, high bitrate video, RTS/CTS

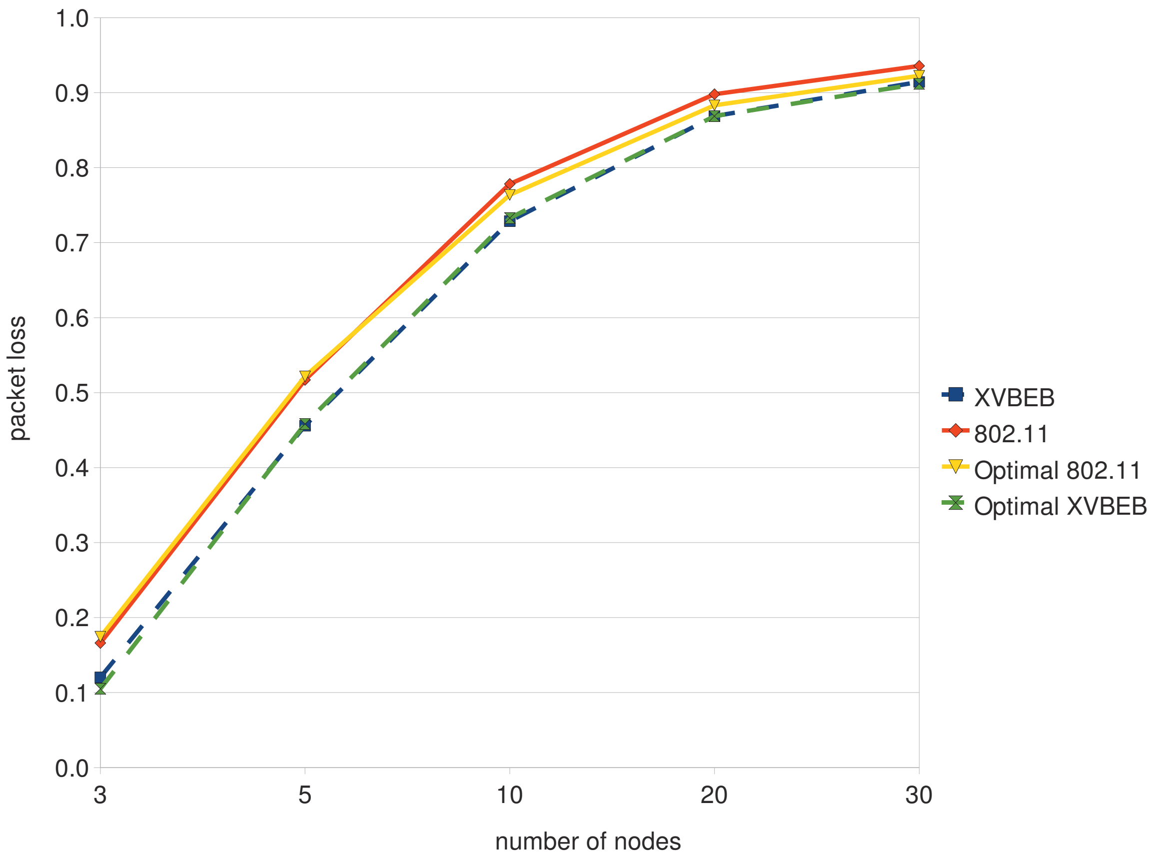

Figure 41: Packet loss ratio, high bitrate video, basic access

Further, the packet loss ratio is evaluated for voice traffic patterns. The VOIP model in NS2 is based on a statistical model presented in [nCK02]. Since voice traffic uses only small portion of the available bandwidth, the simulations are done on a 1Mbps channel. In fact, it turns out that even when there are 50 nodes with one voice channel per node, competition for channel resources rarely occurs. Therefore, to ensure the backoff scheme is called often enough to evaluate its performance, the network is offered 300 voice channels. For example, when there are 3 competing nodes, each node maintains 100 voice channels.

As observed in Figures 42 and 43, the XVBEB protocol again outperforms 802.11.

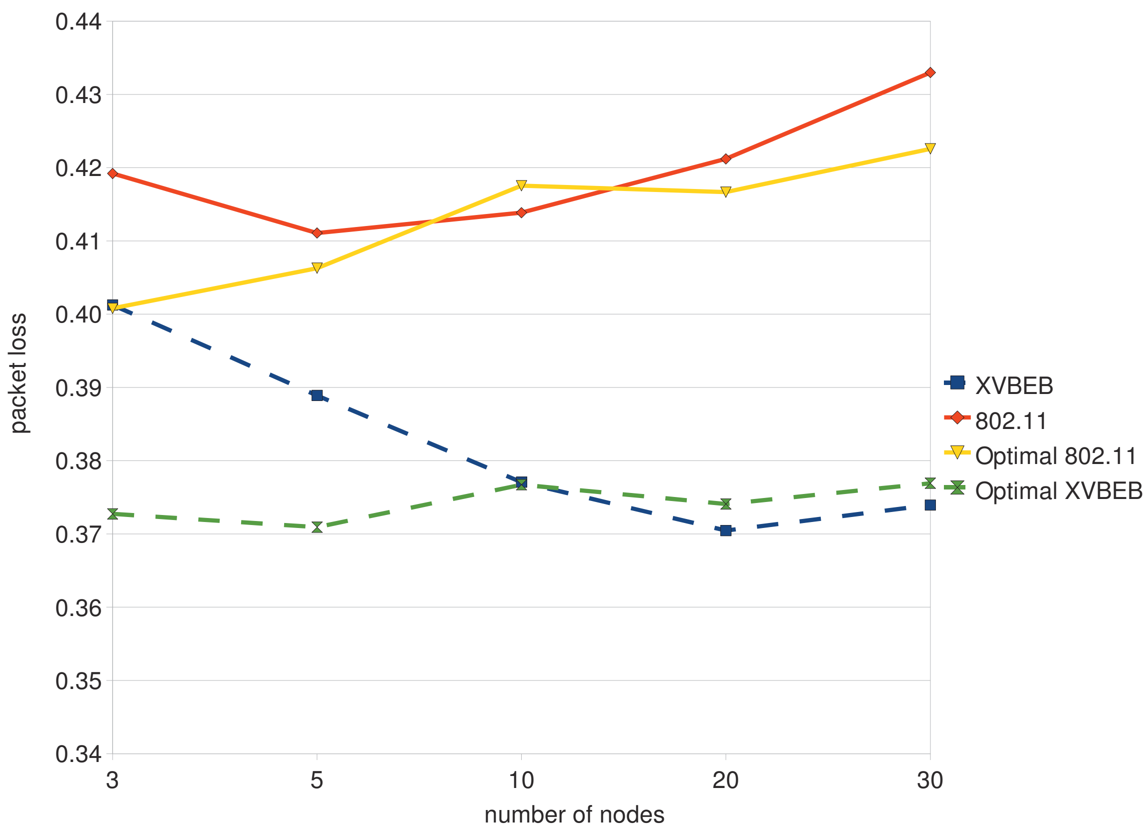

Figure 42: Packet loss ratio, voice traffic, RTS/CTS

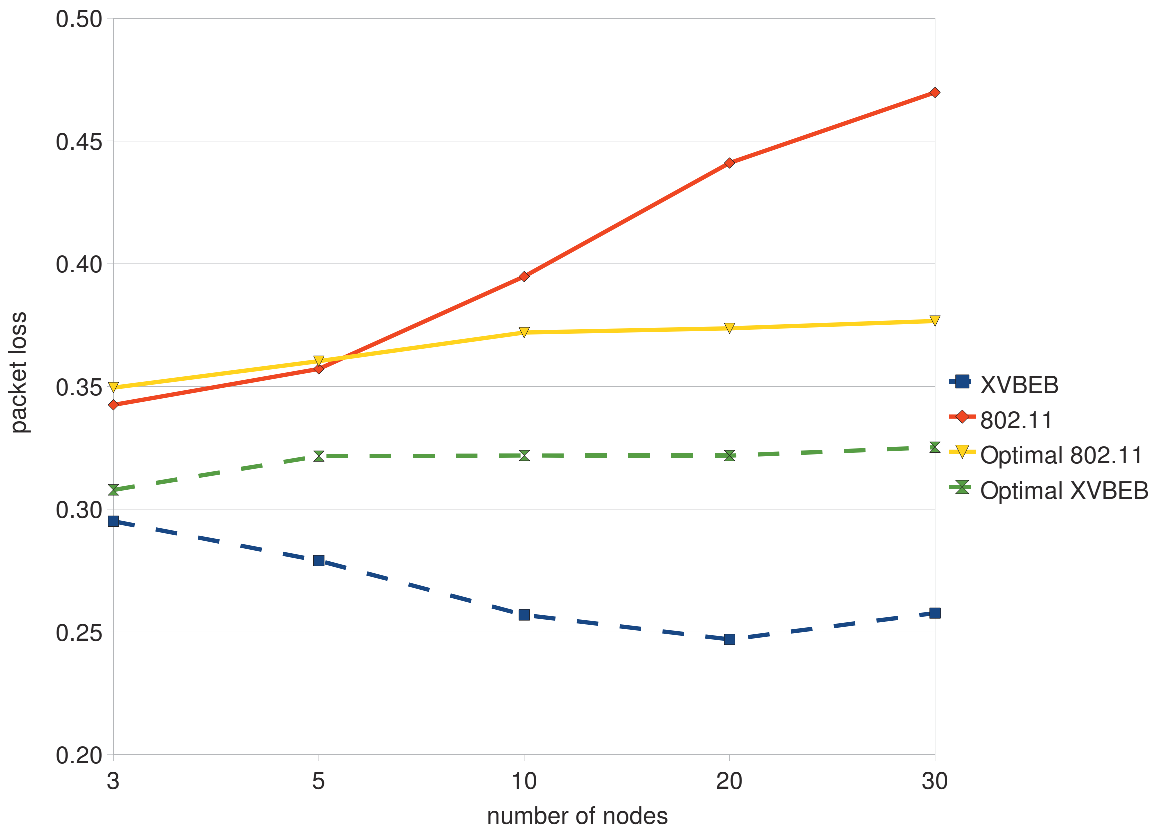

Figure 43: Packet loss ratio, voice traffic, basic access

6.3.4 Packet delay

As in Section 6.3.3, the packet delay and delay variation are evaluated based on the relevant video and voice traffic patterns. The packet delay variation is measured as an average of the inter-packet delay variations as defined in [DC02]. Here again the access point acts a sink, all participating nodes generate video or voice traffic at the previously defined rates.

Figures 44, 45, 46, 47, 48 and 49 illustrate that the both XVBEB algorithms exhibit lower delay than both 802.11 protocols for low medium and high bit rate video streams in both channel access methods.

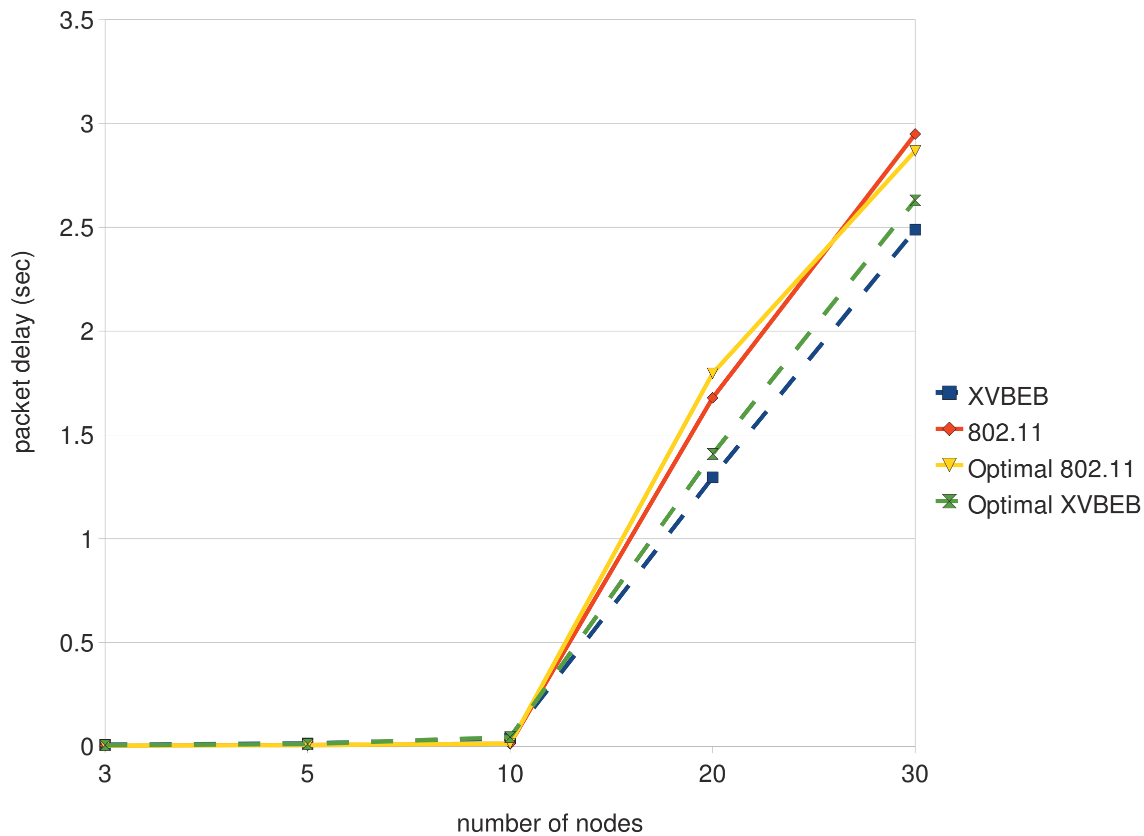

Figure 44: Packet delay, low bitrate video, RTS/CTS

No change in packet delay performance is being noticed when voice traffic is simulated in ns-2; again, XVBEB (Figures 50 and 51) does better than 802.11.

Finally, as observed in Figures 52 to 59, packet delay variation is the only evaluated parameter where 802.11's performance is comparable to XVBEB. Yet, the XVBEB procedure manifests superior performance at many points.

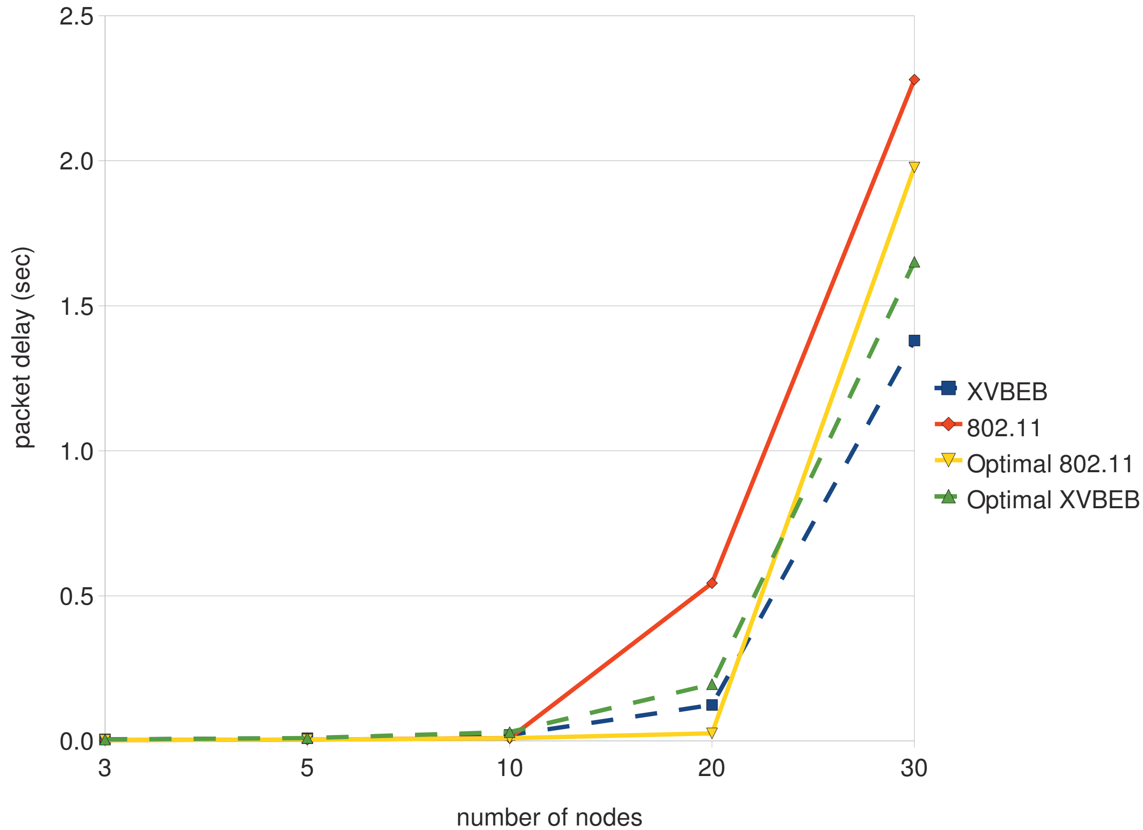

Figure 45: Packet delay, low bitrate video, basic access

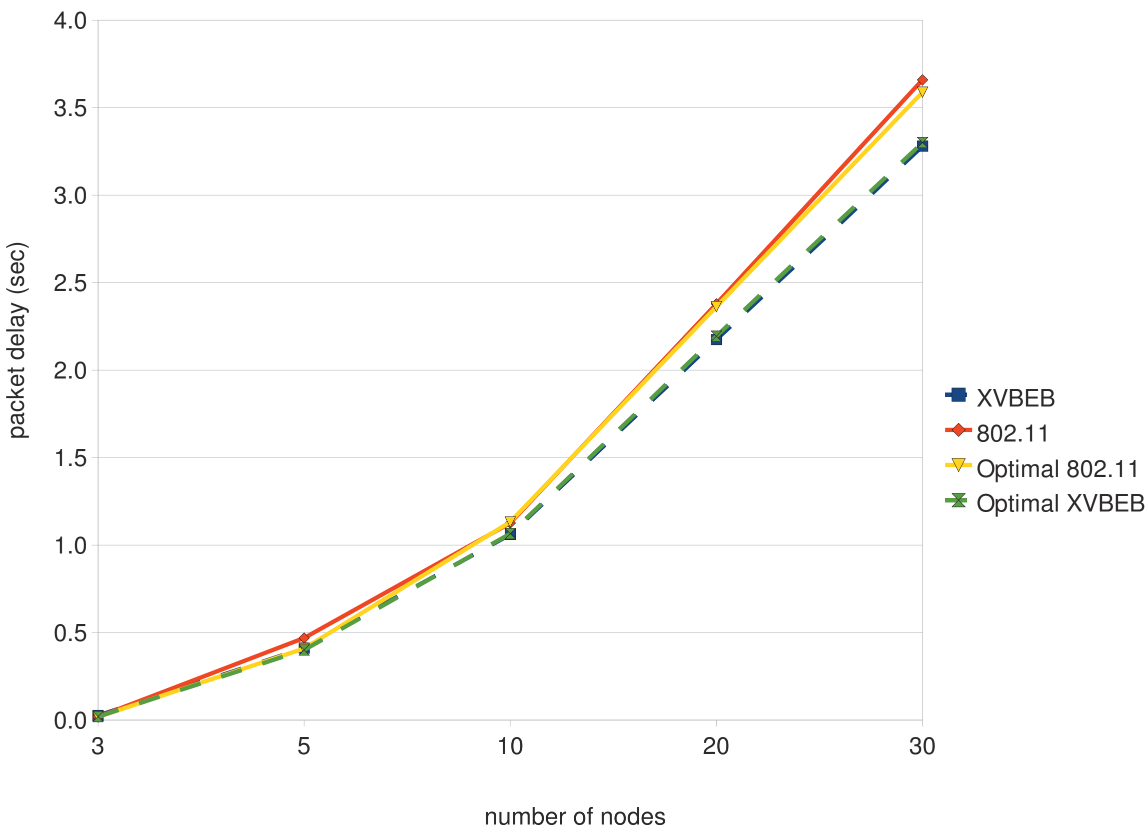

Figure 46: Packet delay, medium bitrate video, RTS/CTS

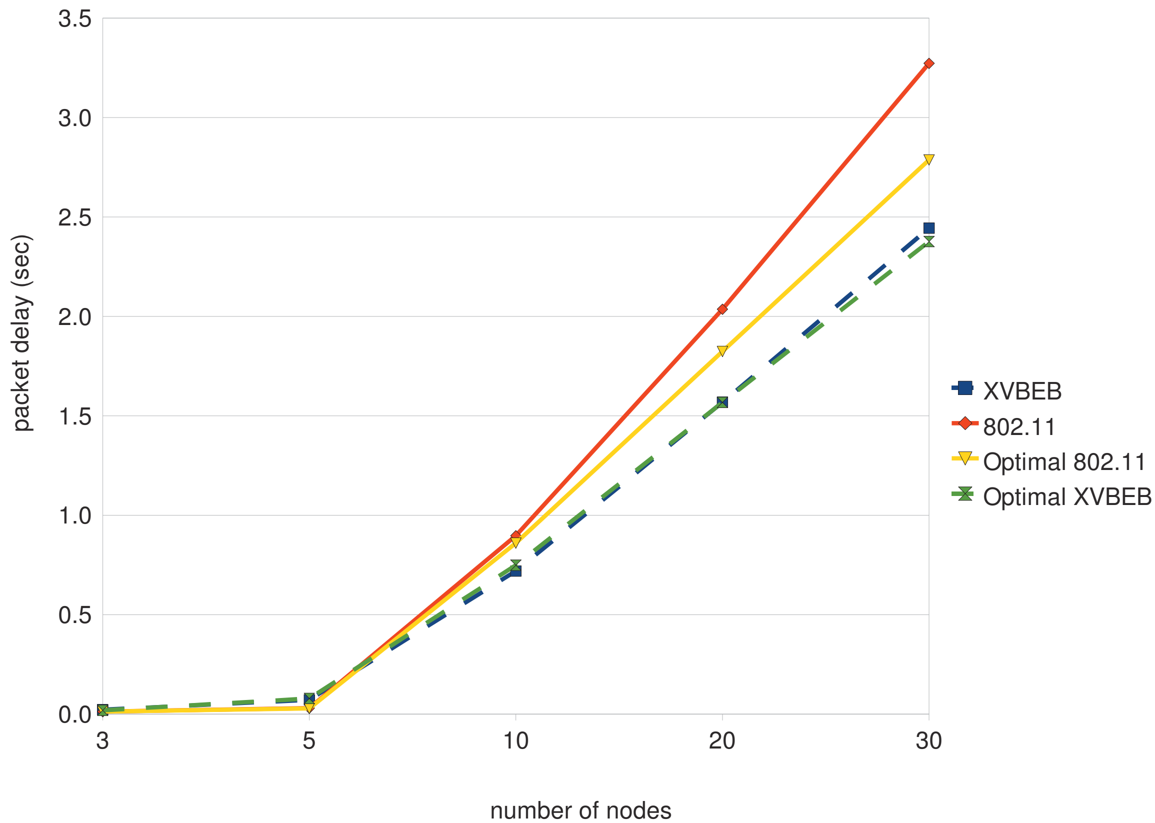

Figure 47: Packet delay, medium bitrate video, basic access

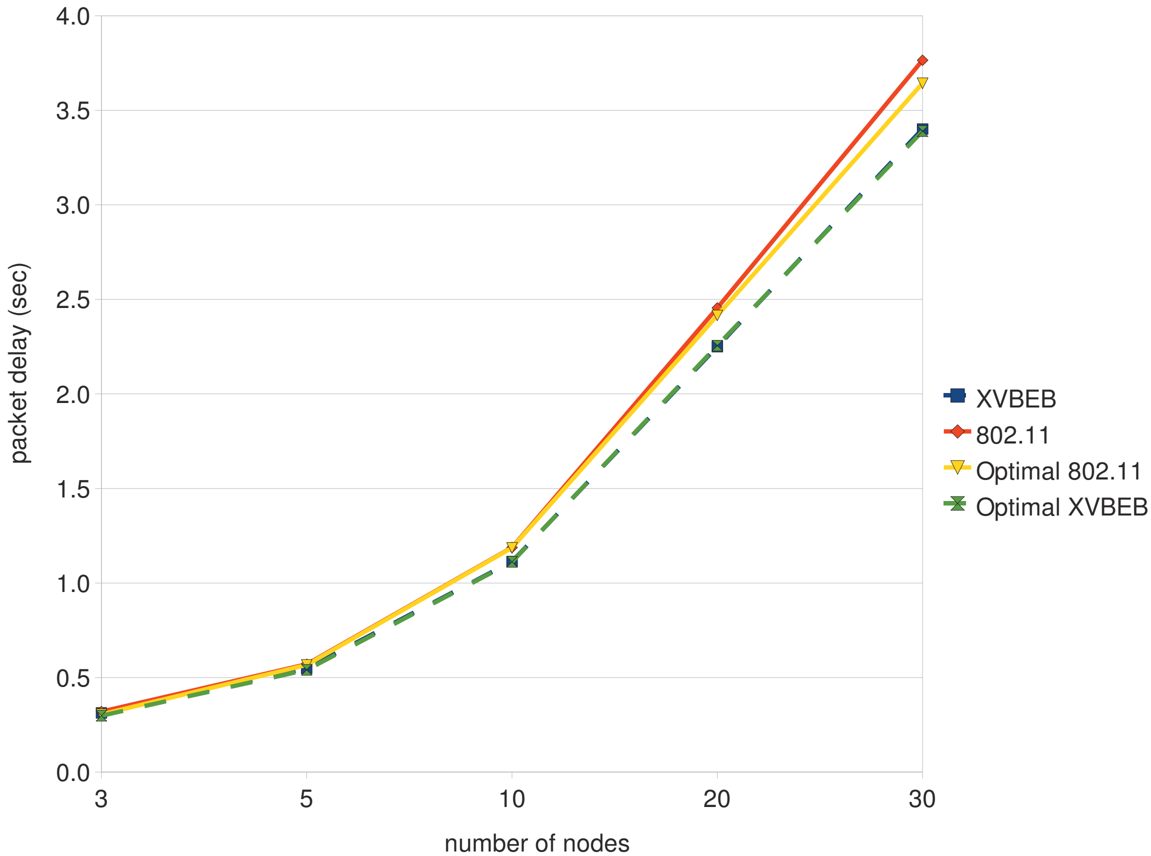

Figure 48: Packet delay, high bitrate video, RTS/CTS

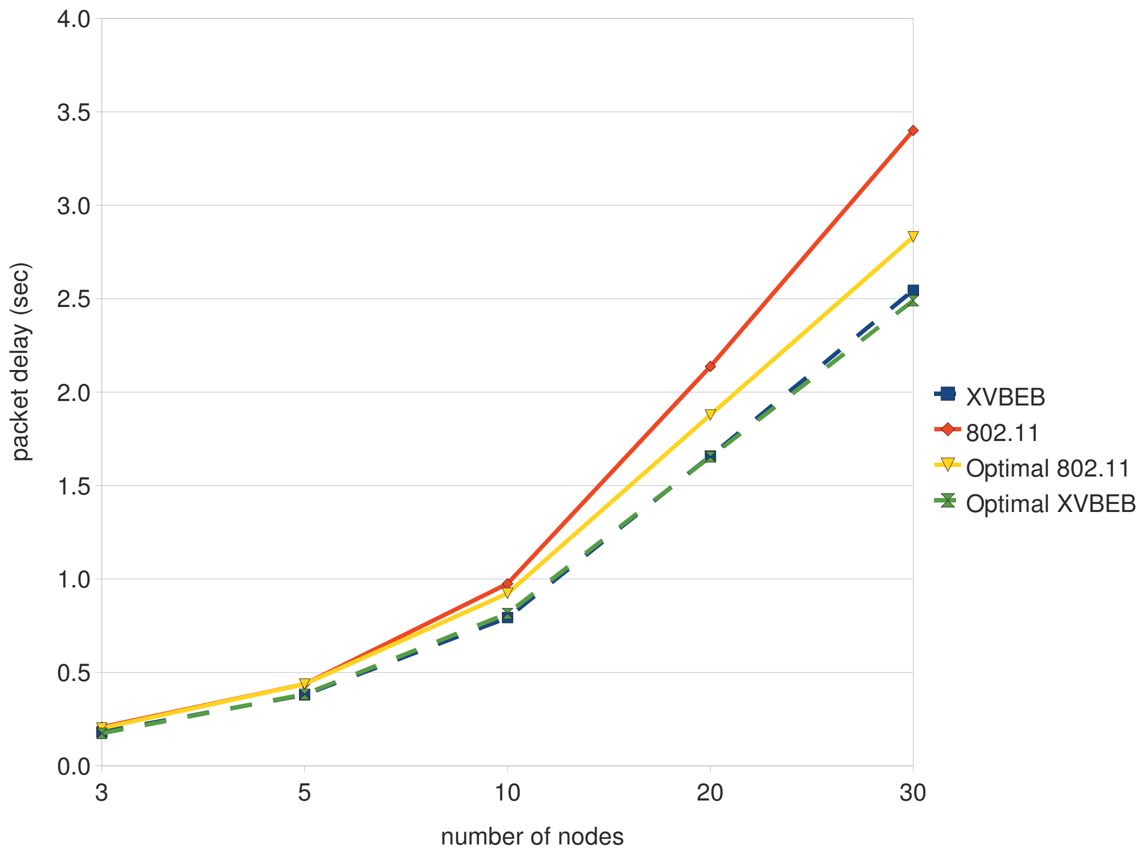

Figure 49: Packet delay, high bitrate video, basic access

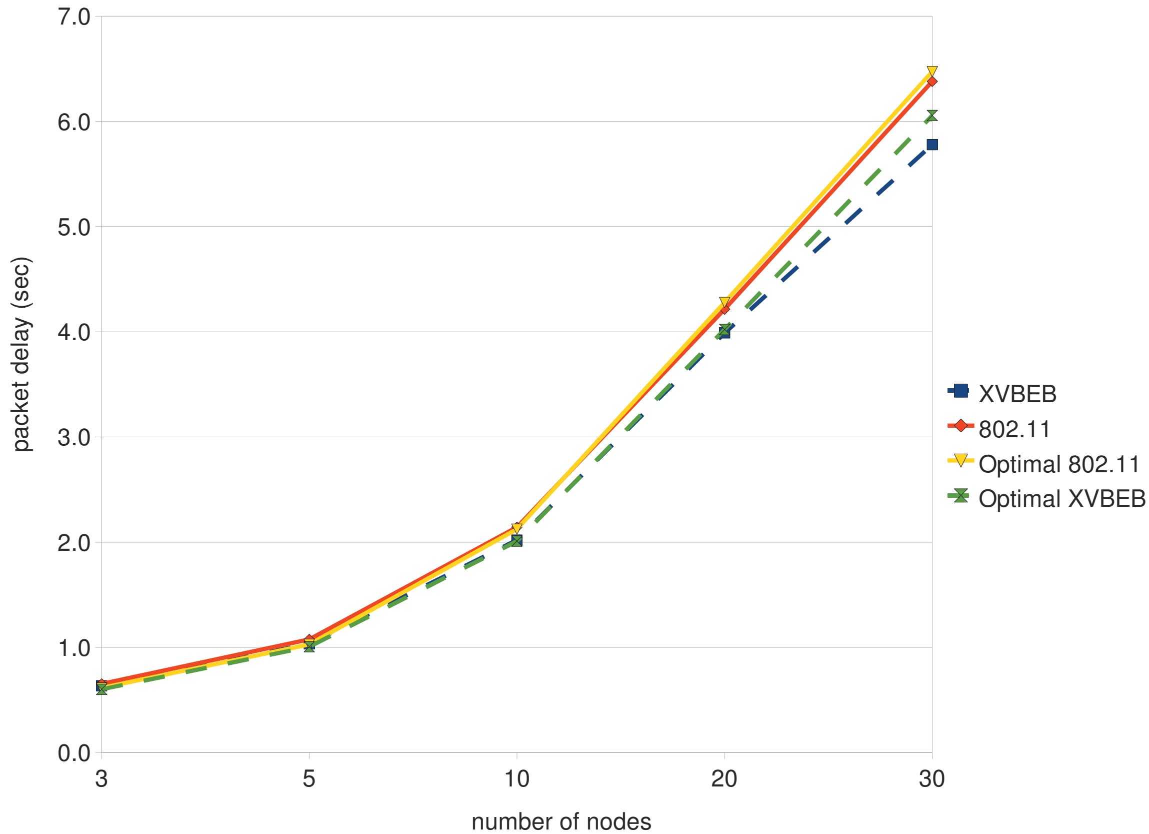

Figure 50: Packet delay, voice traffic, RTS/CTS

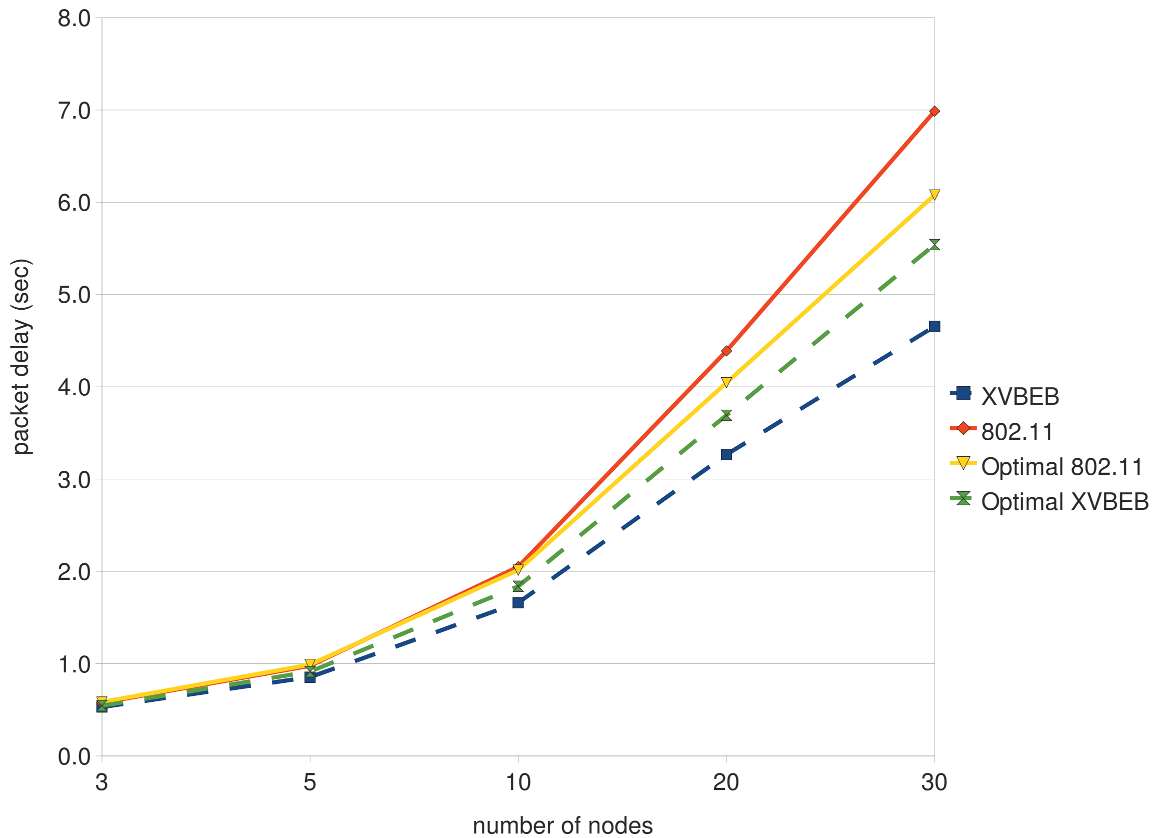

Figure 51: Packet delay, voice traffic, basic access

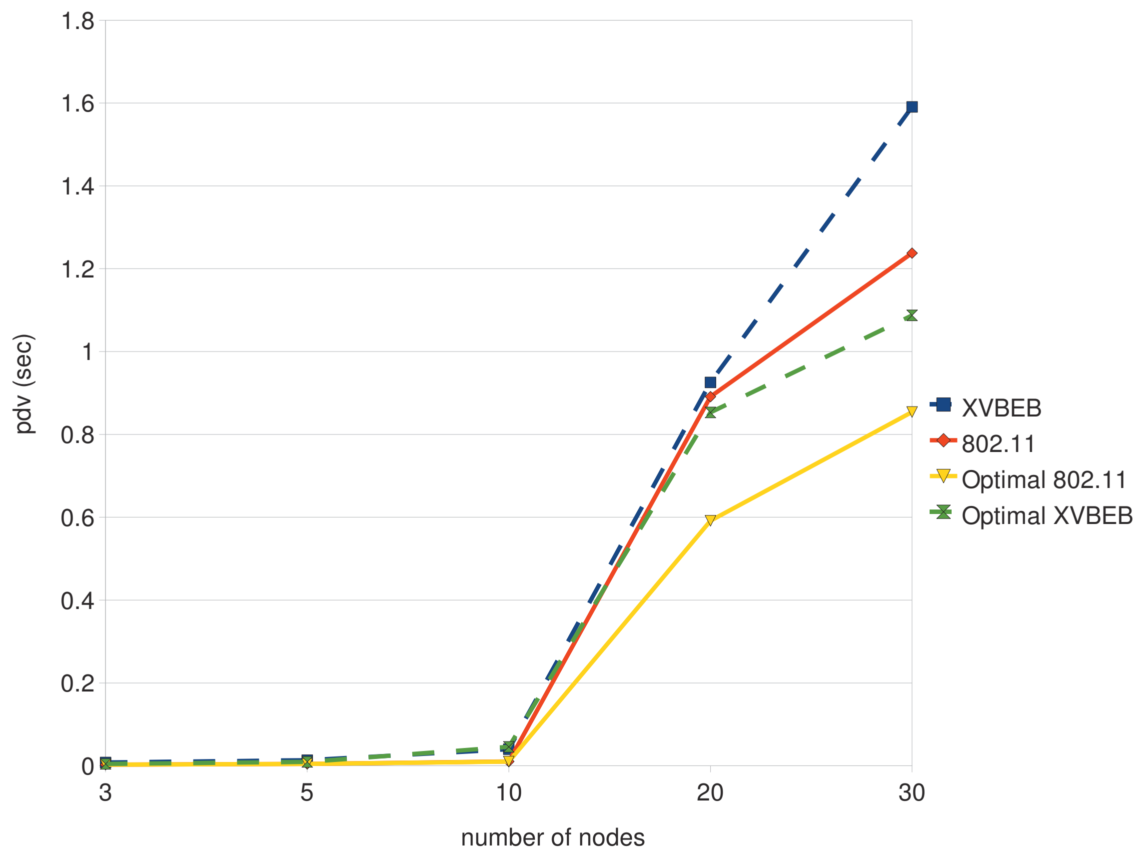

Figure 52: Packet delay variation, low bitrate video, RTS/CTS

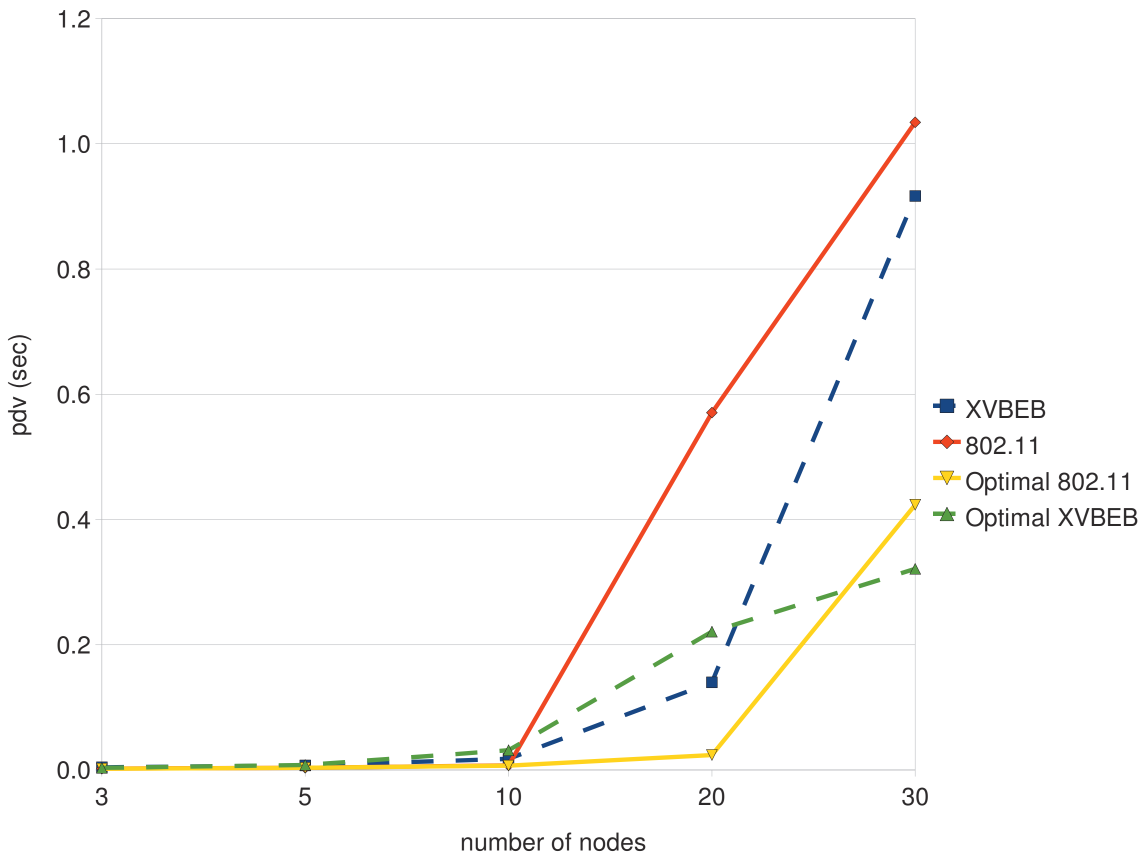

Figure 53: Packet delay variation, low bitrate video, basic access

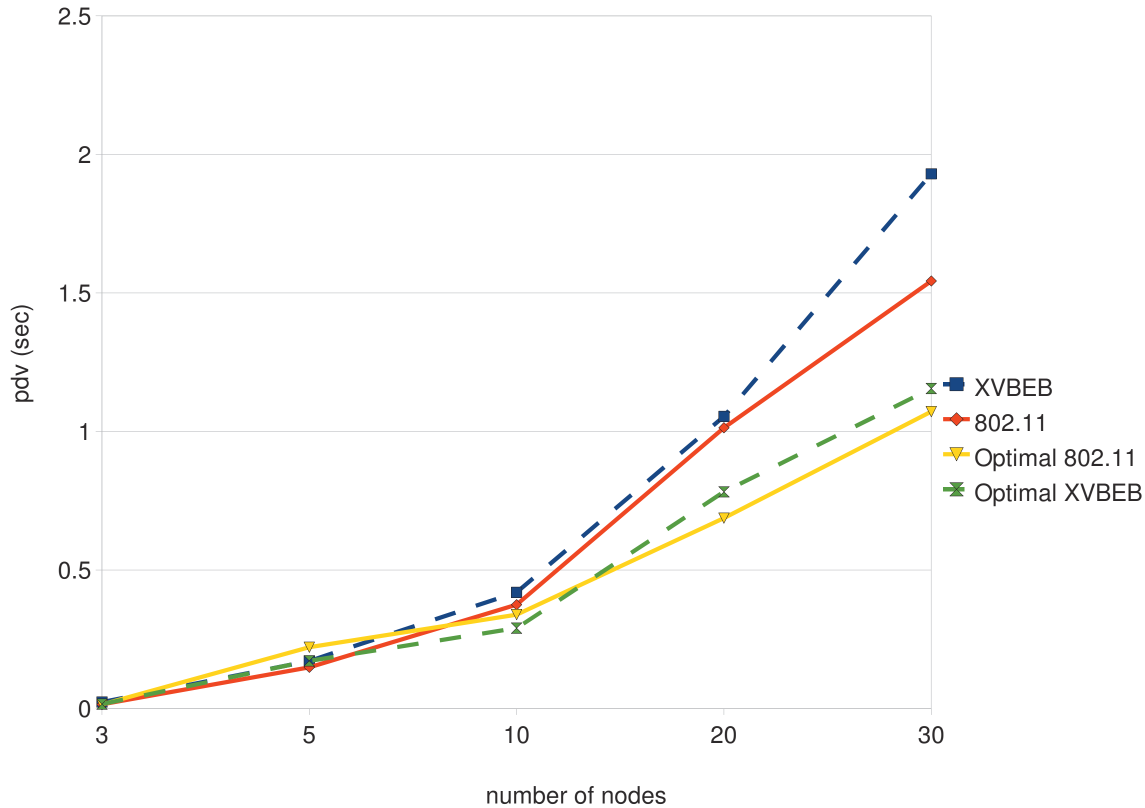

Figure 54: Packet delay variation, medium bitrate video, RTS/CTS

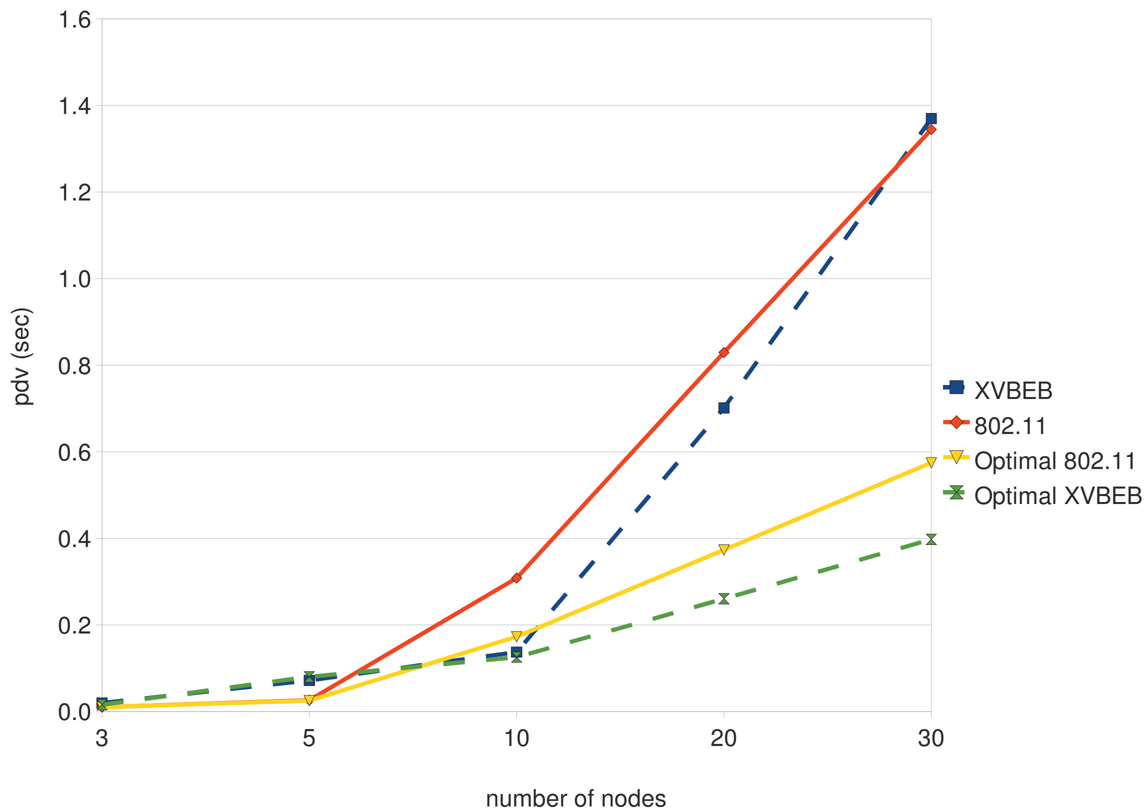

Figure 55: Packet delay variation, medium bitrate video, basic access

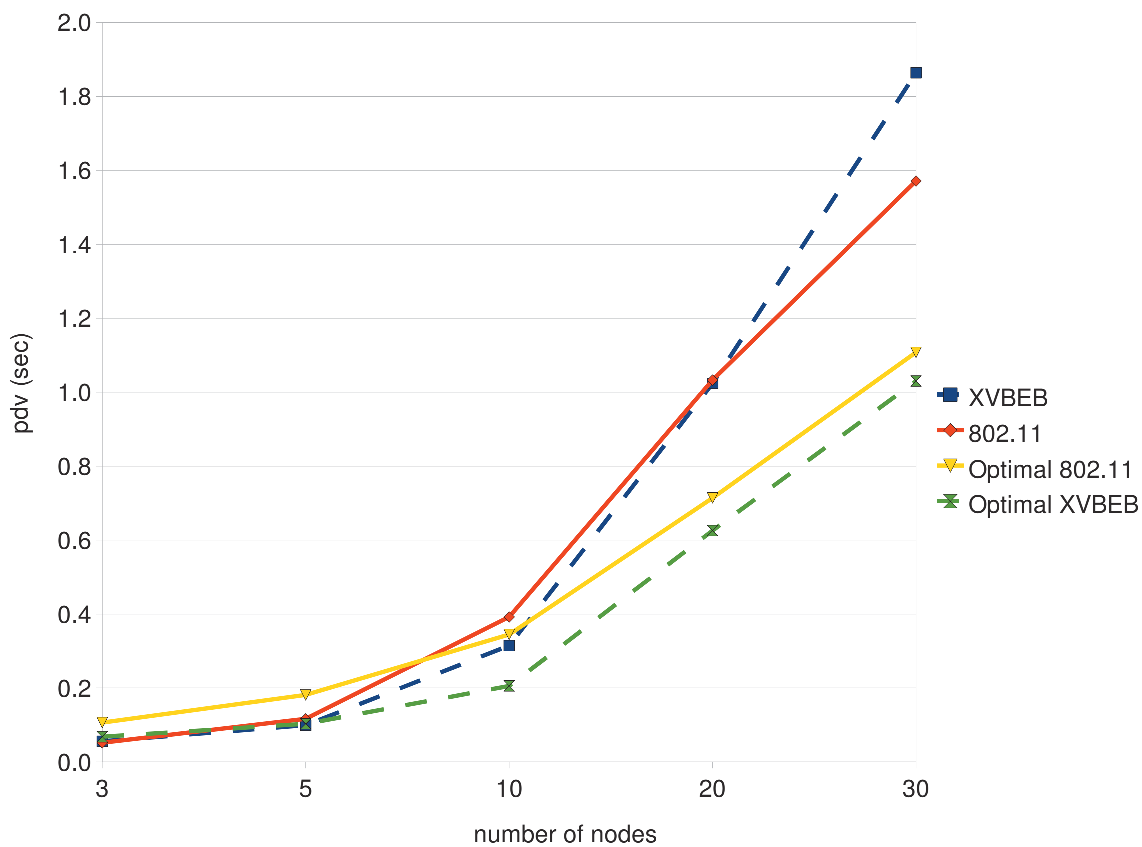

Figure 56: Packet delay variation, high bitrate video, RTS/CTS

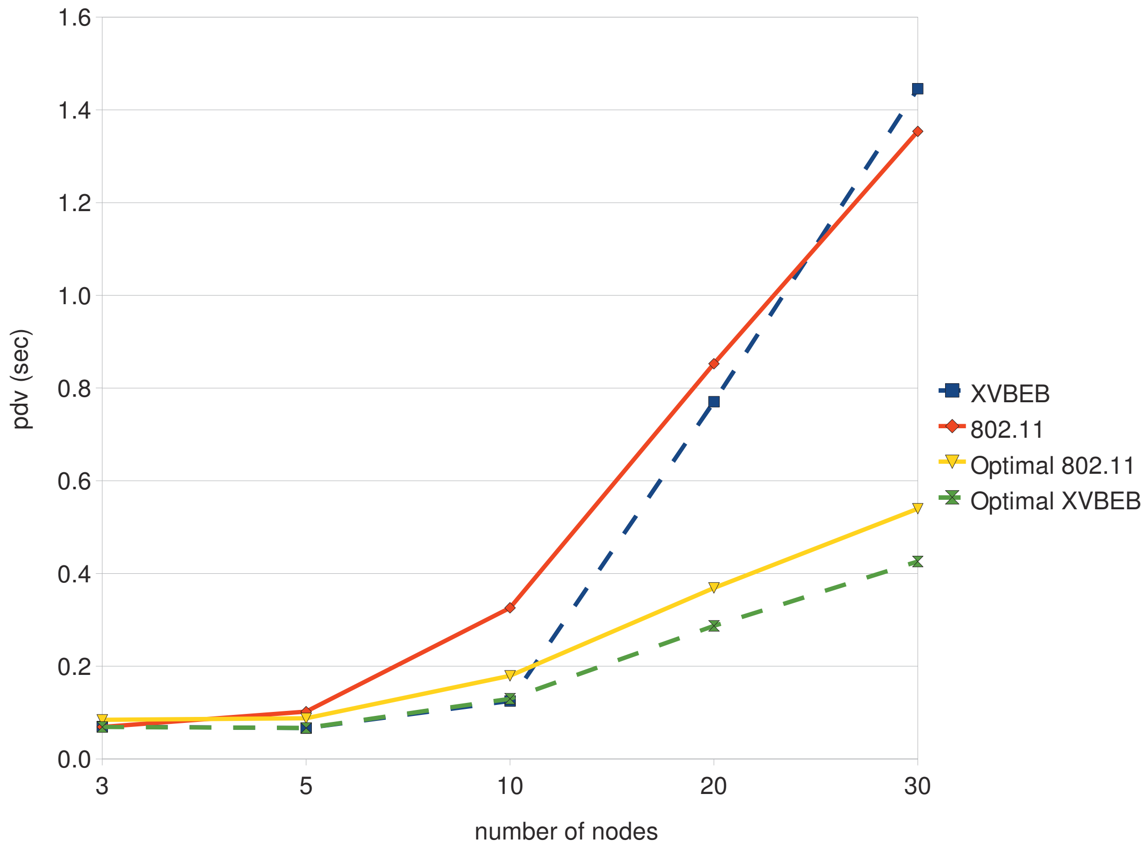

Figure 57: Packet delay variation, high bitrate video, basic access

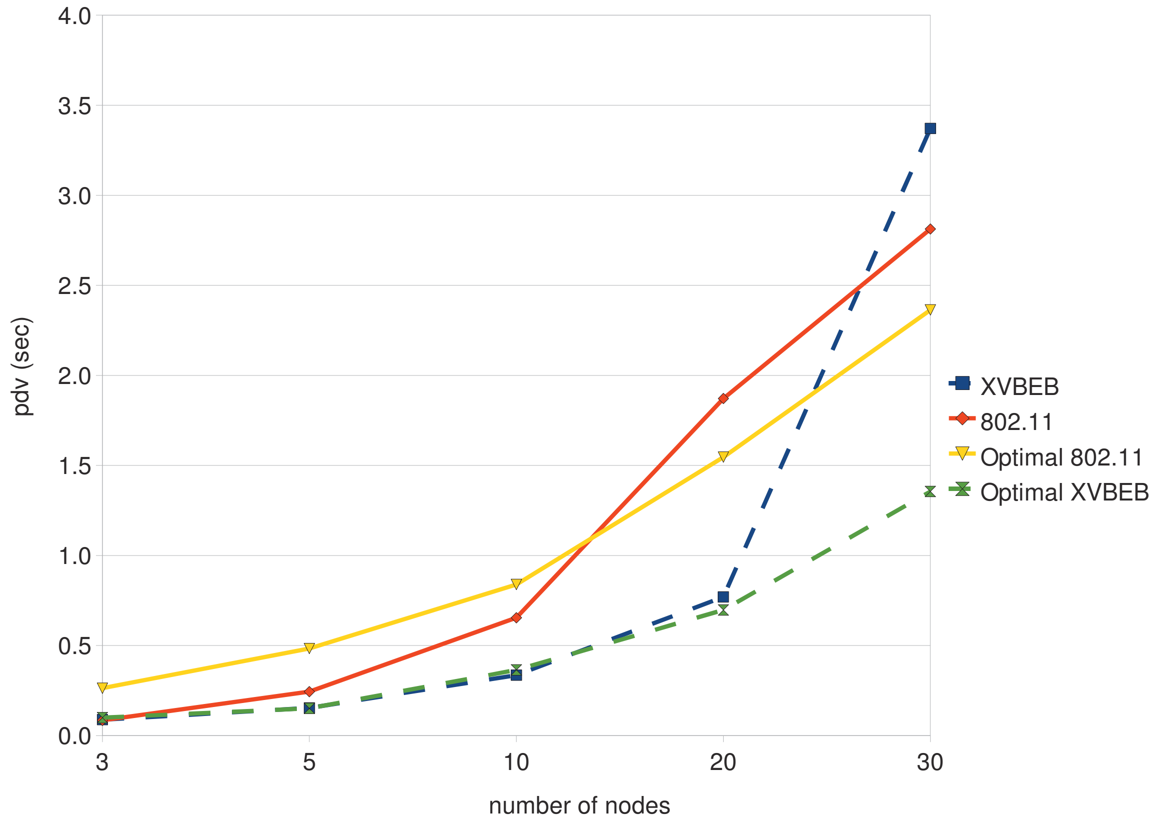

Figure 58: Packet delay variation, voice traffic, RTS/CTS

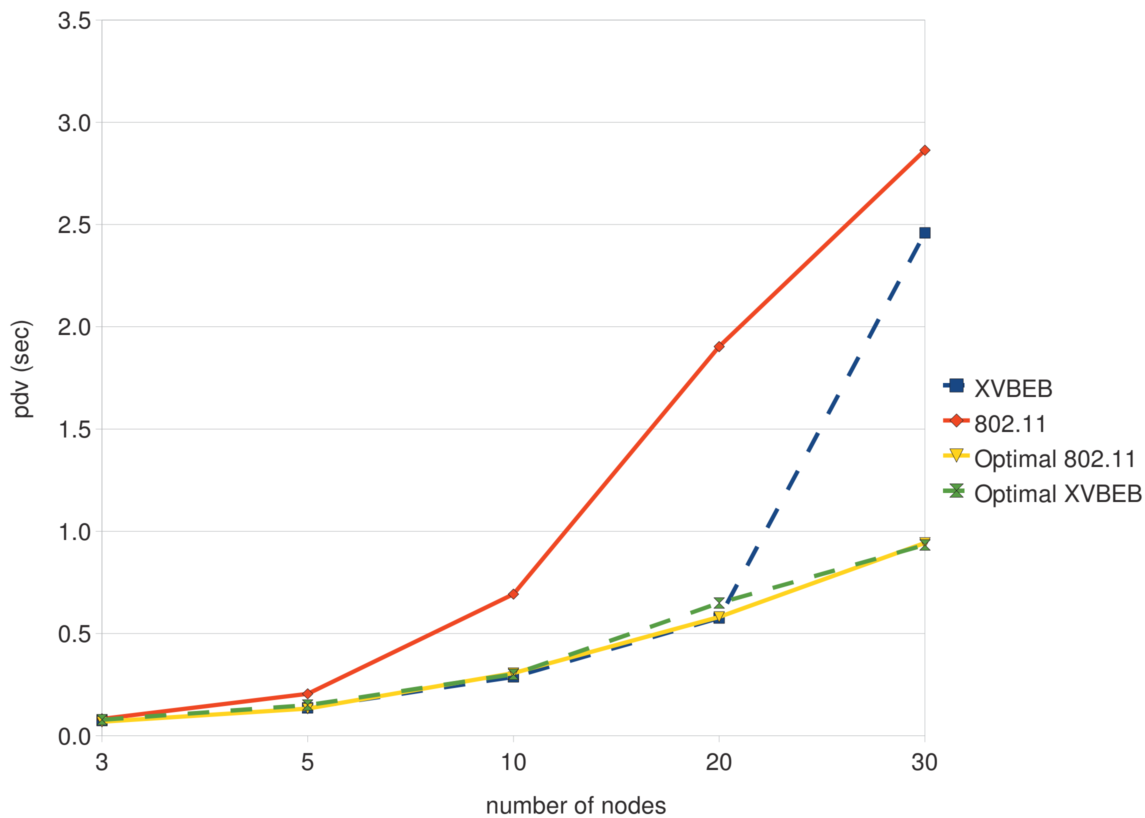

Figure 59: Packet delay variation, voice traffic, basic access

Chapter 7

Conclusions

In this thesis, we analyzed the problem of selfishness detection and prevention on behalf of the wireless nodes. In particular, we focused our attention on greedy nodes that misbehave by deviating from the 802.11 backoff procedure.

We first used a game-theoretic framework to represent a snapshot version of the media access contention resolution algorithm as a static strategic game. Further, we established an exact condition based on the number of the players and their strategies under which it is possible to design utility function such that the players' unique best response would be to choose their strategies according to a desired a priori specified distribution. We explicitly illustrated how to design the utilities when the condition is satisfied. In terms of the abstracted CSMA/CA backoff procedure, the unique Nash equilibrium of the game corresponds to protocol compliance on behalf of the wireless stations.

We also investigated practical methods for selfishness detection. We proposed a new protocol called XVBEB that allows to detect selfish stations based on the choices of their backoff values, which is not generally possible in IEEE 802.11. We showed how to deduce the backoff value choices of a node employing XVBEB using the timeline of channel events. Then, we demonstrated how to determine with a desired degree of accuracy whether the difference in the collected backoff values from the expected sample distribution is due to chance or because a station is misbehaving. Finally, we evaluated the performance of XVBEB and compared it with IEEE 802.11. Our simulations showed that XVBEB outperforms IEEE 802.11 in terms of saturated throughput, packet loss and delay in various situations.

Future works aims at using the game theoretic results to design a mechanism that could be used to provide incentives to players (nodes) in order to induce protocol compliance. There are several challenges to overcome. First, the dynamic nature of the CSMA/CA backoff procedure needs to be addressed, possibly by enhancing the repeated game model discussed in Section 4.3. A second challenge is the fact that a player's strategy is essentially its backoff value, and complete or perfect knowledge about backoff values used by players is unlikely to be available. Finally, the games we design focus exclusively on the utility function of players, which in fact is the sum of the payoffs used to incentivize participants and their internal valuation. The model should perhaps be extended to take into account the internal valuations. For example, in terms of the CSMA/CA procedure, urgent (real-time) traffic would be valued higher than regular data packets.

Another extension to the work in this thesis seeks to assess further the performance of the XVBEB protocol by providing theoretical and experimental analysis for the expected number of collisions and access patterns. Furthermore, the behavior of XVBEB should be evaluated in the quality of service context in order to determine how the protocol deals with changing priority traffic. Additionally, more attention should be brought to different misbehaving patterns, such as following the specifications in the lower backoff stages (e.g. $CW = 32$, $CW = 64$) and acting selfishly in the higher backoff stages ($CW = 512$, $CW = 1024$).

Finally, other backoff algorithms should be examined for resilience against selfish behavior and their performance should be evaluated. One such possibility is to require the nodes to choose only prime numbers as their backoff values.

Bibliography

[Abr70] Norman Abramson. The ALOHA system: another alternative for computer communications. In *Proceedings of the November fall joint computer conference*, pages 281–285, 1970.

[AE03] L. Anderegg and S. Eidenbenz. Ad hoc-VCG: a truthful and cost-efficient routing protocol for mobile ad hoc networks with selfish agents. In *Proceedings of 9th Annual International Conference on Mobile Computing and Networking*, pages 245–259, September 2003.

[AEAJ03] E. Altman, R. El-Azouzi, and T. Jimenez. Slotted ALOHA as a stochastic game with partial information. In *Proceedings of WiOpt'03*, 2003.

[Bia00] Giuseppe Bianchi. Performance analysis of the IEEE 802.11 distributed coordination function. *IEEE Journal on Selected Areas in Communications*, (3):535–547, 2000.

[CCHD07] L. Chen, T. Cui, Low. S. H., and J. C. Doyle. A game-theoretic model for medium access control. In *Proceedings of WICON*, 2007.

[CGAH05] M. Cagalj, S Ganeriwal, I. Aad, and J.-P. Hubaux. On selfish behavior in CSMA/CA networks. In *Proceedings of IEEE INFOCOM 2005*, volume 4, pages 2513–2524, March 2005.

[CGM04] M. Conti, E. Gregori, and G. Maselli. Cooperation issues in mobile ad hoc networks. In *Proceedings of IEEE ICDCSW*, pages 803–808, March 2004.

[CJ03] T. Clausen and P. Jacquet. Optimized link state routing protocol OLSR. Technical report, IETF RFC 3626, 2003.

[Cla71] Edward H. Clarke. Multipart pricing of public goods. *Public Choice*, 11:17–33, 1971.

[CRB09] Alvaro A. Cárdenas, Svetlana Radosavac, and John S. Baras. Evaluation of detection algorithms for mac layer misbehavior: theory and experiments. *IEEE/ACM Transactions on Networking*, 17:605–617, April 2009.

[DB05] D. Djenouri and N. Badache. New approach for selfish nodes detection in mobile ad hoc networks. In *Proceedings of SecQoS'05*, pages 288–294, 2005.

[DC02] C. Demichelis and P. Chimento. IP packet delay variation metric for IP performance metrics (IPPM). RFC 3393, November 2002.

[DNP03] R. Dash, Jennings N., and D. Parkes. Computational-mechanism design: A call to arms. *IEEE Intelligent Systems*, pages 40–47, November 2003.

[DV05] X. James Dong and Pravin Varaiya. Saturation throughput analysis of IEEE 802.11 wireless LANs for a lossy channel. *IEEE Communications Letters*, 9:100–102, 2005.

[FBW02] Zuyuan Fang, Brahim Bensaou, and Yu Wang. Performance evaluation of a fair backoff algorithm for IEEE 802.11 DFWMAC. In *MobiHoc '02*, pages 48–57, 2002.

[Fer96] Thomas S. Ferguson. *A Course in Large Sample Theory*. Chapman and Hall/CRC, 1996.

[FP03] E. Friedman and D. Parkes. Pricing WiFi at starbucks - issues in online mechanism design. In *Proceedings of Fourth ACM Conf. on Electronic Commerce (EC'03)*, pages 240–241, 2003.

[Gib92] R. Gibbons. *Game Theory for Applied Economists*. Princeton University Press, 1992.

[GN11] Antoniy Ganchev and Lata Narayanan. Selfishness detection for backoff algorithms in wireless networks. In *Proceedings of IEEE STWiMob*, 2011. To appear.

[GNA11] Antoniy Ganchev, Lata Narayanan, and Chadi Assi. Performance evaluation of backoff algorithms for medium access in wireless networks. In *Proceedings of IEEE iCOST*, 2011. To appear.

[GNS06] Antoniy Ganchev, Lata Narayanan, and Sunil M. Shende. Mechanisms to induce random choice. In *Proceedings of WINE*, pages 124–135, 2006.

[GNS08] Antoniy Ganchev, Lata Narayanan, and Sunil M. Shende. Games to induce specified equilibria. *Theoretical Computer Science*, 409(3):341–350, 2008.

[GNS09] Antoniy Ganchev, Lata Narayanan, and Sunil Shende. A tight characterization of strategic games with a unique equlibrium. In *Proceedings of the First ICST international conference on Game Theory for Networks*, GameNets'09, pages 366–373, 2009.

[GPHC] M. Gerla, G. Pei, X. Hong, and T. Chen. Fisheye state routing protocol FSR for ad hoc networks. Technical report, IETF INTERNET-DRAFT.

[Gro73] Theodore Groves. Incentives in teams. *Econometrica*, 41(4):617–31, July 1973.

[HP06] Jun He and Hung Keng Pung. Performance modelling and evaluation of IEEE 802.11 distributed coordination function in multihop wireless networks. *Computer Communications*, 29(9):1300 – 1308, 2006.

[IEE07] Wireless LAN medium access control (MAC) and physical layer (PHY) specification, 2007.

[JCH98] Raj Jain, Dah-Ming Chiu, and W. Hawe. A quantitative measure of fairness and discrimination for resource allocation in shared computer systems. *CoRR*, 1998.

[JMH] D. Johnson, D. Maltz, and Y.-C. Hu. The dynamic source routing protocol for mobile ad hoc networks DSR. Technical report, IETF INTERNET-DRAFT.

[KLS01] M. Kearns, M. Littman, and S. Singh. Graphical models for game theory. In *Proceedings of UAI*, pages 253–260, 2001.

[KMW08] Brett Myors Kevin Murphy and Allen Wolach. *Statistical Power Analysis: A Simple and General Model for Traditional and Modern Hypothesis Tests, 3rd Edition*. Routledge Academic, 2008.

[Kon01] Jerzy Konorski. Protection of fairness for multimedia traffic streams in a non-cooperative wireless LAN setting. In *Proceedings of the 6th International Conference on Protocols for Multimedia Systems*, pages 116–129, 2001.

[Kon02] Jerzy Konorski. Multiple access in ad-hoc wireless LANs with non-cooperative stations. In *Proceedings of NETWORKING '02*, pages 1141–1146, 2002.

[KT75] L. Kleinrock and F. A. Tobagi. Packet switching in radio channels: Part I -carrier sense multiple-access modes and their throughput-delay characteristics. *IEEE Transactions on Communications*, 23:1400–1416, 1975.

[KV04] P. Kyasanur and N. Vaidya. Selfish MAC layer misbehavior in wireless networks. *IEEE Transactions on Mobile Computing*, pages 502–516, April 2004.

[LLK+06] Venkata Nishanth Lolla, Lap Kong Law, Srikanth V. Krishnamurthy, Chinya V. Ravishankar, and Dharmaiah Manjunath. Detecting MAC layer back-off timer violations in mobile ad hoc networks. In *International Conference on Distributed Computing Systems*, page 63, 2006.

[MGLB00] S. Marti, T. Guili, K. Lai, and M. Baker. Mitigating routing misbehavior in mobile ad hoc networks. In *Proceedings of ACM MOBICOM*, pages 255–265, 2000.

[ML] Ashraf Matrawy and Ioannis Lambadaris. NS2 contributed code.

[MM02] P. Michiardi and R. Molva. CORE: A collaborative reputation mechanism to enforce node cooperation in mobile ad hoc networks. In *Proceedings of Communications and Multimedia Security*, pages 107–121, September 2002.

[MN07] Hadi Minooei and Hassan Nojumi. Performance evaluation of a new backoff method for IEEE 802.11. *Computer Communications*, 30(18):3698 – 3704, 2007.

[MW01] A.B. MacKenzie and S.B. Wicker. Selfish users in ALOHA: a game theoretic approach. In *Proceedings of IEEE Vehicular Technology Conference*, pages 1354–1357, October 2001.

[nCK02] Chen nee Chuah and Randy H. Katz. Characterizing packet audio streams from internet multimedia applications. In *Proceedings of the IEEE ICC*, pages 119–9, 2002.

[OR96] M. Osbourne and A. Rubenstein. *A Course In Game Theory*. The MIT Press, 1996.

[Par01] D. Parkes. *Iterative Combinatorial Auctions: Achieving Economic and Computational Efficiency*. PhD thesis, Univesity of Pennsylvania, May 2001.

[PBRD03] C. Perkins, E. Belding-Royer, and S. Das. Ad hoc on demand distance vector AODV routing. Technical report, IETF RFC 3561, 2003.

[RBK05] Svetlana Radosavac, John S. Baras, and Iordanis Koutsopoulos. A framework for mac protocol misbehavior detection in wireless networks. In *Proceedings of the 4th ACM workshop on Wireless security*, WiSe '05, pages 33–42, 2005.

[RHA04] M. Raya, J. P. Hubaux, and I. Aad. DOMINO: A system to detect greedy behavior in IEEE 802.11 hotspots. In *Proceedings of MobiSys*, pages 84–97, 2004.

[RLC06] Yanxia Rong, Sang Kyu Lee, and Hyeong-Ah Choi. Detecting stations cheating on backoff rules in 802.11 networks using sequential analysis. In *Proceedings of INFOCOM*, pages 1–13, 2006.

[Rob75] Lawrence G. Roberts. ALOHA packet system with and without slots and capture. *SIGCOMM Computer Communication Review*, 5:28–42, April 1975.

[Ros04] Sheldon M. Ross. *Introduction to probability and statistics for engineers and scientists (3. ed.)*. Academic Press, 2004.

[RT99] E.M. Royer and C-K Toh. A review of current routing protocols for ad hoc mobile wireless networks. *IEEE Personal Communications*, 6:46–55, April 1999.

[TGN09] I. Tinnirello, L. Giarre, and G. Neglia. The role of the access point in Wi-Fi networks with selfish nodes. In *Proceedings of International Conference on Game Theory for Networks*, pages 631–637, May 2009.

[Vic61] William Vickrey. Counterspeculation auctions and competitive sealed tenders. *Journal of Finance 16*, pages 8–37, 1961.

[WCLH05] Shao-Cheng Wang, Yi-Ming Chen, Tsern-Huei Lee, and Ahmed Helmy. Performance evaluations for hybrid IEEE 802.11b and 802.11g wireless networks. In *Proceedings of Performance, Computing, and Communications Conference*, pages 111–118, 2005.

[WPL+02] Haitao Wu, Yong Peng, Keping Long, Shiduan Cheng, and Jian Ma. Performance of reliable transport protocol over IEEE 802.11 wireless LAN: Analysis and enhancement. In *Proceedings of IEEE INFOCOM*, pages 599–607, 2002.

[ZA02] Eustathia Ziouva and Theodore Antonakopoulos. CSMA/CA performance under high traffic conditions: throughput and delay analysis. *Computer Communications*, 25(3):313 – 321, 2002.

[ZCY03] S. Zhong, J. Chen, and Y. R. Yang. Sprite: A simple, cheat-proof, credit-based system for mobile ad hoc networks. In *Proceedings of IEEE INFOCOM*, pages 1987–1997, March 2003.